

See discussions, stats, and author profiles for this publication at: <https://www.researchgate.net/publication/327118518>

Structural influence of the geometry of masonry vaults – Brick tiling patterns for compression shells using geodesic coordinates

Thesis · November 2016

DOI: 10.13140/RG.2.2.23041.71521

CITATION

1

READS

2,742

1 author:

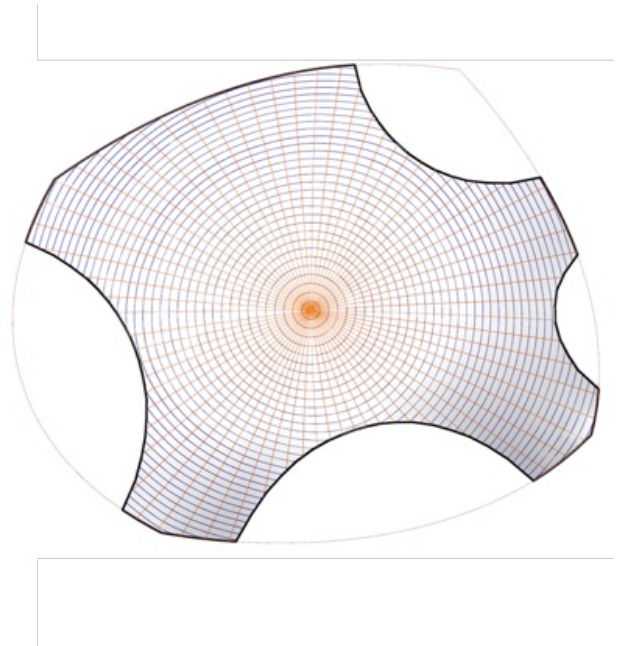
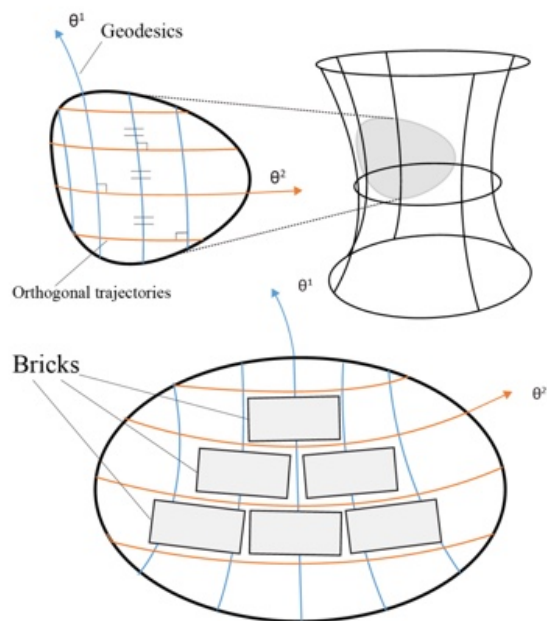


[Emil Adiels](#)

Chalmers University of Technology

10 PUBLICATIONS 15 CITATIONS

[SEE PROFILE](#)



Structural influence of the geometry of masonry vaults

Brick tiling patterns for compression shells using geodesic coordinates

Master's thesis in Structural Engineering and Building Technology

EMIL ADIELS

MASTER'S THESIS 2016:88

Structural influence of the geometry of masonry vaults

Brick tiling patterns for compression shells using geodesic coordinates

EMIL ADIELS



Department of Applied Mechanics
Division of Material and Computational Mechanics
CHALMERS UNIVERSITY OF TECHNOLOGY
Gothenburg, Sweden 2016

Structural influence of the geometry of masonry vaults
Brick tiling patterns for compression shells using geodesic coordinates
EMIL ADIELS

© EMIL ADIELS, 2016.

Supervisor: Chris J K Williams, Bath University
Examiner: Mats Ander, Department of Applied Mechanics, Chalmers

Master's Thesis 2016:88
Department of Applied Mechanics
Division of Material and Computational Mechanics
Chalmers University of Technology
SE-412 96 Gothenburg
Telephone +46 31 772 1000

Cover: Polar geodesic coordinates applied onto a form found compression shell structure.

Typeset in L^AT_EX
Printed by [Name of printing company]
Gothenburg, Sweden 2016

Structural influence of the geometry of masonry vaults
Brick tiling patterns for free-form shells using geodesic coordinates
EMIL ADIELS
Department of Applied Mechanics
Chalmers University of Technology

Abstract

In this thesis, we propose a strategy for generating patterns for brick laying on compression free-form shells. The strategy is based on geodesic coordinates which guarantees an equal length between its coordinates curves, which for brickwork means an equal spacing between the bed joints. The implementation is done for polar geodesic coordinates using dynamic relaxation. The procedure is implemented in a parametric design framework and evaluated on a test case. Our study revealed that the proposed strategy has potential of contributing in the design of complex brick shells and also being a piece in the puzzle of understanding patterns of historical vaults.

Keywords: masonry, architectural geometry, brick, shells, polar geodesic coordinates, differential geometry

Acknowledgements

This thesis work would not have been possible without the help and inspiration from some special people. Firstly I would like to thank my supervisor Prof. Chris Williams, examiner Dr. Mats Ander and my opponents Alexander Sehlström and Erica Henrysson. I would also like to thank Prof. Karl-Gunnar Olsson, Prof. John Ochsendorf at MIT and Francis Aish at Foster and Partners for taking time and being inspirational. Special thanks to Carl Hoff, Isak Näslund, Emil Poulsen and Johanna Riad for many interesting collaborations and conversations over the years in this subject.

Emil Adiels, Gothenburg, November 2016

Contents

List of Figures	xiii
------------------------	-------------

List of Tables	xxi
-----------------------	------------

1	Introduction	1
1.1	Bricks	2
1.2	Shells in architecture	2
1.3	Finding forms of equilibrium	3
1.3.1	Numerical methods	4
1.3.2	Development of form-found bricks shells	5
1.4	Geometry	6
1.4.1	Mathematical mappings	7
1.4.2	Brick patterns on shells	8
1.5	Design processes in computational environments	9
1.5.1	Design scheme	10
1.6	Research task	10
1.6.1	Aim	11
1.6.2	Purpose	11
1.6.3	Method	11
1.6.4	Limitations	12
2	Theory	13
2.1	Structural theory of masonry structures	13
2.1.1	Structural design	13
2.1.2	Limit design principles	15
2.1.2.1	Safety factor	16
2.2	Differential geometry	16
2.2.1	Curves in space	17
2.2.1.1	Geometry of the space curve	19
2.2.1.2	Curvature and Torsion	20
2.2.2	Surfaces	20
2.2.2.1	Geometry on a surface	22
2.2.2.2	Geodesics	25
2.2.2.3	Normal and geodesic curvature	25
2.2.2.4	Geodesic coordinates	26
2.3	Membrane theory of shells	30

2.4	Numerical solvers and form finding	33
2.4.1	Force density method(FDM)	33
2.4.2	Dynamic relaxation(DR)	34
3	Method	39
3.1	Part 1: form-finding	41
3.2	Part 2: Polar geodesic coordinates	42
3.2.1	From continuous to discrete mathematics	43
3.2.1.1	Discrete polar geodesic coordinates	43
3.2.1.2	Discrete geodesics	44
3.2.1.3	Simulate geodesics using dynamic relaxation	45
3.2.2	Procedure	46
4	Results	51
4.1	Model preparation and generation	51
4.2	Test case: polar geodesic coordinates on shell	53
4.2.1	Visual output	53
4.2.2	Discrete geodesics	54
4.2.3	Geodesic segment length	55
4.2.4	Maximum angle difference of mesh face	57
4.2.5	Transformation of discrete to continuous surface	60
5	Discussion	61
5.1	Reflections	61
5.1.1	Organisation of the method	61
5.1.2	Credibility of the method	61
5.1.3	Implementation	62
5.1.3.1	Computational efficiency	62
5.1.3.2	Form generation	62
5.1.4	Design	63
5.1.4.1	General and polar geodesic coordinates	63
5.1.4.2	Edge-conditions	64
5.2	Future work and improvements	65
6	Conclusion	67
	Bibliography	69
A	Appendix 1	I
A.1	Bricks	I
A.1.1	The brick	I
A.1.2	Brick Making	II
A.1.3	Craftsmanship	II
A.1.4	Brick formats and terminology	V
A.2	Differential geometry	VI
A.2.1	First fundamental Form	VI
A.2.2	Second fundamental Form	VIII

A.2.3	Christoffel Symbols	IX
A.2.4	Gauss-Codazzi Equations	XI
A.2.5	Gaussian and Mean Curvature	XI
A.2.5.1	Principal Curvature	XII
A.3	Tensor Analysis	XIII
A.3.1	Index notation	XIII
A.3.2	2nd order Tensors	XIII
A.4	Material	XIII
A.4.1	Material Properties	XIII
A.4.2	Mortar	XV
A.5	Geometry	XVI
A.5.1	Stereotomy	XVI
A.6	Form Finding	XVIII
A.6.1	Graphical Methods	XVIII
A.6.2	Analytical Methods	XIX
A.6.3	Physical methods	XX
A.7	Results	XX
A.7.1	Model preparation	XXI
A.7.2	Parametric Framework	XXVI

List of Figures

1.1	To the left, terminology for the brick faces and different types of joints in a brick constellation [11]. To the right it shows that bricks laid along the brick joints [31].	2
1.2	To the left a staircase by the Guastavino company showing both structural and geometrical complexity achievable using brick vaults[7]. To the right the roof construction on <i>Citricos Caputto fruit packing plant</i> , by Dieste [48].	6
1.3	A free-form compression shell that was developed and built by the Block Research Group at ETH in Zurich [43].	6
1.4	Draping a cylinder with a plane is very easy. Trying a similar procedure with a sphere it is proven impossible without modifications or crumbling of the paper.	7
1.5	The Mercator projection, which maps the sphere coordinates onto a plane, invented 1569 by <i>Gerardus Mercator</i> is still used in modern applications such as Google Maps[32] to illustrate the coordinates of the earth onto a two dimensional map.[37]	8
1.6	It is possible to find records of how to tessellate traditional vaults with bricks. This illustration shows the brick patterns and guidelines for a Cavetto vault, top, and a Saucer dome below [31]	9
1.7	A possible parametric design process that will be used to adress the research in a design context.	10
1.8	The thesis work will only concern a small portion of the whole design process. It will concern the tessellation and form generation in the initial conceptual phase.	12
2.1	Collapse mechanism of masonry vault by an asymmetric load. The vault cannot contain the line of thrust within its geometry. This leads to the formation of plastic hinges at those locations where the line of thrust exceeds or hits the boundaries. This is not a problem until a sufficient number of hinges are formed to make the structure collapse[8].	14
2.2	Typical cracks in Gothic vaults. " <i>Pol Abraham(1934) distinguished between the 'hinging' cracks near the crown, the 'Sabouret' cracks parallel to the wall ribs and the separation of the vault from the walls.</i> " [8]	15

2.3	The theoretical limit condition for masonry voussoirs. If the position of the compressive axial force is placed a distance $t/2$ from the center a hinge will be formed. This represents a block of infinite stress capacity since a normal stone or brick would crush when the contact area gets to small. Therefore, there are some safety factors that need to be applied, see figure 2.4. [14]	16
2.4	The middle third rule applied to a block, if going axial force is less than $1/3$ from the edge it will result in tension which will cause possible hinges, redrawn from [3]	17
2.5	Example of curves in Cartesian coordinates, redrawn from [5]	17
2.6	A parametrized curve is constructed by a locus of points in space based on a coordinate vector. To the right one can see how the position of the curve is related to a one-dimensional parameter. . . .	18
2.7	The geometry of the curve with its tangent, \mathbf{t} , principal normal \mathbf{n} and binormal \mathbf{b} vectors, redrawn from [5]	19
2.8	Two examples of surfaces made of ribbed wood structures. To the left is a "Monkey saddle"- surface described in Cartesian coordinates $z = x^3 - 3xy^2$, to the right a Hyperbolic paraboloid $z = (y^2)/(b^2) - (x^2)/(a^2)$	21
2.9	Parametrizes surface in three dimensional space \mathbb{R}^3 , is described using a position vector which is $\mathbf{r}(\theta^1, \theta^2)$ and how it relates to the parametrization in \mathbb{R}^2	22
2.10	The coordinate curves are straight lines in domain \mathbb{R}^2 that forms the curved net on the surface in \mathbb{R}^3	22
2.11	basis vectors of a surface described using curvilinear coordinates. \mathbf{a}_1 and \mathbf{a}_2 are the ,the covariant basis vectors which are the tangent to coordinate curves. \mathbf{a}^1 and \mathbf{a}^2 are the contravariant basis vectors and can be described in equation 2.19 above.	23
2.12	A vector \mathbf{p} can be constructed using either covariant or contravariant basis vectors.	24
2.13	Straight ribbons laid out flat on a surface will follow the geodesics on that surface[4].	25
2.14	There are two possible boundary conditions when constructing a geodesic on a surface. Either one specifies two points and finds the geodesic between those, illustrated to the left, or one specify a starting point and direction and the geodesic is aloud propagates without restriction, illustrated to the right.	26
2.15	The curvature κ , for a curve $\mathbf{C}(t)$ that lies in the surface, can be divided into two separate parts κ_n , normal curvature, and κ_g which is the geodesic curvature.	26
2.16	A Geodesic coordinate set which consists of two types of coordinate curves, geodesics and parallel trajectories to the geodesics. Notice the right angle in the intersection between the two types of curves. Redrawn picture from [1]	27

2.17	Interpretation of Theorem 1, of Struik [1], which states that if one parallel trajectory is found for a set of geodesics a parallel trajectory is found at an equal distance from the first parallel trajectory.	28
2.18	A polar geodesic coordinate set redrawn from [1]. The polar geodesic coordinates set possess the same properties as an arbitrary geodesic set, see figure 2.16, the difference is that the geodesics meet in a pole.	29
2.19	Since the length between two orthogonal trajectories bricks, assuming uniform height, might be placed between them. [52]	30
2.20	Equilibrium for a three dimensional membrane element in curvilinear coordinates.	31
2.21	The two kinds of loading referring to loading in normal direction from equation 2.50, to the left, and the in plane loading from equation 2.49, to the right.	32
2.22	A node connected to three bars with load applied in the z-direction with labeled nodes and internal forces.	33
2.23	Flow diagram showing the computational procedure for FDM. This diagram is redrawn from [3]	35
2.24	Visualization of dynamic relaxation applied on a plane mesh that is under gravitational load where the corner points are fixed. It shows how the structure reach equilibrium tracing through time. Initial state at $t = 0$ and equilibrium at $t = 4$	36
2.25	Flow diagram describing the different stages of Dynamic Relaxation. A reconstruction from [3], where axial and shear forces has been replaced with a more general definition of forces only. The main idea of dynamic relaxation is to transform a residual force into an acceleration leading to a new position. Iterate this process until the residual force vanish, meaning that the equilibrium of external and internal forces is found.	37
3.1	The method separates the form-finding and the generation of polar geodesic coordinates. Decoupling of the process enables more freedom to change and alter different aspects of the design.	39
3.2	The theoretical framework of the generation of polar geodesic coordinates. From theory to formulating a mathematical model that is implemented in a numerical solver.	40
3.3	To enhance the user interaction in the design process a user interface will extend the connection between the parametric development environment and the 3d modelling software.	41
3.4	The method should be integrated in a easily navigated design scheme where the designer can change the design thorough different parameters.	42
3.5	The flow diagram for the FDM routine is formalised based on the user interaction diagram of figure 3.4.	43
3.6	To the left the continuous definition of polar geodesic coordinates and to the right a discrete interpretation. For the discrete polar geodesic coordinate the angles are not necessarily orthogonal.	44

3.7	Definition of a point on a discrete geodesic curve on a continuous surface. A point, that is part of set of points forming a discrete curve, is connected by vectors A and B to its adjacent neighbouring points. The vectors A and B should be contained within a plane together with the normal vector of the surface.	45
3.8	The mechanical equivalent of zero geodesic curvature is that there is no difference between the force $\mathbf{s}_1 + \mathbf{s}_2$ and its projection onto the normal, \mathbf{a}_3 , in that point.	46
3.9	The DR procedure in which the points are connected with pre-tensioned springs. In the final state the residual force is parallel with the normal vector in that point.	47
3.10	The procedure of generating the polar geodesic coordinates on a surface.	49
4.1	The connection between the 3d modelling software Rhinoceros and the parametric design plug-in is enhanced by a user interface.	52
4.2	The code in grasshopper structured in different units. Starting from the input of geometry one can follow the procedure to the generation of polar geodesics on the surface.	52
4.3	Output of discrete geodesic coordinates in top view	53
4.4	Output of discrete geodesic coordinates in right view	53
4.5	Output of discrete geodesic coordinates in front view	54
4.6	Output of discrete geodesic coordinates in back view	54
4.7	Graphical output of the angle between the normal and the cross product of the two connecting vectors to each point. The angle is evaluated in the range 89 and 91 degrees.	55
4.8	Analysis of the length of the discrete lines between the geodesic points. The figure above consists of all segments, both geodesics and orthogonal trajectories. Below the analysis is done with only the geodesic segments. The analysis shows great length consistency of the geodesic elements with small deviations.	56
4.9	The analysis criteria where the result is the subtraction of the maximum and the minimum angle of each face.	57
4.10	Analysis with two types of mesh resolution, the top is coarser and below is a small patch that is of very fine resolution. They are evaluated between 0 and 10 degrees.	58
4.11	Analysis of the fine resolution mesh, same model as in figure 4.10 but with the evaluation ranging between 0 and 2 degrees to give a more detailed analysis.	59
4.12	Comparison between the form-found mesh, in blue, and the surface generated from that mesh in grey which is used for the generation of geodesic coordinates.	60
4.13	The average deviation going from the discrete surface, the form-found mesh, to the continuous surface that is used during the dynamic relaxation is relatively small compared to the size of the mesh face.	60
5.1	In Bath abbey each fan vault has its geometry based on a pole. The geometry then meets in the aisle roof. [47]	64

5.2	Problems that can occur along the edges if the edges and the orthogonal trajectories differ. A good design approach would be to design the edges are described by an orthogonal trajectory.	65
5.3	It is possible to construct the geodesic coordinates by generating geodesics orthogonal to a curve, using for instance the edge curve. There is a possibility though that the geodesics will propagate on the surface in such a way that they intersect each other.	65
A.1	A traditional method of brick making is by putting it into wooden forms. Today this is not very common and the bricks are usually pressed by a machine. This method gives the brick marks of the form and also results in some deformation and transformations from the cuboid. The deformations is in general not a problem due to the adaptability for tolerances of the mortar joints. This method is more in line with traditional brick making then the wire-cutting method. [30]	II
A.2	An industrialised way of making bricks using a wire-cutter. This results in concise and precise forms of the brick with less deformations. The feeling of these bricks are usually more industrial. [30]	III
A.3	Principles of a tunnel kiln. Above is the different stages and below one can follow the difference in temperature during these stages [10] .	IV
A.4	Typical tools for a brick layer from a Swedish brick layer handbook from 1938. 1)Plumb 2)spatula 3)spirit level 4)Wooden jointer 5)Hammer for brick cutting [31]	IV
A.5	The bricks should all be level in the horizontal direction. The most common way to achieve this is to use string that is attached between to rods. [31]	V
A.6	To the left one can see how the bricklayer uses a spatula to apply mortar to both the brick and the place of the brick. To the right one can see how the brick layer can use both the spirit level and a plumb to ensure geometrical correctness [31]	V
A.7	Different sizes formats of typical brick constellations. [11]	VI
A.8	The first fundamental form is way of describing how the measure of lengths on the surface will behave and propagate. If two surfaces has the same first fundamental form means that the length of a mapped curve will have the same length as before mapping. Since the plane and the cylinder has the same first fundamental form the curve will have the same length if mapping between these surfaces.	VII
A.9	The sphere and the plane does not have the same FF and therefore it is not possible to mapp these curves between the two without constraints. If flattening out a sphere on the plane, to the right, one might understand the geometrical issue graphically.	VII

A.10	A surface with a tangent plane in the point $P = \mathbf{r}(\theta^1, \theta^2)$. The point Q is described as increment from P, $Q = \mathbf{r}(\theta^1 + d\theta^1, \theta^2 + d\theta^2)$. The second fundamental form is the measure of how much the surface deviates from a tangent plane, in this figure the measure d . Redrawn from [24]	VIII
A.11	On the left is the elliptic case, In the middle the hyperbolic case and to the right the parabolic case.	IX
A.12	Geometric representation of Christoffel Symbol of Second kind	X
A.13	Geometric representation of Christoffel Symbol of First kind	X
A.14	To the left is a sphere which has positive curvature in two directions. In the middle is a hyperparaboloid which has both positive and negative curvature in its saddle point, which results in negative Gaussian curvature. To the right is the cylinder which has positive in one and zero curvature in the second direction which results in zero Gaussian curvature.	XII
A.15	The flexural strength and Young modules compared to the compressive strength of bricks. These pictures are remakes from[25]	XIV
A.16	Brick are part of category called ceramics which has relatively low elastic modulus compared to most metals. [25]	XV
A.17	The properties of bricks are very much controlled and related to the composition of the raw material and the kiln temperature. [10]	XV
A.18	Sketches and drawings from a notebook of Stereotomy from 1896 showing how structures are discretized and how those elements are constructed.[28]	XVI
A.19	The stone vault at Hotel de Ville by <i>Jules Hardouin Mansart</i> is a famous example of stereotomy in architecture [49]	XVII
A.20	Blocks can be generated from a discrete surface representation with computational methods [18]	XVII
A.21	Stone blocks that have been fabricated using digital fabrication methods [19]	XVIII
A.22	Graphic statics applied to vault with differently shaped elements. To the right on can see triangles forming of the internal and external forces which illustrates equilibrium.[9]	XIX
A.23	Example of graphic statics applied to a hanging cable. Figure to the left shows the collected force polygons and how they relate to the internal forces of the hanging cable. To the right one can see the global equilibrium illustrated. [9]	XIX
A.24	Soap-film experiment to achieve minimal surfaces from the research of Frei Otto [34]	XX
A.25	It is easy to apply and change the boundary conditions. One can draw initial lines that are then projected onto the edge of the bottom form.	XXI
A.26	It is possible to change the force densities to get different properties and attributes to the form.	XXII
A.27	It is possible to adjust the position of the pole depending on the aesthetics or the properties of the form itself.	XXIII

A.28	Dynamic relaxation is applied to generate the geodesics. it is possible to analyse during the process by either looking at the values for each point, top picture, or look graphically, bottom picture.	XXIV
A.29	The generation of the geodesics are done at this stage. And it is now possible to generate the polar geodesic coordinate based on the points from the previous stage.	XXV
A.30	The grasshopper definition made for this thesis.	XXVI

List of Tables

A.1	The chemical composition of different types of brick clay. The proportions are described in percentage. [12]	I
-----	--	---

1

Introduction

For a long time, bricks have been used in construction of vaults and shells in architecture. In history the shapes of the shells have been a selected few and often based on rotational surfaces and intersection between those. With time methods for generating more structurally optimal shapes have been developed. These can be more mathematically complex and also individual between projects. The concept of brick constructions is based on the modular manufacturing of bricks. The standardized building system is viable due to the applicable paste, mortar, which fills gaps and connects bricks.

The complex nature associated with shells makes construction methods, structural theory and tessellation complicated. This section will give an introduction and contextual orientation in the subject of brick shells. It will cover different aspects of brick shells such as traditional crafts, development of shells, form finding and geometry, and in the end defining the area and question of research.

1.1 Bricks

Brick structures consists of bricks that are either stacked or glued together using mortar forming an almost weaved structure. Bricks are artificial stones that are made of heated clay and formed into specific cuboid formats. Depending on fabricating technique the bricks form either a perfect cuboid or can become more or less distorted. The mortar, which initially is a fluid paste, makes it possible to not only connect the bricks but also compensate differences and evenly distribute the stresses between the bricks. This makes it possible to reach a high level of originality between the elements but still be a modular fabrication concept. So even though the format and repetition is one of the key features bricks also contains significant materiality and uniqueness.

Brick structures are usually made in different types of patterns where the layers, or courses, are specified along by the mortar bed joints. For a vertical structure the bed joints become horizontal and for vaults they follow the curvature of the surface and therefore become curved. A brick layer will produce the structure layer by layer.

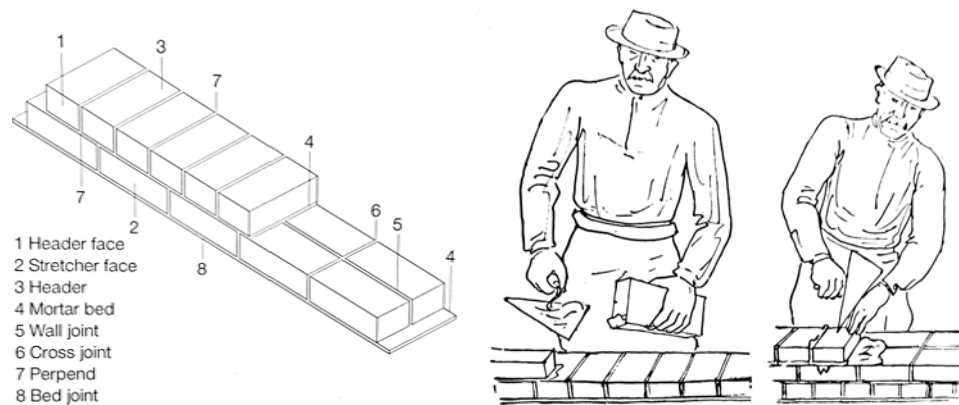


Figure 1.1: To the left, terminology for the brick faces and different types of joints in a brick constellation [11]. To the right it shows that bricks laid along the brick joints [31].

To read more about bricks, brick making, production and craftsmanship please see appendix A.1.

1.2 Shells in architecture

Shells are a special type of structure or structural element used in architecture and engineering. They are sometimes mentioned as vaults in architecture while in engineering usually referred as only shells. What is significant about shells is their form and mechanical behaviour. Its form can be described as a surface which is curved in one or two directions. Mechanically it can convert external loads into mainly forces in the plane of the surface, inflicting little or no bending [3].

Historically masonry shells are usually based on simple geometric forms like rotational surfaces cut by planes or by other rotational surfaces [31]. Their design

emphasises production and visual aspects rather than governed by structural efficiency. During the late 19th century *Rafael Guastavino* started designing masonry shells with the relatively new method of graphic statics, and by so taking the first steps into modern age of masonry shells. This meant that engineers could more easily design shells based on their optimal form. With time the shapes of shells has proven to be endless with new techniques of construction, materials and numerical simulations, see figure 1.3.

Since there are so many types and shapes of shells it can be convenient to categorize them into different families or branches. One can say that it is possible to derive the form of the shells based on three paradigms. [3]

- *Freeform, free-curved or sculptural shells* - These shells are generated without taking into account logic or structural action performance.
- *Mathematical, geometrical or analytical shells* - These shapes have been derived directly from mathematical expressions of surfaces, such as for instance the hyperparaboloid. The choice of these expressions can be based on parameters such as accurate geometrical analyses or sleek fabrication strategies.
- *Form Found shells* - These are shells that have their form described by structural performance. They can have been generated using one of the form finding techniques described in 1.3. One can say in general that the shape coincides with a state of static equilibrium.

1.3 Finding forms of equilibrium

The term form-finding usually refers to the process of finding a shape that is in static equilibrium under a certain design load. This usually applies to shapes of shells or membranes where an efficient geometry is hard to conceive using analytical derivation or reasoning. Linkwitz [3] expresses it as, *"As part of the conceptual design of structures, especially domes, shells and membrane structures, generating adequate structural shape is crucial to the load-bearing behaviour and aesthetic expression of design. Their shapes cannot be freely chosen and conceived directly, due to the intrinsic interaction between form and forces. For such a problem one needs form finding."*

Typical structures that require form finding include:

- soap films within a given boundary.
- prestressed, or hanging fabric membranes.
- prestressed, or hanging cable nets.
- compression structures like masonry and concrete shells.

Even though the shape cannot be chosen freely the designer has measures of controlling and influence the outcome. These are examples of different parameters chosen by the designer:[3]

- *Boundary Conditions*, which implies the supports and conditions at the edges.
- *External loads*, the type and magnitude of the load.
- *Topology and Geometry*, what is the initial condition of the geometry and how are the members connected.

- *Internal force distribution*, this controls how the forces are distributed and transferred between structural members.

There are different methods that applies to form-finding. In recent years with more powerful computers form-finding has almost been implying numerical methods using computers. The art of form finding though goes back in history, and the simplest method can be performed with a pencil and ruler. A way of categorizing them can be done in this way:

- *Graphical Methods*, this includes methods such as graphics statics where the interactions and amplitudes of forces in a structure can be drawn graphically. More in depth detail can be read in appendix A.6.1
- *Physical Methods*, this implies methods that resemble the structural behaviour through real physical objects. This can be done through hanging chains that inverts to a catenary or cloth that is pretensioned to simulate fabric structures. Further reading can be done in section A.6.3
- *Analytical Methods* derives the form based on the equilibrium equations for a specific structure and load-case. Assuming a type of loading and stress distribution it is possible to attain the form for such a specific case. In the case of shells, it might be very complicated and not always possible to find a solution. Read further regarding analytical methods in appendix A.6.2
- *Numerical Methods* uses the power of computing to solve large sets of equations or iteratively find solutions for nonlinear problems. This is probably the most common in modern days when trying to find equilibrium states of structures. This will be described more in detail in section 1.3.1

1.3.1 Numerical methods

Numerical methods have emerged with the possibility to solve large sets of equations quickly using computers. Rather than solving equations equilibrium analytically one can find solutions through iterations, which sometimes is easier but more computationally heavy. There are many examples of numerical methods of form-finding and they are usually spoke of as quite different, but they all share the same basic idea. A common recipe can be formulated for numerical form-finding methods [3]:

1. *Discretization of geometry*. This means that the initial geometry or form needs to be broken down into elements such as lines or surface elements.
2. *Connectivity of internal and external forces*, it is necessary to have a clear topology of how the members are connected and how the external loading and boundary conditions apply.
3. *Equilibrium conditions and equations*. The equilibrium conditions define how the internal and external forces and boundary relate to each other.
4. *A solver*, a method for how the equilibrium equations can be solved.

This template allows for big diversity if to design a form finding method. To give a bit of structure to this diversity one can describe different *form-finding families*[3].

1. *Stiffness Matrix Methods*, these are based on using standard elastic and geometric matrices. These have a strong connection to traditional structural analysis and *Finite Element Method (FEM)*.
2. *Geometric Stiffness Methods*, these are material independent where the equilibrium is achieved only with a geometrical stiffness. The most common and influential of these is the *Force Density Method (FDM)*, where the equilibrium equations are based on the ratio of element force to element length. Extensions have been done and different methods have been emerged such as the *Thrust Network Analysis (TNA)*.
3. *Dynamic Equilibrium Methods*, these methods have a dynamic based equilibrium condition, i.e. the second Law of Newton $\sum F = ma$ which is different compared to statics where the sum of forces always are equal to zero. Examples of these methods are *Dynamic Relaxation (DR)* and *Particle-Spring (PS)* systems. You can read further about DR in section 2.4.2. The figure 2.24 can give an idea of how a DR or PS can behave for a quadratic mesh fixed in the corners.

1.3.2 Development of form-found bricks shells

Prior to the nineteenth century the shapes of and proportions of masonry shells was based on experience and intuitive methods. Since they were unreinforced the bending capacity needed to be ensured by thicker vaults which resulted in over dimensioned structures that was not only heavy but also uneconomical[23]. Pure brick structures in general lacks tensile capacities which results in very low bending capacity. To make slender and efficient brick shells one must either have a form that ensures compression only stresses, i.e. no moments, or add bending capacity in terms of steel reinforcement.

Three important events in the development of form-found brick shells in modern time can be presented as:

1. *Implementation of graphic statics* - *Rafael Guastavino (1842 - 1908)* implements graphical form-finding methods in the design of brick shells. Enabling slender shells that are based on the thrust line ensuring compression stresses in the structure. This reinvention of the traditional vault made it into a contender with the new materials at the time, such as steel.[7]
2. *Reinforced brick vaults* - Breaking conventional form-play with his reinforced brick structures *Eladio Dieste (1917 - 2000)* created new categories of shapes and design not seen in this field, see right figure of 1.2. Reinforcement had been implemented previously by for instance the Guastavino company but in traditional vaults.
3. *Computational form-finding* - During the second half of the 20th century computational methods discovered new complex forms of equilibrium. Though few had been specially made for bricks and masonry. *Philippe Block(1980-)* develops the computational method of TNA that ensures compression only solutions and conducts a full scale testing at Swiss Federal Institute of Technology in Zurich (ETHZ), in 2011, proving new possibilities not seen previously, see figure 1.3.



Figure 1.2: To the left a staircase by the Guastavino company showing both structural and geometrical complexity achievable using brick vaults[7]. To the right the roof construction on *Cítricos Caputto fruit packing plant*, by Dieste [48].



Figure 1.3: A free-form compression shell that was developed and built by the Block Research Group at ETH in Zurich [43].

1.4 Geometry

The geometry of shells makes it necessary to use the theory and properties related to curves and surfaces in space. Form-found shells are efficient in the perspective of structural action but can be very complex to describe mathematically. In general complex forms means complicated tessellation. This chapter will describe why geometry and tessellation is difficult but also that you should not make things more complicated than you need to.

1.4.1 Mathematical mappings

Mathematical mappings has been an area of interest historically and is still very relevant. One might say that a mathematical map is a function that transfer geometry between different domains or surfaces. Examples of different types of mappings [1]:

- *Conformal mapping*, angles are preserved
- *Isometric mapping*, distances are preserved.
- *Equiareal mapping*, areas are preserved.

In architecture one usually wants to cover or represent different surfaces with a certain patterns or facade panels. Imagine that you have drawn a grid on a paper and you want to cover a cylinder with this grid, see figure 1.4. This works perfectly fine and you realise that this is an example of conformal, isometric and equiareal mapping. Doing the same test onto another simple form as the sphere you will run into trouble. One does notice that this exercise is impossible for many shapes without crumbling the paper or cutting parts away distorting and destroying the grid.

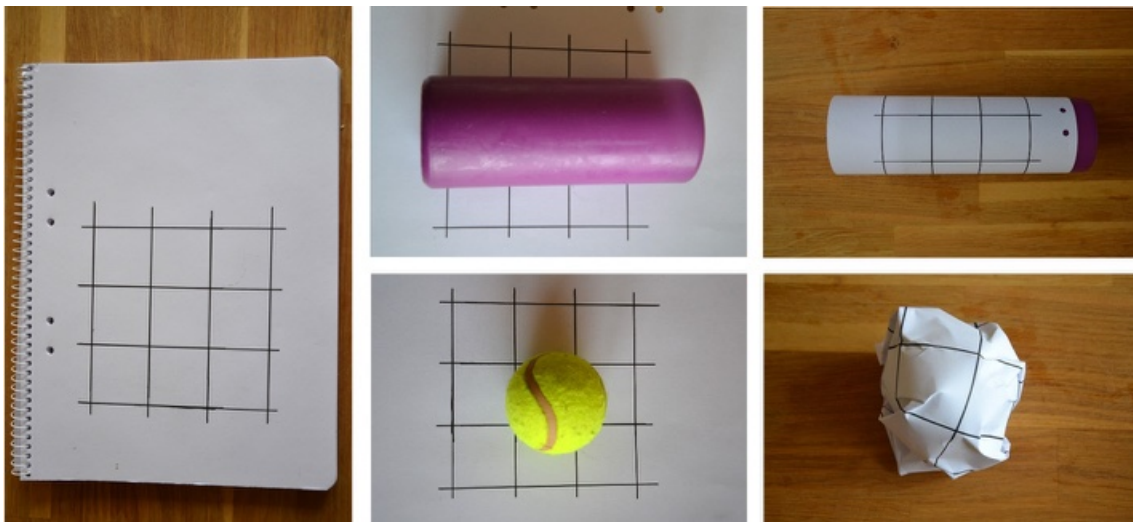


Figure 1.4: Draping a cylinder with a plane is very easy. Trying a similar procedure with a sphere it is proven impossible without modifications or crumbling of the paper.

To make a 2d representation of the earth one would have the inverse problem going from the sphere to the plane. To solve this *Gerardus Mercator* in 1569, made a so called *Mercator Projection*[37]. This is a conformal map that basically projects a sphere onto a cylinder that can be unrolled to a plane. This is of course not a perfect method since the projection becomes different depending on your distance to the equator, and the poles cannot even be projected, i.e the distances are not accurate. 550 years later this method is still used in applications such as *Google Maps*[32].

It is clear that Mercator projection has clear disadvantages but also has the advantage that the map does not contain any gaps or holes which a more accurate map would need. A more accurate map does not mean that you would have higher success finding your goal, probably the opposite in this case. This tells us that geometry is complicated but also that you do not have to solve all issues to still find it useful.

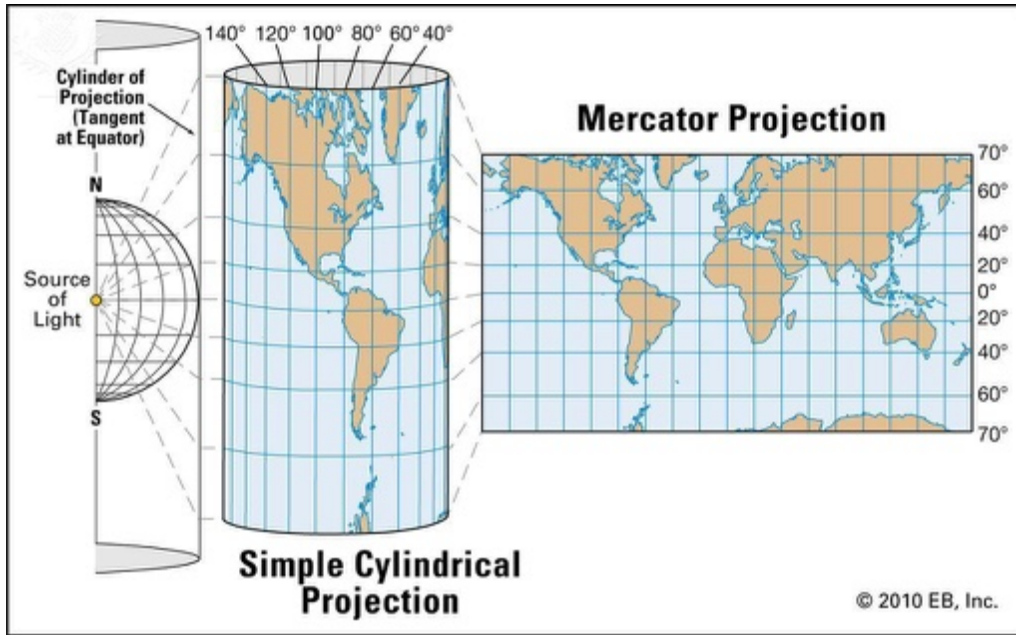


Figure 1.5: The Mercator projection, which maps the sphere coordinates onto a plane, invented 1569 by *Gerardus Mercator* is still used in modern applications such as Google Maps[32] to illustrate the coordinates of the earth onto a two dimensional map.[37]

1.4.2 Brick patterns on shells

In section 1.4.1 it became clear that geometry and tessellation might be complicated even for simple shapes. Though there are many built examples in history and illustrations of how to cover traditional vaults in old handbooks for bricklayers. There are some important aspects to think of regarding historical tessellation of brick shells.

1. The forms are often based on simple mathematical functions that are used in a repetitive manner in history.
2. The mortar makes it possible to compensate deviations and geometrical limitations, both globally and locally. This means that it allows some tolerance from the exact mathematical solution.
3. Brick layers does not mark every bricks position but rather the guidelines for each layer, i.e the direction and propagation of the brick joints, see figure 1.6.
4. Craftsmen and brick layers were in general much more skilled in this field compared to today.[31]

These bullet points and the fact that it is hard to find any theory regarding the derivation of these drawings could emphasize an empirical approach. An empirical approach is of course possible if working on similar types of geometries. Form-found shells that are dependent on project specific parameters can be unique from case to case in their global geometry which does not favor an empirical approach. There have been built form-found examples, see figure 1.3, and attempts to make theoretical strategies for generating brick patters. It is though hard to find much information upon success regarding the latter.[51]

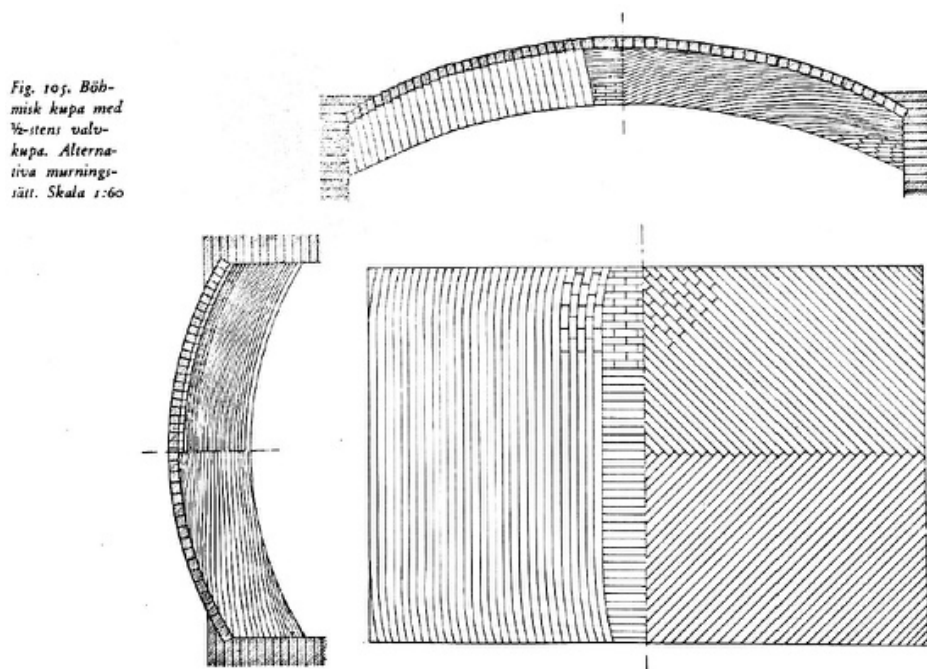


Figure 1.6: It is possible to find records of how to tessellate traditional vaults with bricks. This illustration shows the brick patterns and guidelines for a Cavetto vault, top, and a Saucer dome below [31]

1.5 Design processes in computational environments

Design processes of today involves the possibility of, or even demands, incorporating computers that enables numerical solving capabilities and high user interaction. Parametric design is relatively new concept in architecture that emerged during the late 20th century with raised level of computational power. One can say that parametric design is a design paradigm that allows describing your design abstraction, idea or concept through logic using measurable parameters. This means that you can fully or partially drive your design based on algorithmic thinking and performance parameters. *"Algorithmic thinking allows designers to rationalize, control, iterate, analyze and search for solutions in a defined solution space."* [21] Concepts of parametric design has been incorporated in graphical algorithm editors such as *Grasshopper3d*, *Dynamo* and *Generative Components*. It is therefore relatively easy these days to integrate for instance numerical methods of form-finding and tessellation strategies in an user friendly design environment.

1.5.1 Design scheme

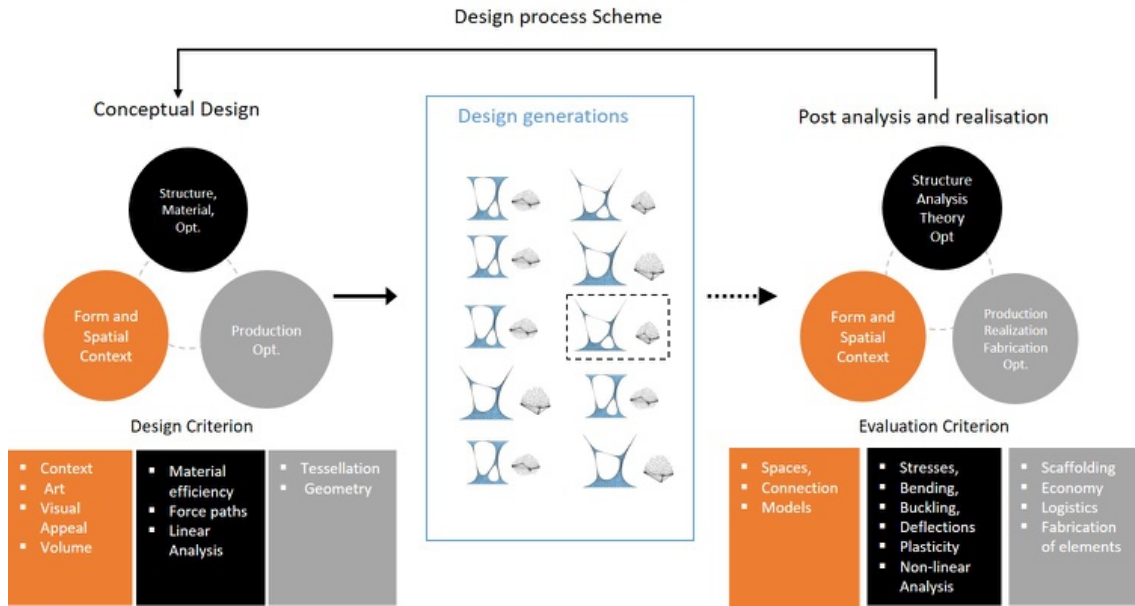


Figure 1.7: A possible parametric design process that will be used to adress the research in a design context.

A parametric design scheme might be structured in many different ways. In figure 1.7 is an example of a scheme to use in a design process made for this thesis. The main idea is to have a conceptual design phase and a post analysis design phase. These are based on three main categories; the categories could either be the same or different for the two stages. From the categories chosen design and evaluation criterion can be made to narrow the design solution space and rank different alternatives. Criterion can be based on both measurable or non-measurable metrics depending on category. In this example the categories are the same for both stages but the criterion goes from free and basic to advanced and refined. For instance, the structural optimization in the conceptual phase could assume axial forces and linear behaviour. In the realization stage bending and shear capacities are evaluated in a non-linear analysis. The best design can then be feed back and the design and evaluation criterion is evaluated and developed further based on previous design iteration. This process should be iterated until sufficient design is achieved.

1.6 Research task

From the contextual orientation in the subject it is possible to state some important findings:

1. Bricks are placed in layers following the bed joint and that deviance's can be handled by adjusting the mortar connecting the bricks.
2. Architectural drawings over brick tessellations describe the bed joints. This emphasizes that the most vital information is the position and propagation of the bed joint along the surface and not the position of each brick.

3. The global geometry of the shell is very influential on its behaviour.
4. Brick shells need internal compression stresses solutions if not reinforced.
5. Mercator proved that it might not be necessary for the solution to solve all aspects of a geometrical problem for it to be meaningful.

The contextual review of the subject of masonry shell structures has led to the following research question:

Is it possible to use polar geodesic coordinates as a means of achieving brick tessellation patterns of form-found shell structures?

1.6.1 Aim

The aim of this thesis is to combine craftsmanship, geometry, mechanics of shells and computational into a generic method of generating tiling patterns on form-found shells. The method should be possible to apply in an architectural design context.

1.6.2 Purpose

Through history until modern times the methods of tessellation and tiling of brick structures have been made mostly on empirical studies. Therefore, forms in history have been restricted to a few. Advances in theory, computational power and fabrication methods have extended the range and complexity of viable shapes. This means that the shells can be uniquely designed for each architectural project. Therefore, an empirical approach might not be applicable meaning theoretical methods are required. Until this day there have been few or none generic methods for this purpose.

1.6.3 Method

The research question will be put into a parametric design context where two parts will be separated out, *form finding*, which generates a global geometry to perform tessellation, and *tessellation* of brick patterns. The design scheme was chosen based on the figure 1.7 in previous chapter. This is illustrated in figure 1.8 which highlights the different parts focused on in the thesis.

Both parts should be implemented in the parametric environment *Grasshopper3d*, which is plug-in to the 3d modelling software *Rhinoceros3d*.

There are two parts in this:

1. Gain a theoretical ground to base a tessellation procedure on that connects geometry and fabrication.
2. Transform this to a computational method that can be implemented in a parametric framework.

This is done by using the knowledge gained in the literature review and going into depth to the areas of *Differential geometry*, *Structural design of masonry vaults*, *Mechanics of Shells* and *Computational methods*.

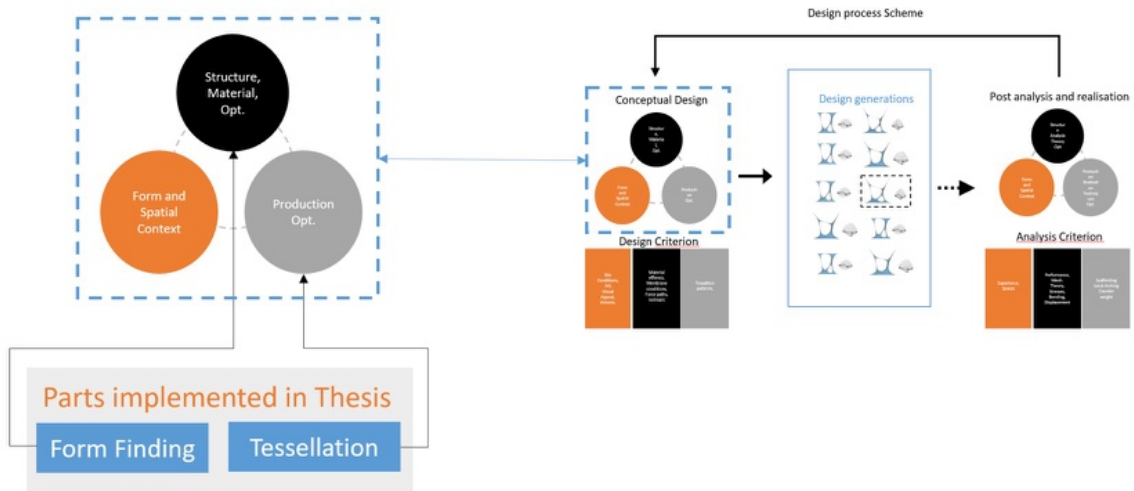


Figure 1.8: The thesis work will only concern a small portion of the whole design process. It will concern the tessellation and form generation in the initial conceptual phase.

1.6.4 Limitations

This report will only concern brick structures, meaning module blocks with the same dimensions, and no other types of masonry structures such as stone or concrete. The structural theory though applies to all masonry structures. The report will concern compressive brick shell structures and not conventional brick structures. Compression structures meaning in this case structures where the form ensures equilibrium in compressive axial forces and where reinforcement is not necessary in theory. The forms generated are of conceptual nature meaning that no detailed calculations or instability checks are made, such as buckling.

The implementations will be programmed in a parametric development environment, but no effort will be made to develop and evaluate different parametric design processes. The code will be implemented using the object-oriented language C#. The methods are though general and should be possible to implement using most languages.

2

Theory

This section will cover theory related to the research question. It will cover the following areas:

1. *Structural theory of masonry structures*. This section describes a plastic design approach for masonry structures.
2. *Differential geometry*, the theory of curves and surfaces necessary for understanding polar geodesic coordinates.
3. *Membrane theory of shells*, this section describes general theory of membrane shells in curvilinear coordinates of free-form shells. It can be seen as a explanatory compliment to theory described by Green and Zerna[26].
4. *Numerical solvers*. This section describes the algorithms for the numerical solvers that will be used for the form-finding and geodesic generation onto the form-found surface.

2.1 Structural theory of masonry structures

Masonry is a composition or assemblage of building elements. The most common types of these elements are stones and bricks. It can though be in any shape it can be done with or without mortar but the structural action is similar. According to Heyman [8] it is wise to and convenient to regard a masonry building as a collection of dry stones or bricks that are placed on one another to to form a stable structure. The mortar cannot be accounted since it may have reduced its structural influence with time - it cannot be assumed to add strength to the construction. The stability of the structure relies on the compaction under the gravity of its components. "*A general state of compressive stress exists, but only feeble tensions can be resisted.*"[8]

2.1.1 Structural design

Heyman [8] uses a masonry arch to illustrate this as in figure 2.1. The load applied on the arch is its self-weight and an external point load. The stresses are low and the deflection negligible until a certain magnitude of the point load is reached and it collapses. The stresses are still low in the structure but the internal forces cannot be held inside the geometry of the arch. This leads to the formation of four frictionless hinges that turns the structure into a collapse mechanism.

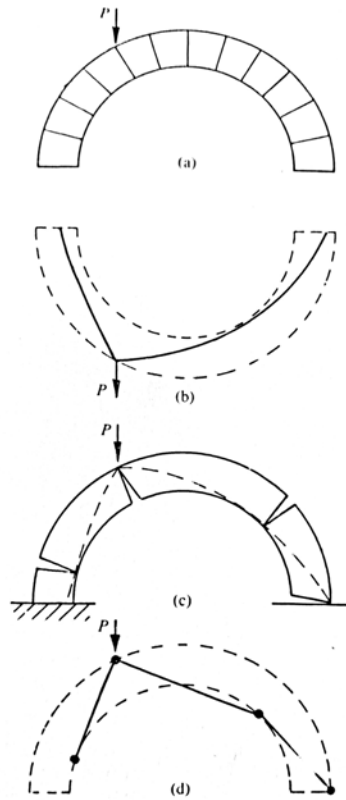


Figure 2.1: Collapse mechanism of masonry vault by an asymmetric load. The vault cannot contain the line of thrust within its geometry. This leads to the formation of plastic hinges at those locations where the line of thrust exceeds or hits the boundaries. This is not a problem until a sufficient number of hinges are formed to make the structure collapse[8].

Heyman [8] imposes a method based on plastic analysis for the structural design of masonry rather than the elastic analysis. One reason is that an elastic solution might not be possible, an arch consisting of rigid blocks will not deform themselves and will therefore not obey the rules of elastic analysis. Another reason is that there are uncertainties regarding the structure and how the boundary conditions change with time. Therefore, an elastic analysis might change dramatically with time. The so-called plastic designer accepts that there are infinite ways to achieve equilibrium and that the solution he has found is just one of them. The plastic designer takes this into account and applies the theorems of plasticity to ensure that the structure will not fail. Two common plasticity theorems are:

- *The lower bound, or safe theorem*
- *The upper bound, or unsafe theorem*

Heyman[8] suggest the lower bound approach in what he calls the "master safe theorem". Even though masonry structures do not follow elastic analysis principles one can still apply elastic equilibrium solutions in plastic design. If one finds an elastic solution for the structure with respect to the structural criterion the structure should stand. This means that one can find more or less efficient solutions leading to

more or less slender structures, but all will stand, i.e on the safe side. For masonry structures this criteria is as stated when the internal forces can be contained within the geometrical boundaries of the structure. As long as the settlements are within margin the safe theorem ensures that future cracks formed should not endanger the collapse of the structure. Cracks can be considered as a natural behaviour and since the geometry bears little change the internal forces should still be contained. For large complex structures it can be hard to evaluate the difference between dangerous, as in figure 2.1, and natural cracking. Figure 2.2 illustrates some typical cracks in a Gothic vault that can be difficult to judge for the inexperienced engineer.

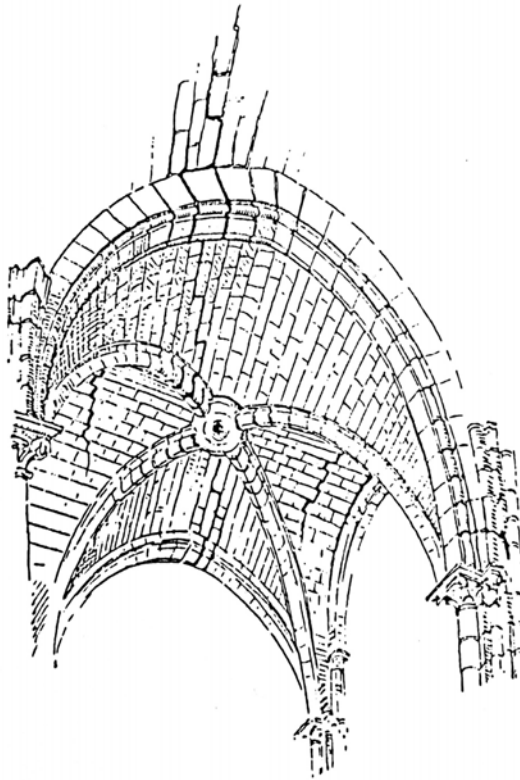


Figure 2.2: Typical cracks in Gothic vaults. *"Pol Abraham(1934) distinguished between the 'hinging' cracks near the crown, the 'Sabouret' cracks parallel to the wall ribs and the separation of the vault from the walls."* [8]

2.1.2 Limit design principles

The limit design principles Heyman purposes for masonry is similar to those used for plastic design of steel frames. This implies that hinges formed causes the structure to become a mechanism. To be able to apply the same theory and theorems for masonry structures Heyman makes three assumptions for the properties of the material:[14]

1. *Stone has no tensile strength.*
2. *The general stress levels are so low that, for the purposes of calculation, the compressive strength of stone is effectively infinite.*

3. *Sliding of one stone upon another cannot occur.*

The hinges are formed when, as shown in figure 2.1, the line of thrust cannot contain itself inside the geometry. A thrust that follows the center line of the structure results in pure axial forces, and when moving outside it results in a minor moment that until a certain point that will be negligible due to the compression of the self-weight.

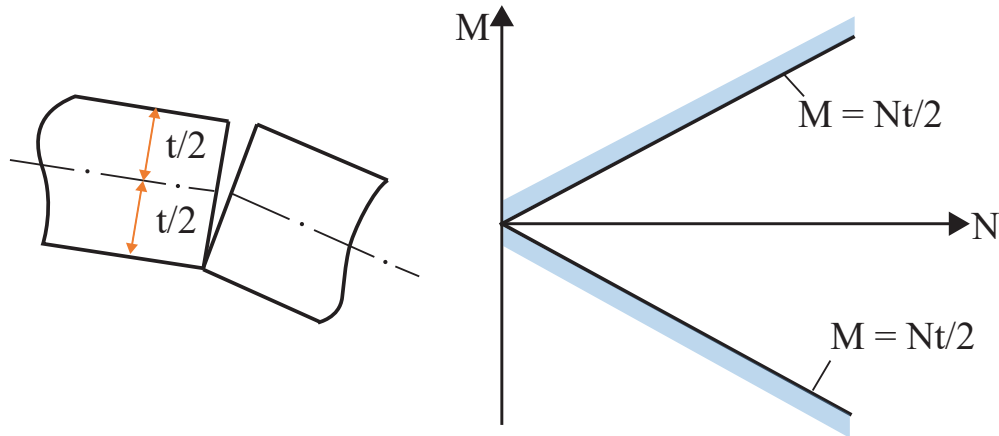


Figure 2.3: The theoretical limit condition for masonry voussoirs. If the position of the compressive axial force is placed a distance $t/2$ from the center a hinge will be formed. This represents a block of infinite stress capacity since a normal stone or brick would crush when the contact area gets too small. Therefore, there are some safety factors that need to be applied, see figure 2.4. [14]

This represents a block of infinite stress capacity since a normal stone or brick would crush when the contact area gets too small. Therefore, there are some safety factors that need to be applied.

2.1.2.1 Safety factor

As stated previously in section 2.1.2 a masonry structure is assumed to have zero tensile capacity. Therefore one seeks a structural solution where the line of thrust lies in the center line of the cross section, which implies an ideal uni-formal compression stress distribution along the cross section. The important aspect is though that there should be no tensile stress distribution over the cross section. A rule that can be applied to ensure no tensile stress is that the resultant force should be within the middle third of the cross section, see figure 2.4. Going outside the middle third one will get a part of the cross section with a tensile force component and the risk of forming plastic hinges.

2.2 Differential geometry

This section will handle definitions and description of the properties of curves and surfaces. This will be based on classical differential geometry which implies continuous and smooth curves and surfaces. This means that we assume that the surfaces

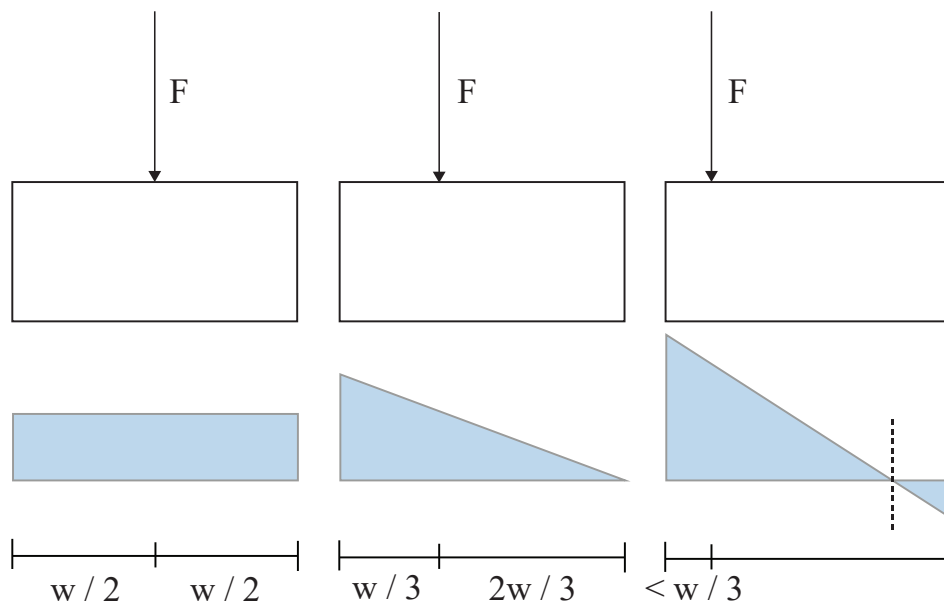


Figure 2.4: The middle third rule applied to a block, if going axial force is less than $1/3$ from the edge it will result in tension which will cause possible hinges, redrawn from [3]

and curves are differentiable and that there exists normals and tangents in each point.

This section will cover the most essential parts related to the research task and method. Further reading for some of the concepts can be found in appendix A.2.

2.2.1 Curves in space

There are many examples of Curves and most of you have used various of them. Common examples might be a line, a parabola or a circle, see figure 2.5.

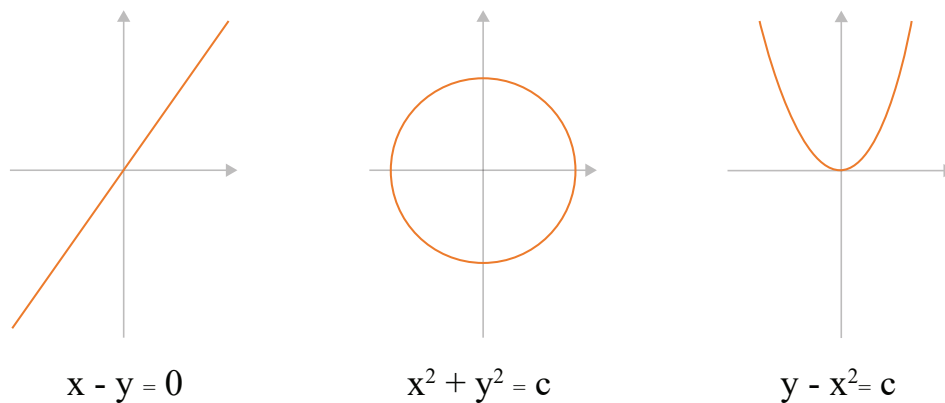


Figure 2.5: Example of curves in Cartesian coordinates, redrawn from [5]

Using the notation in figure 2.5 means that you describe them in a Cartesian equation $f(x, y) = c$, where f is a function of x and y and c is a constant. From this point of view we see a curve as a set of points namely [5]

$$\mathcal{C} = \{(x, y) \in \mathbb{R}^2 \mid f(x, y) = c\}$$

It is sometimes more efficient to describe curves in another way, as parametrized curves. Where the curve is described by a vector \mathbf{c} of a scalar parameter t (in \mathbb{R}^2 for a plane curve, in \mathbb{R}^3 for a curve in space), see figure 2.6 .

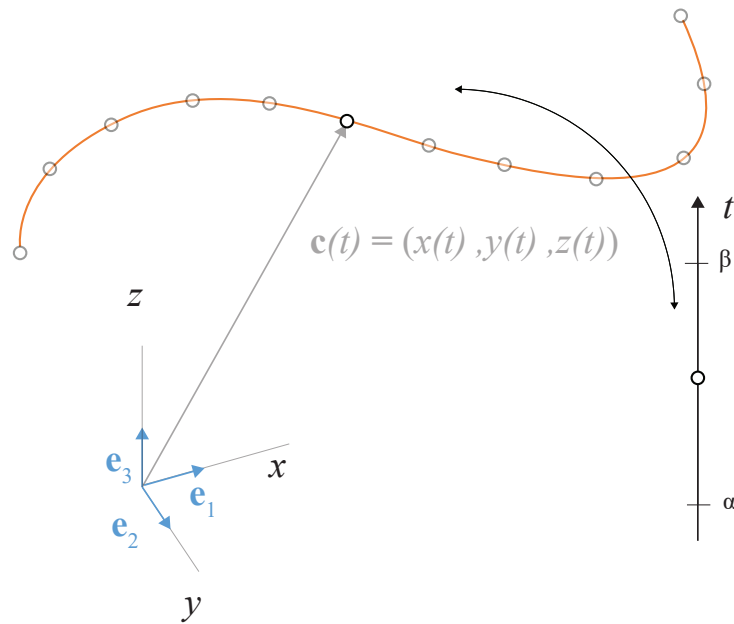


Figure 2.6: A parametrized curve is constructed by a locus of points in space based on a coordinate vector. To the right one can see how the position of the curve is related to a one-dimensional parameter.

Stoker[24] describes a *regular* curve as the locus defined by a vector

$$\mathbf{c}(t) = x(t)\mathbf{e}_1 + y(t)\mathbf{e}_2 + z(t)\mathbf{e}_3, \quad \alpha \leq t \leq \beta \quad (2.1)$$

such that the functions $x(t), y(t), z(t)$ have continuous second or third derivatives, in the interval of α and β , and such that the derivative of $\mathbf{c}(t)$ with respect to t is not zero.

$$\frac{\mathbf{c}(t)}{dt} = \mathbf{c}'(t) = (x'(t), y'(t), z'(t)) \neq 0 \quad (2.2)$$

The locus means that a set of points are related and governed by a set of equations or rules, in this case the rules of the curve. The latter statement ensures that the mapping of t into the space of (x, y, z) is one-to-one. When we speak of curves later on we impose that they are regular curves.

To give an example when this is useful we can take the circle which can be described as $x^2 + y^2 = 1$. A common choice to parametrize is to choose $x = \cos(t)$ and $y = \sin(t)$ which clearly holds the initial statement $\cos(t)^2 + \sin(t)^2 = 1$.

Written in parametric form $\gamma(t) = (\cos(t), \sin(t))$. A useful property of this parametrization is that we can differentiate this expression infinitely many times. This is very useful when computing the properties of the curve, which will be obvious in the section 2.2.1.2.

2.2.1.1 Geometry of the space curve

If we have a curve $c(t)$, where the parameter t is not necessarily an unit speed parametrization, it is possible to express the curve in what is called an arch length parametrization. The arch length of the curve is defined by the integral

$$s(t) = \int_{t_0}^{t_1} \sqrt{\frac{dc}{dt} \cdot \frac{dc}{dt}} dt \quad (2.3)$$

With an arch length parametrization, we ensure that the tangent of the curve is a unit speed vector, which can be quite convenient. Evaluating a curve in a point, we define a tangent, \mathbf{t} , a principal normal, \mathbf{n} , and a binormal vector, \mathbf{b} , of the curve, see figure 2.7. The tangent and principal normal vector lies in what is called the osculating plane.

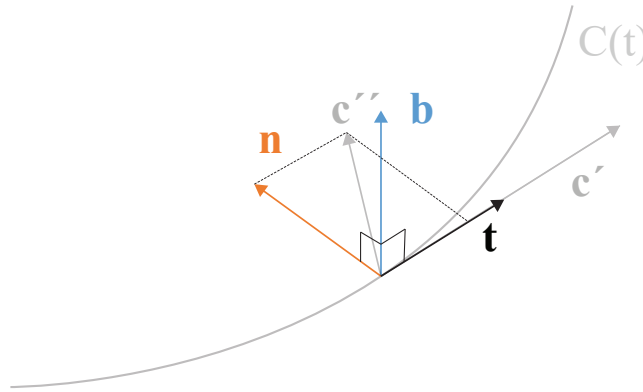


Figure 2.7: The geometry of the curve with its tangent, \mathbf{t} , principal normal \mathbf{n} and binormal \mathbf{b} vectors, redrawn from [5]

If we have a unit speed curve with s as arch length parameter we have the tangent defined as

$$\mathbf{t} = \frac{dc}{ds}, \quad \mathbf{t} \cdot \mathbf{t} = 1 \quad (2.4)$$

Note that dc/dt is also a tangent but not necessarily a unit vector. The principal vector, \mathbf{n} , is defined as following if we still assume s as our arch length parameter.

$$\mathbf{n} = \frac{1}{\kappa} \frac{d\mathbf{t}}{ds} \quad (2.5)$$

Where κ is the curvature in that specific point of the curve. It is easy to get the binormal vector \mathbf{b} due to the following relations between the vectors.

$$\mathbf{b} = \mathbf{t} \times \mathbf{n}, \quad \mathbf{n} = \mathbf{b} \times \mathbf{t}, \quad \mathbf{t} = \mathbf{n} \times \mathbf{b} \quad (2.6)$$

2.2.1.2 Curvature and Torsion

Curvature can be seen as a measure of how much a curve deviates from a straight line [2], or as Struik [1] defines it as a measure of the rate of change of the tangent moving along the curve. *Torsion* can be seen as a measure of the rate of change of the osculating plane.

The definition of curvature, κ , for regular curves $\mathbf{c}(t)$, can be expressed as [1].

$$\kappa = \frac{\|d^2\mathbf{c}/dt^2 \times d\mathbf{c}/dt\|}{\|d\mathbf{c}/dt\|^3} \quad (2.7)$$

For arch length parameter curves it is a bit more convenient and κ can be defined as

$$\kappa = \|d^2\mathbf{c}/ds^2\| \quad (2.8)$$

A similar definition can be made for torsion, τ , as for the curvature for a regular curve with an arbitrary parameter t .

$$\tau = \frac{d^3\mathbf{c}/dt^3 \cdot (d\mathbf{c}/dt \times d^2\mathbf{c}/dt^2)}{\|d\mathbf{c}/dt \times d^2\mathbf{c}/dt^2\|^2} \quad (2.9)$$

It is possible to read the applied properties of the curve in vector form using the *Frenet - Serret equations*, which implies.

$$d\mathbf{t}/ds = \kappa\mathbf{n} \quad (2.10)$$

$$d\mathbf{n}/ds = -\kappa\mathbf{t} + \tau\mathbf{b} \quad (2.11)$$

$$d\mathbf{b}/ds = \tau\mathbf{n} \quad (2.12)$$

2.2.2 Surfaces

Surfaces in three-dimensional space are two dimensional objects, meaning that we can describe them in a two dimensional domain using two parameters, it can be u, v or θ^1, θ^2 . Surfaces range from quite simple, as the plane, to very complex such as fractals. In mathematics it is quite uncommon to handle surfaces that are possible to parametrize as whole, like the sphere or the cylinder. More common is that only a part, or patch, is parametrized[24]. In figure 2.8 are two physical examples of surfaces in space, a "Monkey Saddle"- surface and a Hyperbolic paraboloid.



Figure 2.8: Two examples of surfaces made of ribbed wood structures. To the left is a "Monkey saddle"- surface described in Cartesian coordinates $z = x^3 - 3xy^2$, to the right a Hyperbolic paraboloid $z = (y^2)/(b^2) - (x^2)/(a^2)$

A proper mathematical definition of regular surfaces can be found in most books of concerning differential geometry. One of the most comprehensible for non-mathematicians is made by Stoker[24].

A *regular surface* is defined as follows.

1. A surface is a locus of points in the Euclidean three-space defined by the end points of a vector $\mathbf{r} = \mathbf{r}(\theta^1, \theta^2)$, depending on two real parameters θ^1 and θ^2 , see figure 2.9.

$$\mathbf{r}(\theta^1, \theta^2) = x_1(\theta^1, \theta^2)\mathbf{e}_1 + x_2(\theta^1, \theta^2)\mathbf{e}_2 + x_3(\theta^1, \theta^2)\mathbf{e}_3 \quad (2.13)$$

with $x_i(\theta^1, \theta^2)$ being the components of the vector. These real functions are assumed to be defined over an open connected domain of a Cartesian θ^1, θ^2 - plane and to have continuous fourth partial derivatives.

2. The vectors $\mathbf{r}_{,\alpha} = \partial\mathbf{r}/\partial\theta^\alpha$, to be called coordinate vectors, or covariant base vectors, are assumed to be linearly independent:

$$\frac{\partial\mathbf{r}}{\partial\theta^1} \times \frac{\partial\mathbf{r}}{\partial\theta^2} \neq 0 \quad (2.14)$$

To give an example of how to parametrize a surface one can take the sphere. A sphere can be described in Cartesian coordinates as:

$$x^2 + y^2 + z^2 = R^2 \quad (2.15)$$

where R is the radius. Writing this example in the general form we get:

$$x_1 = R \cos(\theta^1) \sin(\theta^2), \quad x_2 = R \sin(\theta^1) \cos(\theta^2), \quad x_3 = R \sin(\theta^2) \quad (2.16)$$

In the coming sections surfaces are described using parametric form.

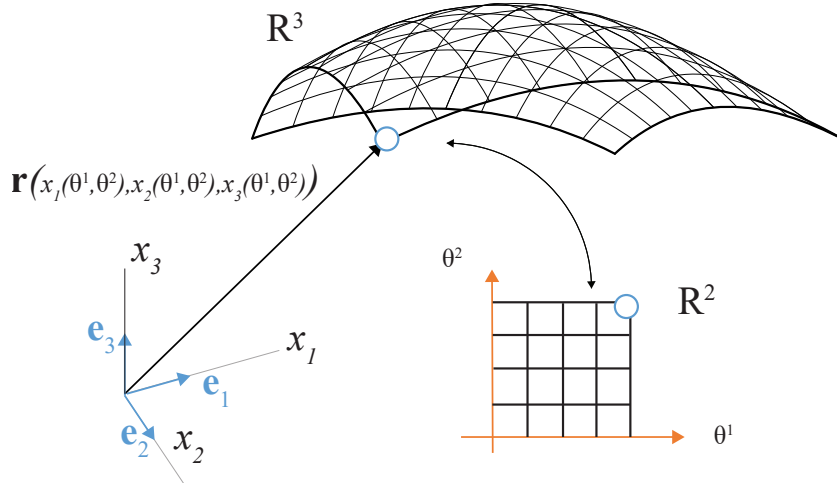


Figure 2.9: Parametrizes surface in three dimensional space \mathbb{R}^3 , is described using a position vector which is $\mathbf{r}(\theta^1, \theta^2)$ and how it relates to the parametrization in \mathbb{R}^2 .

2.2.2.1 Geometry on a surface

To orientate on the surface one can see the surface having a mapped set of curves, like a net. These are what is called coordinate curves and are the curves that are generated when parameter θ^1 has a constant value and θ^2 is allowed to vary, and vice versa, see figure 2.10.

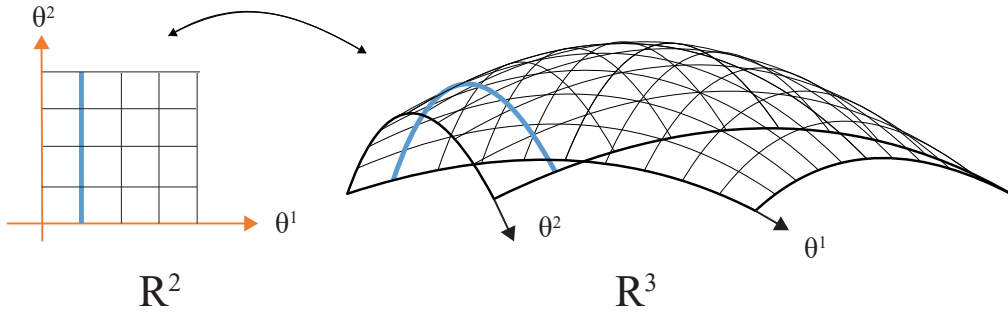


Figure 2.10: The coordinate curves are straight lines in domain \mathbb{R}^2 that forms the curved net on the surface in \mathbb{R}^3 .

This type of orientation along these curves on the surface is called curvilinear coordinates. The orientation of these curves can be chosen after convenience by changing the parameters of the position vector, \mathbf{r} , to say $\bar{\theta}^1$ and $\bar{\theta}^2$, defined as

$$\bar{\theta}^1 = \phi(\theta^1, \theta^2), \quad \bar{\theta}^2 = \phi(\theta^1, \theta^2) \quad (2.17)$$

A commonly used type of curve linear coordinates are for instance geodesic coordinates which is described in detail in section 2.2.2.4.

To describe properties of the geometry on the surface one can use two pair of base vectors, covariant and contravariant base vectors, as in [26], see figure 2.11. The

covariant basis vectors, \mathbf{a}_α , are the tangent vectors of the curve linear curves on the surface and they are defined as:

$$\mathbf{a}_\alpha = \frac{\partial \mathbf{r}}{\partial \theta^\alpha} = \frac{\partial x}{\partial \theta^\alpha} \mathbf{e}_1 + \frac{\partial y}{\partial \theta^\alpha} \mathbf{e}_2 + \frac{\partial z}{\partial \theta^\alpha} \mathbf{e}_3 = \mathbf{r}_{,\alpha}, \text{ for } \alpha = 1, 2 \quad (2.18)$$

The covariant base vectors are rarely orthogonal to each other, but are however always orthogonal to the normal of the surface and therefore lies in the tangent plane of the surface. The contravariant basis vectors, \mathbf{a}^α , also lies in the tangent plane of the surface and are defined through the covariant basis vectors[3]. This is described in equation 2.19 and illustrated in figure 2.11.

$$\mathbf{a}_\alpha \cdot \mathbf{a}^\beta = \delta_\alpha^\beta \quad (2.19)$$

$$\mathbf{a}_\alpha \cdot \mathbf{a}^3 = 0 \quad (2.20)$$

Where δ_α^β is the *Kronecker delta* and has the properties $\delta_\alpha^\beta = 0$ if $\alpha \neq \beta$ and $\delta_\alpha^\beta = 1$ if $\alpha = \beta$.

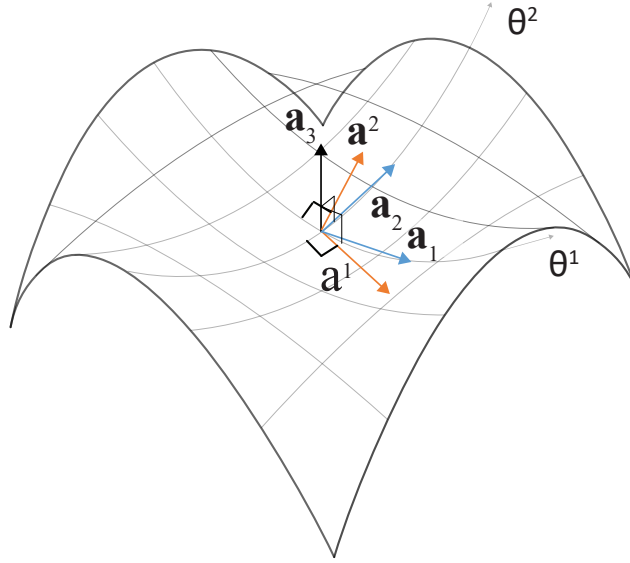


Figure 2.11: basis vectors of a surface described using curvilinear coordinates. \mathbf{a}_1 and \mathbf{a}_2 are the covariant basis vectors which are the tangent to coordinate curves. \mathbf{a}^1 and \mathbf{a}^2 are the contravariant basis vectors and can be described in equation 2.19 above.

The use of the two sets of basis vectors can be illustrated by this example [3]. By specifying a vector \mathbf{p} it can be written in both contravariant and covariant basis vectors. And depending on the situation one might use one or the other or a combination.

$$\mathbf{p} = p_x \mathbf{e}_1 + p_y \mathbf{e}_2 + p_z \mathbf{e}_3 \quad (2.21)$$

$$\mathbf{p} = p^\alpha \mathbf{a}_\alpha + p\mathbf{a}^3 = p^1 \mathbf{a}_1 + p^2 \mathbf{a}_2 + p\mathbf{a}^3 \quad (2.22)$$

$$\mathbf{p} = p_\alpha \mathbf{a}^\alpha + p\mathbf{a}^3 = p_1 \mathbf{a}^1 + p_2 \mathbf{a}^2 + p\mathbf{a}^3 \quad (2.23)$$

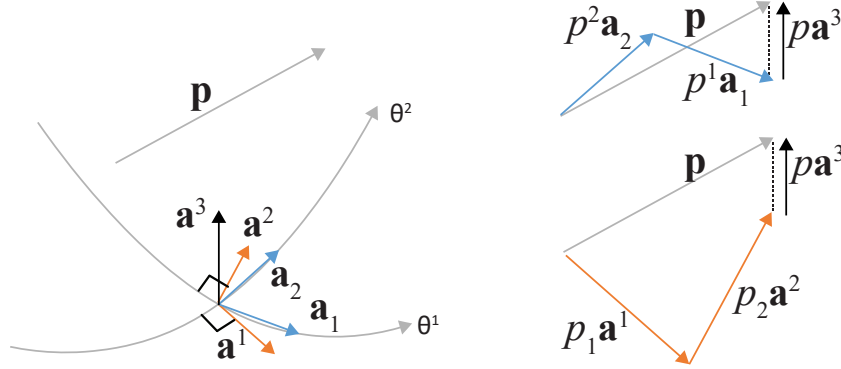


Figure 2.12: A vector \mathbf{p} can be constructed using either covariant or contravariant basis vectors.

The properties such as length and curvature can be described using the basis vectors. The length of a line element of ds can be described using Pythagoras:

$$ds^2 = \mathbf{dr} \cdot \mathbf{dr} = a_{\alpha\beta} d\theta^\alpha d\theta^\beta = a^{\alpha\beta} d\theta_\alpha d\theta_\beta \quad (2.24)$$

Equation 2.24 is what is called the *First fundamental Form* [26] and describes distances on the surface. $a_{\alpha\beta}$ are the components of the metric tensors and can be defined as:

$$a_{\alpha\beta} = \mathbf{a}_\alpha \cdot \mathbf{a}_\beta = \begin{bmatrix} a_{11} & a_{12} \\ a_{21} & a_{22} \end{bmatrix} \quad (2.25)$$

$$a^{\alpha\beta} = \mathbf{a}^\alpha \cdot \mathbf{a}^\beta = \begin{bmatrix} a^{11} & a^{12} \\ a^{21} & a^{22} \end{bmatrix} \quad (2.26)$$

The quantity a can be seen as the determinant of the covariant metric tensor.

$$a = a_{11}a_{22} - a_{12}^2 \quad (2.27)$$

To measure the curvature of the surface, which refer to what is called the *Second fundamental Form*, the following definition is used:

$$- \mathbf{dr} \cdot d\mathbf{a}_3 = b_{11}(d\theta^1)^2 + 2b_{12}d\theta^1 d\theta^2 + b_{22}(d\theta^2)^2 \quad (2.28)$$

$$b_{\alpha\beta} = \mathbf{a}_3 \cdot \mathbf{a}_{\alpha,\beta} = \begin{bmatrix} b_{11} & b_{12} \\ b_{21} & b_{22} \end{bmatrix} \quad (2.29)$$

Read more about the First and Second fundamental form in appendix A.2.1 and A.2.2.

2.2.2.2 Geodesics

The most common description of a geodesic curve is that it follows the shortest path between two points on a surface. More interesting might be to think of the experience of moving along a geodesic on the surface. Presley [5] describes it as even though the curve does not in fact look straight the notion is that we are progressing in a straight direction, i.e we do not need to turn to keep ourselves on the curve.

To visualize this on a physical surface one can mount a straight paper strip upon the surface, without wrinkling the paper. *A straight piece of paper laid over a smooth surface will follow a geodesic on the surface*" [4]. This is visualised in the figures 2.13 where the ribbons are geodesics on the surface.

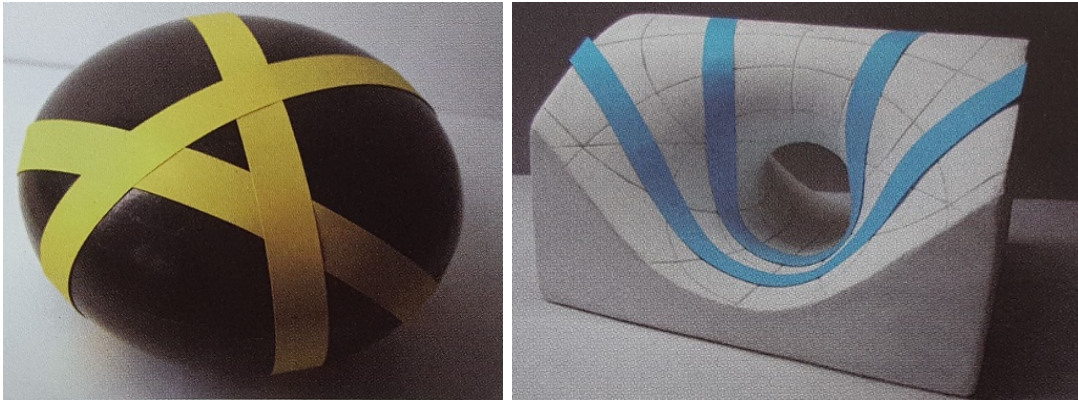


Figure 2.13: Straight ribbons laid out flat on a surface will follow the geodesics on that surface[4].

So you can think of a geodesic as a shortest path between A and B but you can also say that standing in A there is a geodesic in every direction. *"Through every point of the surface passes a geodesic in every direction. A geodesic is uniquely determined by an initial point and tangent at that point"*[1] This means that one can construct a geodesic by either specifying two points, i.e finding the shortest path, or by specifying the starting point and direction, see figure 2.14.

To describe geodesics in a more mathematical way you would say that the geodesic curvature is zero in every point on the curve.

2.2.2.3 Normal and geodesic curvature

Recall from section 2.2.1.2 the curvature is defined as $d\mathbf{t}/ds = \kappa\mathbf{n}$ for a unit speed curve. This is also true even if the curve lies on a surface. It is though possible to separate the curvature into two parts, *geodesic curvature*, κ_g , and *normal curvature*, κ_n , and refer it to the framework and properties of the surface. This gives a better understanding of how the curvature relates to the surface since the principal normal vector for space curves might be hard to anticipate. In figure 2.15 it is possible to get an idea of how the geodesic curvature and the normal curvature behaves on the surface.

$$\kappa\mathbf{n} = \kappa_n\mathbf{a}_3 + \kappa_g\mathbf{a}_3 \times \mathbf{t} \quad (2.30)$$

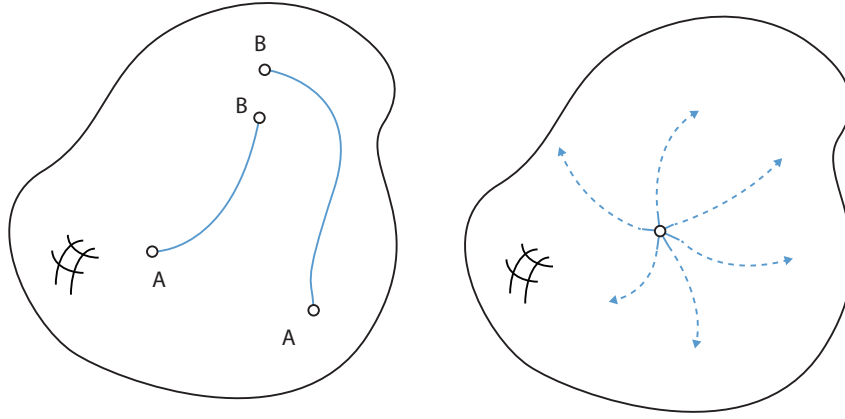


Figure 2.14: There are two possible boundary conditions when constructing a geodesic on a surface. Either one specifies two points and finds the geodesic between those, illustrated to the left, or one specify a starting point and direction and the geodesic is aloud propagates without restriction, illustrated to the right.

$$\kappa_n = d^2\mathbf{c}/ds^2 \cdot \mathbf{a}_3, \quad \kappa_g = d^2\mathbf{c}/ds^2 \cdot (\mathbf{a}_3 \times \mathbf{t}) \quad (2.31)$$

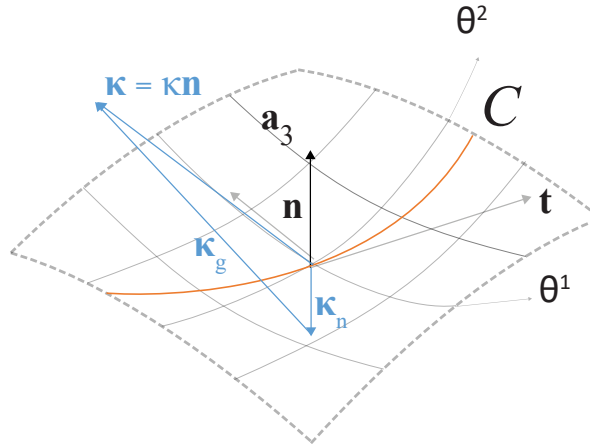


Figure 2.15: The curvature κ , for a curve $\mathbf{C}(t)$ that lies in the surface, can be divided into two separate parts κ_n , normal curvature, and κ_g which is the geodesic curvature.

One particular important case is when the geodesic curvature is zero and the curvature is only based on the normal curvature. Those curves that fulfills those requirements are called geodesics.

2.2.2.4 Geodesic coordinates

The geodesic coordinates are based on two different sets of coordinate curves that forms what is called a geodesic set. The first set of curves are geodesics and the

other set are curves that intersect the geodesics at a right angle, and is therefore called orthogonal trajectories to the geodesics. The parametric curves are chosen as $\theta^2 = \text{constant}$ and the orthogonal trajectories as $\theta^1 = \text{constant}$ [17], see figure 2.16.

Struik[1] states that *"Equation 2.32(in this thesis) is called the 'geodesic form' of the line element and (θ^1, θ^2) form a set of 'geodesic coordinates'; or, for short, 'geodesic set'. On every surface we can find an infinite number of geodesic sets, depending on an arbitrary curve C_0 , along which the curves $\theta^2 = \text{constant}$ can still be spaced in an arbitrary way."*

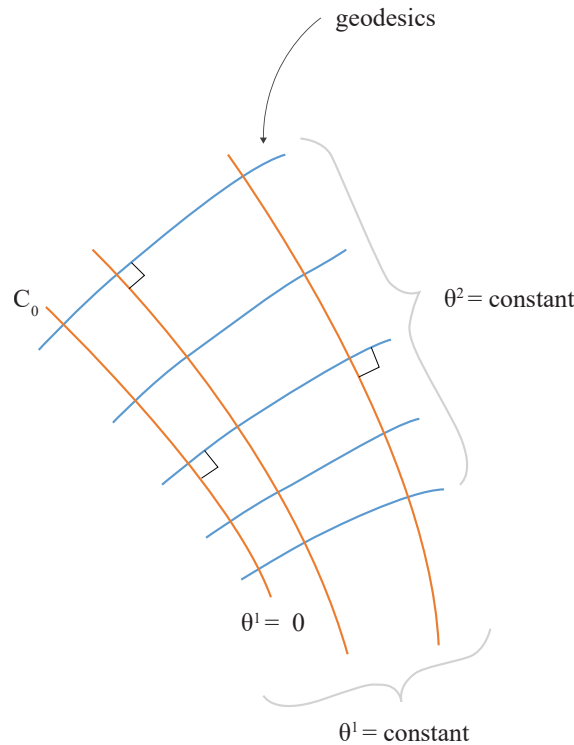


Figure 2.16: A Geodesic coordinate set which consists of two types of coordinate curves, geodesics and parallel trajectories to the geodesics. Notice the right angle in the intersection between the two types of curves. Redrawn picture from [1]

$$ds^2 = (d\theta^1)^2 + a_{22}(\theta^1, \theta^2)(d\theta^2)^2 \quad (2.32)$$

The geodesic form states that $a_{11} = 1$ and $a_{12} = a_{21} = 0$. This means that \mathbf{a}_1 and \mathbf{a}_2 are perpendicular everywhere on the surface since $\mathbf{a}_1 \cdot \mathbf{a}_2 = 0$. Struik[1] also states that the segments on all geodesics included between any two orthogonal trajectories are equal according to this theorem.

Theorem 1 *If geodesics be drawn orthogonal to a curve C , and segments of equal length be measured upon them from C , then the locus of their end points is an orthogonal trajectory of the geodesics.*

This means two things:

1. That the curve segment of the geodesics between orthogonal trajectories are of equal length.
2. If there exist one orthogonal trajectory too the geodesics, one can measure an equal segment length along the geodesics from the intersection to find the next orthogonal trajectory, see figure 2.17.

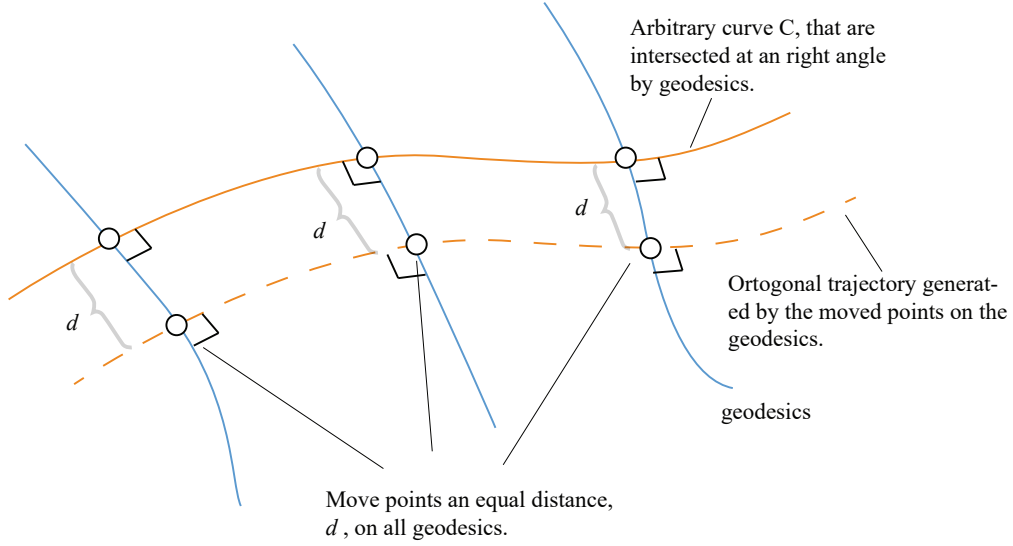


Figure 2.17: Interpretation of Theorem 1, of Struik [1], which states that if one parallel trajectory is found for a set of geodesics a parallel trajectory is found at an equal distance from the first parallel trajectory.

The proof of the geodesic form is done by both Stoker [24] and Williams [17] and can be done as following. Assume that \mathbf{a}_1 and \mathbf{a}_2 are orthogonal and that the distance a_{11} is constant.

$$\mathbf{a}_1 \cdot \mathbf{a}_2 = a_{21} = a_{12} = 0 \quad (2.33)$$

$$a_{11} = 1 = \text{constant} \quad (2.34)$$

Since a_{12} is zero the derivative of a_{12} should equally be zero.

$$\frac{\partial a_{12}}{\partial \theta^1} = \mathbf{a}_1 \cdot \mathbf{a}_{2,1} + \mathbf{a}_{1,1} \cdot \mathbf{a}_2 = 0 \quad (2.35)$$

Similarly the derivative of a_{11} should be zero.

$$\frac{\partial a_{11}}{\partial \theta^2} = \mathbf{a}_1 \cdot \mathbf{a}_{1,2} + \mathbf{a}_{1,2} \cdot \mathbf{a}_1 = 2\mathbf{a}_1 \cdot \mathbf{a}_{1,2} = 2\mathbf{a}_1 \cdot \mathbf{a}_{2,1} = 0 \quad (2.36)$$

Since $\mathbf{a}_1 \cdot \mathbf{a}_{2,1} = 0$ it means that also $\mathbf{a}_{1,1} \cdot \mathbf{a}_2 = 0$ from equation 2.35, hence the coordinate curve θ^1 is a geodesic.

A special case of geodesic coordinates is *Polar geodesic coordinates*. The polar geodesic set is based on that the geodesics has their starting point in a point O, see figure 2.18, the geodesics become a radial set of curves. The orthogonal trajectories become a set of curves in the angular direction that cuts the geodesics at a right angle.

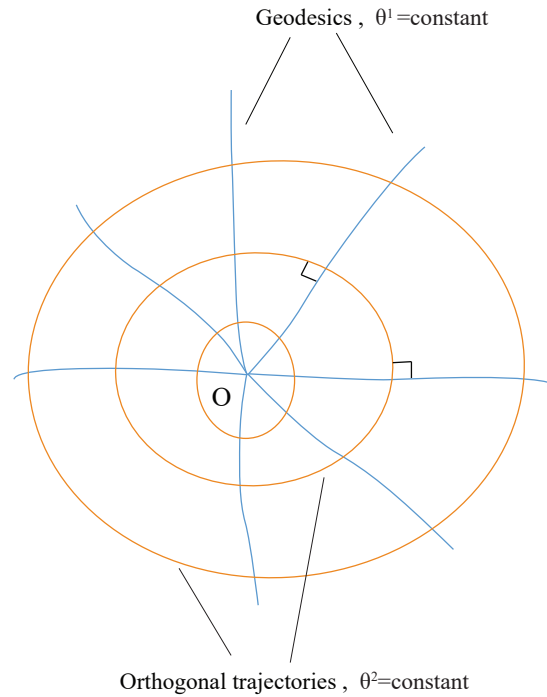


Figure 2.18: A polar geodesic coordinate set redrawn from [1]. The polar geodesic coordinates set possess the same properties as an arbitrary geodesic set, see figure 2.16, the difference is that the geodesics meet in a pole.

The properties of the geodesic coordinates makes it interesting and useful for brick structures, which became clear during a conversation with Williams [52]. The most important for brick patterns is that the height of the brick is made consistent everywhere, as proved above. This means that the orthogonal trajectories follows the bed joints and can be seen as the patterns for the brick courses of the brick structure, see figure 2.19.

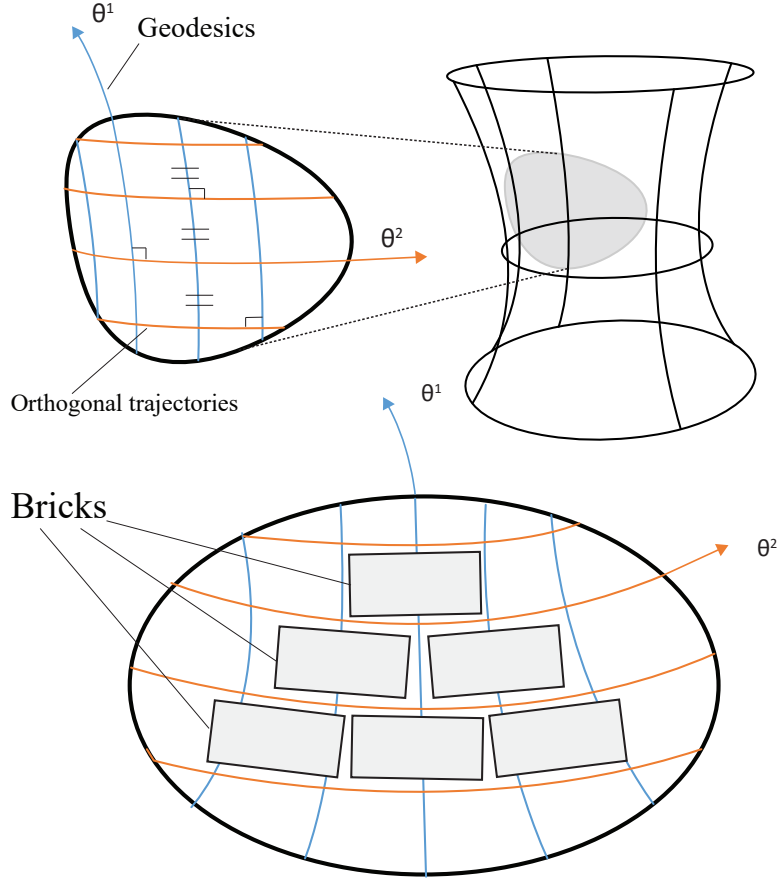


Figure 2.19: Since the length between two orthogonal trajectories bricks, assuming uniform height, might be placed between them. [52]

2.3 Membrane theory of shells

Shells, in which bending moments and thickness can be neglected are called membrane shells. In this section we will derive the equilibrium of free-form membrane elements using curvilinear coordinates. The geometry of the structure is assumed to be known, but no assumptions are made about constitutive or kinematic relations for the structure. There is an advantage to use curvilinear coordinates due to that the basis vectors changes along the surface. This means that the normal and shearing forces for each element always are in the direction of its basis vectors, see figure 2.20. Using for instance Cartesian coordinates of x, y and z might seem more natural but does become complicated for curved elements since it becomes dependent of direction cosines. The equations, notations and definitions are based on Green and Zerna [26] and Williams [20].

Figure 2.20 illustrates a part of membrane surface. It will be considered a small element with edges bounded by the lines $\theta^1, \theta^1 + d\theta^1, \theta^2$ and $\theta^2 + d\theta^2$, where $d\theta^1$ and $d\theta^2$ are considered small.

The membrane force \mathbf{N}_1 is expressed as:

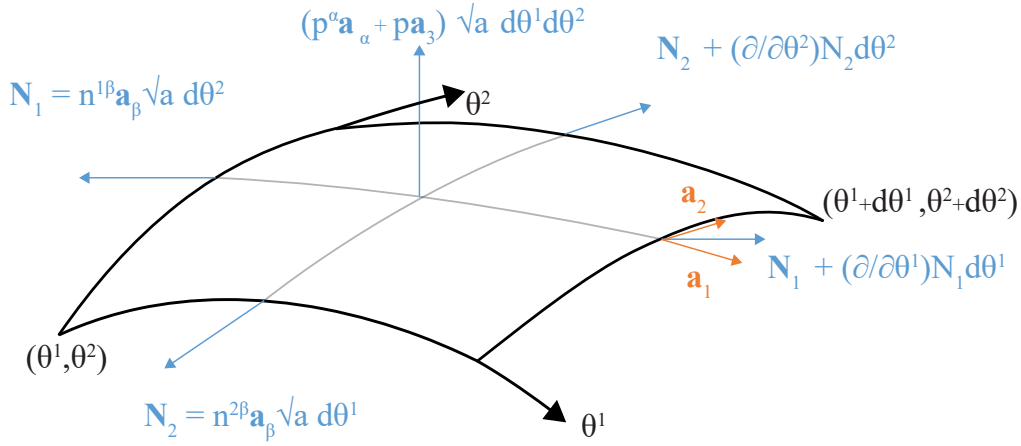


Figure 2.20: Equilibrium for a three dimensional membrane element in curvilinear coordinates.

$$\mathbf{N}_1 = (n^{11}\mathbf{a}_1 + n^{12}\mathbf{a}_2)\sqrt{a}d\theta^2 \quad (2.37)$$

Using Einstein summation convention, it can be reduced to.

$$\mathbf{N}_1 = (n^{1\beta}\mathbf{a}_\beta)\sqrt{a}d\theta^2 \quad (2.38)$$

Similarly for \mathbf{N}_2

$$\mathbf{N}_2 = (n^{2\beta}\mathbf{a}_\beta)\sqrt{a}d\theta^1 \quad (2.39)$$

The tensor, $n_{\alpha\beta}$, contains the surface stress tensor components of the membrane element.

$$n^{\alpha\beta} = \begin{bmatrix} n^{11} & n^{12} \\ n^{21} & n^{22} \end{bmatrix} \quad (2.40)$$

The shell is subjected to external loads denoted by \mathbf{p} and is measured per unit area of the middle surface. The loading is divided into two parts, one in the tangent plane of the the surface and the other in the direction of the normal, see figure 2.21.

$$\mathbf{p} = p^\alpha \mathbf{a}_\alpha + p \mathbf{a}_3 = p^1 \mathbf{a}_1 + p^2 \mathbf{a}_2 + p \mathbf{a}_3 \quad (2.41)$$

The membrane forces and loading can be gathered into the following expression for equilibrium of the membrane shell element:

$$\frac{\partial}{\partial \theta^1} (n^{1\beta} \mathbf{a}_\beta \sqrt{a}) d\theta^2 d\theta^1 + \frac{\partial}{\partial \theta^2} (n^{2\beta} \mathbf{a}_\beta \sqrt{a}) d\theta^1 d\theta^2 + (p^\alpha \mathbf{a}_\alpha + p \mathbf{a}_3) \sqrt{a} d\theta^1 d\theta^2 = 0 \quad (2.42)$$

This can be simplified further:

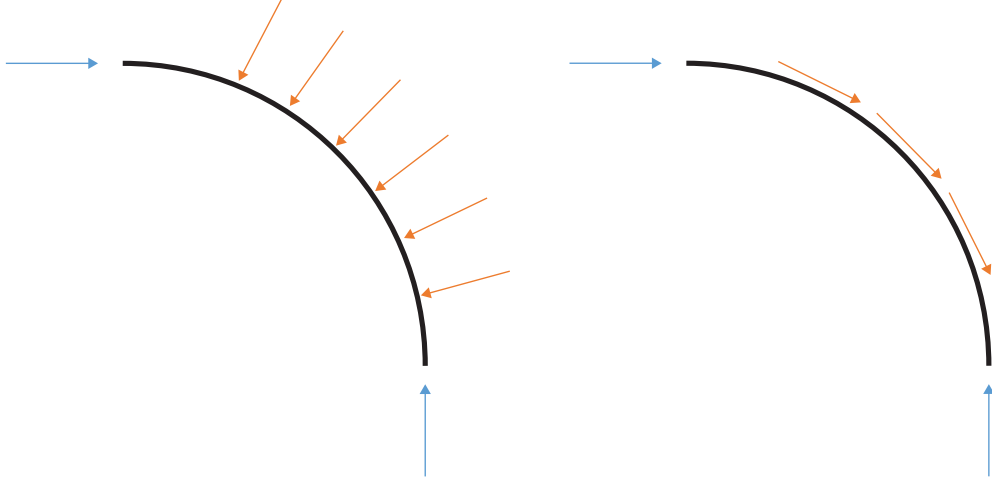


Figure 2.21: The two kinds of loading referring to loading in normal direction from equation 2.50, to the left, and the in plane loading from equation 2.49, to the right.

$$\therefore \frac{\partial}{\partial \theta^\alpha} (n^{\alpha\beta} \mathbf{a}_\beta \sqrt{a}) + (p^\alpha \mathbf{a}_\alpha + p \mathbf{a}_3) \sqrt{a} = 0 \quad (2.43)$$

Dividing 2.43 with \sqrt{a} and using the following condition of the Christoffel symbol $\Gamma_{\lambda\alpha}^\lambda = \frac{\sqrt{a_{,\alpha}}}{\sqrt{a}}$ we get the following expression:

$$n_{,\alpha}^{\alpha\beta} \mathbf{a}_\beta + n^{\alpha\beta} \mathbf{a}_{\beta,\alpha} + n^{\alpha\beta} \mathbf{a}_\beta \Gamma_{\lambda\alpha}^\lambda + (p^\beta \mathbf{a}_\beta + p \mathbf{a}_3) = 0 \quad (2.44)$$

The differentiation of the covariant basis vectors for surfaces is defined [26]

$$\frac{\partial \mathbf{a}_\beta}{\partial \theta^\alpha} = \Gamma_{\alpha\beta}^\lambda \mathbf{a}_\lambda + b_{\alpha\beta} \mathbf{a}_3 \quad (2.45)$$

Inserting 2.45 into 2.44

$$n_{,\alpha}^{\alpha\beta} \mathbf{a}_\beta + n^{\alpha\beta} (\Gamma_{\lambda\alpha}^\beta \mathbf{a}_\beta + b_{\lambda\alpha} \mathbf{a}_3) + n^{\alpha\beta} \mathbf{a}_\beta \Gamma_{\lambda\alpha}^\lambda + (p^\beta \mathbf{a}_\beta + p \mathbf{a}_3) = 0 \quad (2.46)$$

One can now separate equation 2.46 into the two parts, the first containing the basis vectors \mathbf{a}_β , where $\beta = 1, 2$.

$$(n_{,\alpha}^{\alpha\beta} + n^{\alpha\beta} \Gamma_{\lambda\alpha}^\beta + n^{\alpha\beta} \Gamma_{\lambda\alpha}^\lambda + p^\beta) \mathbf{a}_\beta = 0 \quad (2.47)$$

The second part is in the direction of the normal vector, \mathbf{a}_3 .

$$(n^{\alpha\beta} b_{\alpha\beta} + p) \mathbf{a}_3 = 0 \quad (2.48)$$

Equilibrium equations can then be simplified to the following form as in [26]:

$$n^{\alpha\beta} b_{\alpha\beta} + p = 0 \quad (2.49)$$

$$n^{\alpha\beta} |_\alpha + p^\beta = 0 \quad (2.50)$$

Where $n^{\alpha\beta} |_\alpha$ is the covariant differentiation.

$$n^{\alpha\beta}|_{\alpha} = n^{\alpha\beta}_{,a} + \Gamma^{\beta}_{\alpha\rho} n^{\alpha\rho} + \Gamma^{\alpha}_{\alpha\rho} n^{\rho\beta} \quad (2.51)$$

The two equilibrium equations represents the two loading situations in figure 2.21. Equation 2.50 is handling the loading in the plane of the surface(two directions), and equation 2.49 refers to the loading in the direction of the normal.

2.4 Numerical solvers and form finding

The main concepts of form finding and under what circumstances it can be used is described in section 1.3. This chapter will get into detail in how these equilibrium equations and the solving procedure.

2.4.1 Force density method(FDM)

A key concept in Force density method(FDM) is as the name states the "Force densities". The force density is the ratio, that can be defined or chosen, between the force in a bar and its length [3].

$$\text{Force Density, } q, = \frac{\text{Force in bar}}{\text{stressed length of bar}}$$

The FDM is a numerical solver placed under the branch of *Geometric Stiffness Methods*, as described in section 1.3. This means that the solution and internal forces can be derived through the geometry and chosen force densities without the need for material properties, kinematic assumptions or constitutive relations.

To understand the concept one can make an example, this is found more in detail in [3]. In figure 2.22 is a node attached to three bars. The node is also subjected to an external force, \mathbf{p}_i in node i .

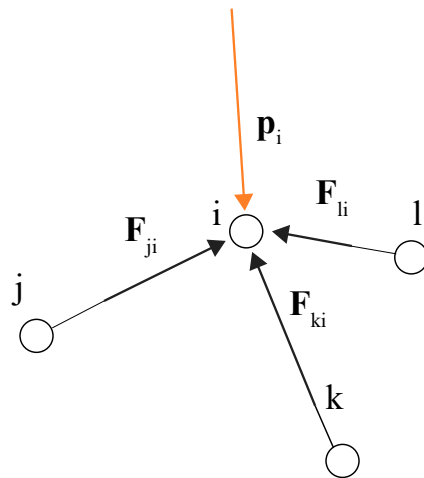


Figure 2.22: A node connected to three bars with load applied in the z-direction with labeled nodes and internal forces.

Equilibrium for node i in the x-direction can be described as follows,

$$\frac{(x_j - x_i)}{l_{ji}}F_{ji} + \frac{(x_k - x_i)}{l_{ki}}F_{ki} + \frac{(x_l - x_i)}{l_{li}}F_{li} + p_{xi} = 0 \quad (2.52)$$

F and l refers to the force and length quantity in each member. It is now possible to apply the definition of the force densities $q_{ji} = F_{ji}/l_{ji}$.

$$(x_j - x_i)q_{ji} + (x_k - x_i)q_{ki} + (x_l - x_i)q_{li} + p_{xi} = 0 \quad (2.53)$$

One can solve this by rewriting the equations in a matrix format and using matrix operations as done in [3]. The \mathbf{C} matrix describes the topology of the system. For the system above it should be a $[3 \times 4]$ matrix for the system above. The condition for the components are described below.

$$C_{ij} = \begin{cases} +1 & \text{if branch } j \text{ ends in node } i \\ -1 & \text{if branch } j \text{ begins in node } i \\ 0 & \text{otherwise} \end{cases} \quad (2.54)$$

The equilibrium equation 2.53 can then be written in matrix form. \mathbf{Q} is a diagonal matrix containing the force densities and \mathbf{x} is a position vector for the nodes and \mathbf{p} is also a vector containing the loads.

$$\mathbf{C}_N^T \mathbf{Q} \mathbf{C} \mathbf{x} + \mathbf{p} = 0 \quad (2.55)$$

\mathbf{C}_N refers to the free nodes and \mathbf{C}_F to the fixed nodes, described as $\mathbf{C} = [\mathbf{C}_N \ \mathbf{C}_F]$. The same goes for position vector \mathbf{x} and matrix \mathbf{D} in equation 2.56. Linkwitz [3] rewrites the equation 2.55 to get it into the standard form for linear equations $\mathbf{A}\mathbf{x}=\mathbf{b}$

$$\mathbf{D}\mathbf{x} + \mathbf{p} = 0 \quad (2.56)$$

$$\mathbf{D}_N = \mathbf{C}_N^T \mathbf{Q} \mathbf{C}_N, \quad \mathbf{D}_F = \mathbf{C}_F^T \mathbf{Q} \mathbf{C}_F \quad (2.57)$$

The node positions of the free nodes can be solved for in a standard manor for linear equations on matrix form for all three directions x,y and z.

$$\begin{aligned} \mathbf{x}_N &= \mathbf{D}_N^{-1}(\mathbf{p}_x - \mathbf{D}_F \mathbf{x}_F) \\ \mathbf{y}_N &= \mathbf{D}_N^{-1}(\mathbf{p}_y - \mathbf{D}_F \mathbf{y}_F) \\ \mathbf{z}_N &= \mathbf{D}_N^{-1}(\mathbf{p}_z - \mathbf{D}_F \mathbf{z}_F) \end{aligned}$$

The solving procedure is described in a flow diagram as in figure 2.23.

2.4.2 Dynamic relaxation(DR)

DR is a numerical procedure that has been commonly used in engineering to find forms of equilibrium for tensile and cable structures[42]. The method was invented in 1965 by Alistair Day to solve sets of non-linear equations. The main concept of dynamics and DR is based on Newton's second law of motion, see equation 2.58.

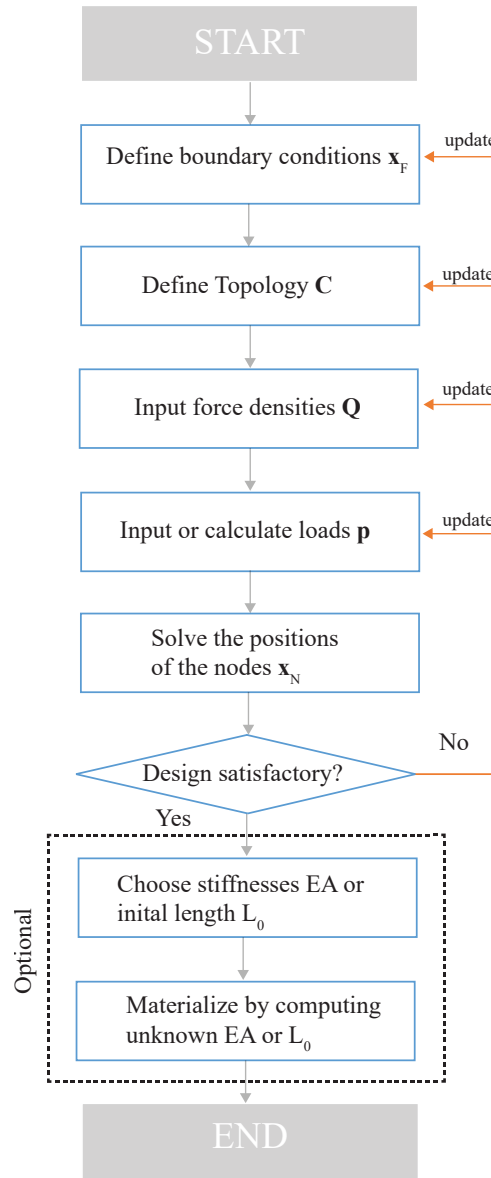


Figure 2.23: Flow diagram showing the computational procedure for FDM. This diagram is redrawn from [3]

This means that the equilibrium equation can result in a residual force that can be interpreted as an acceleration of a (fictitious) mass.

$$\sum F = ma \quad (2.58)$$

Applying Newton's second law it is possible to derive the equation of motion, 2.59, which is a second order differential equation which is the core of structural dynamics. [22].

$$m\ddot{u}(t) + c\dot{u}(t) + ku(t) = p(t) \quad (2.59)$$

$u(t)$ is the displacement parametrized by the time, t , and \dot{u} , \ddot{u} is the first and the

second differentiation of u with respect to time, t , $c(t)$ refers to damping and $p(t)$ is the applied loading. DR will step by step trace the motion in time, using small time increments, finding the position of static equilibrium for a certain loading, stiffness and boundary conditions of the system, see figure 2.24. There are different possibilities on how to structure the time stepping in numerical integration schemes, such as: *Symplectic Euler*, *Fourth Order Runge-Kutta* and *Velocity Verlet Method*. For further reading and how it can be applied see for example Poulsen [41].

A typical flow diagram of dynamic relaxation can be constructed as in figure 2.25. Figure 2.25 is a reconstruction from [3] where axial and shear forces have been replaced with a more general definition of forces only.

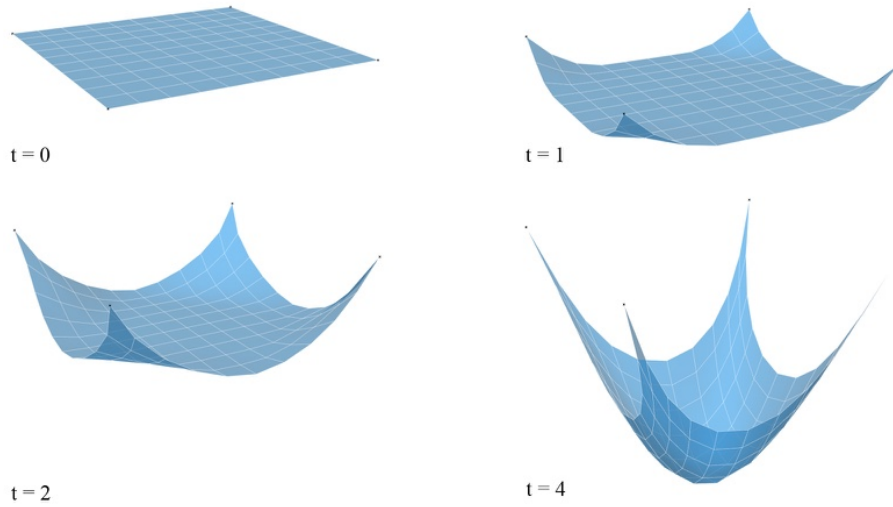


Figure 2.24: Visualization of dynamic relaxation applied on a plane mesh that is under gravitational load where the corner points are fixed. It shows how the structure reach equilibrium tracing through time. Initial state at $t = 0$ and equilibrium at $t = 4$.

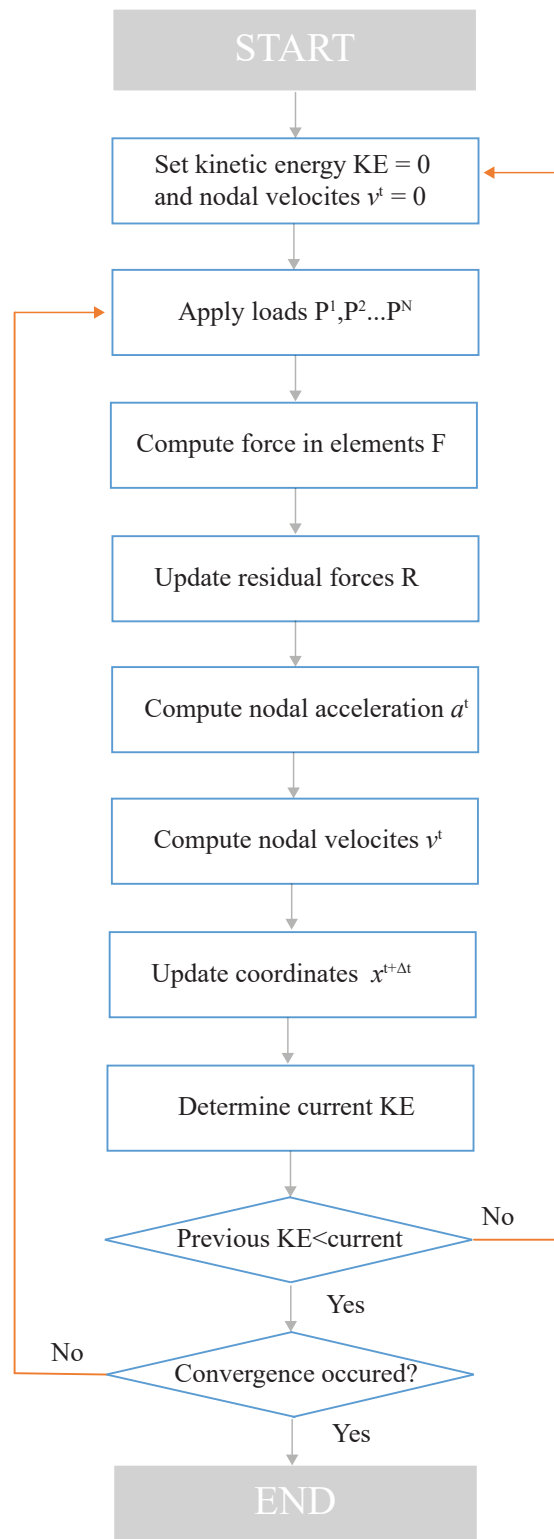


Figure 2.25: Flow diagram describing the different stages of Dynamic Relaxation. A reconstruction from [3], where axial and shear forces has been replaced with a more general definition of forces only. The main idea of dynamic relaxation is to transform a residual force into an acceleration leading to a new position. Iterate this process until the residual force vanish, meaning that the equilibrium of external and internal forces is found.

3

Method

This chapter will describe methods and definitions implemented to solve the research task. The aim is to generate patterns for brickwork on a form-found shell using polar geodesic coordinates. The implemented algorithm and procedure will be derived from the theory described in the previous chapter. The procedure will separate the form generation and the generation of polar geodesic coordinates, see figure 3.1. This means a decoupled process enabling more freedom for the designer in each part.

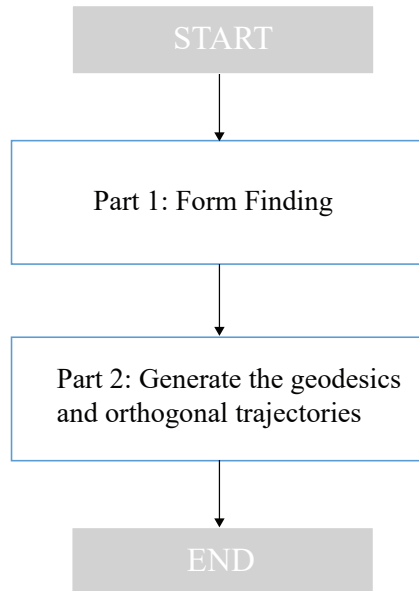


Figure 3.1: The method separates the form-finding and the generation of polar geodesic coordinates. Decoupling of the process enables more freedom to change and alter different aspects of the design.

The form generation will be based on form finding method of FDM. The reason is that it gives direct results based on the solution of the matrix set-up. This means a quick feedback in a design process. A FDM routine based on the theory described in 2.4.1 will be implemented.

Generation of the polar geodesic coordinates will be based on the theory of polar geodesic coordinates in section 2.2.2.4 and implemented using DR, section 2.4.2. To connect the theory and the numerical solver the continuous theory of 2.2.2.4 was transformed to discrete equivalent theory. The discrete mathematics can be applied

in a mathematical model which is solved using DR. The theoretical framework is illustrated in figure 3.2.

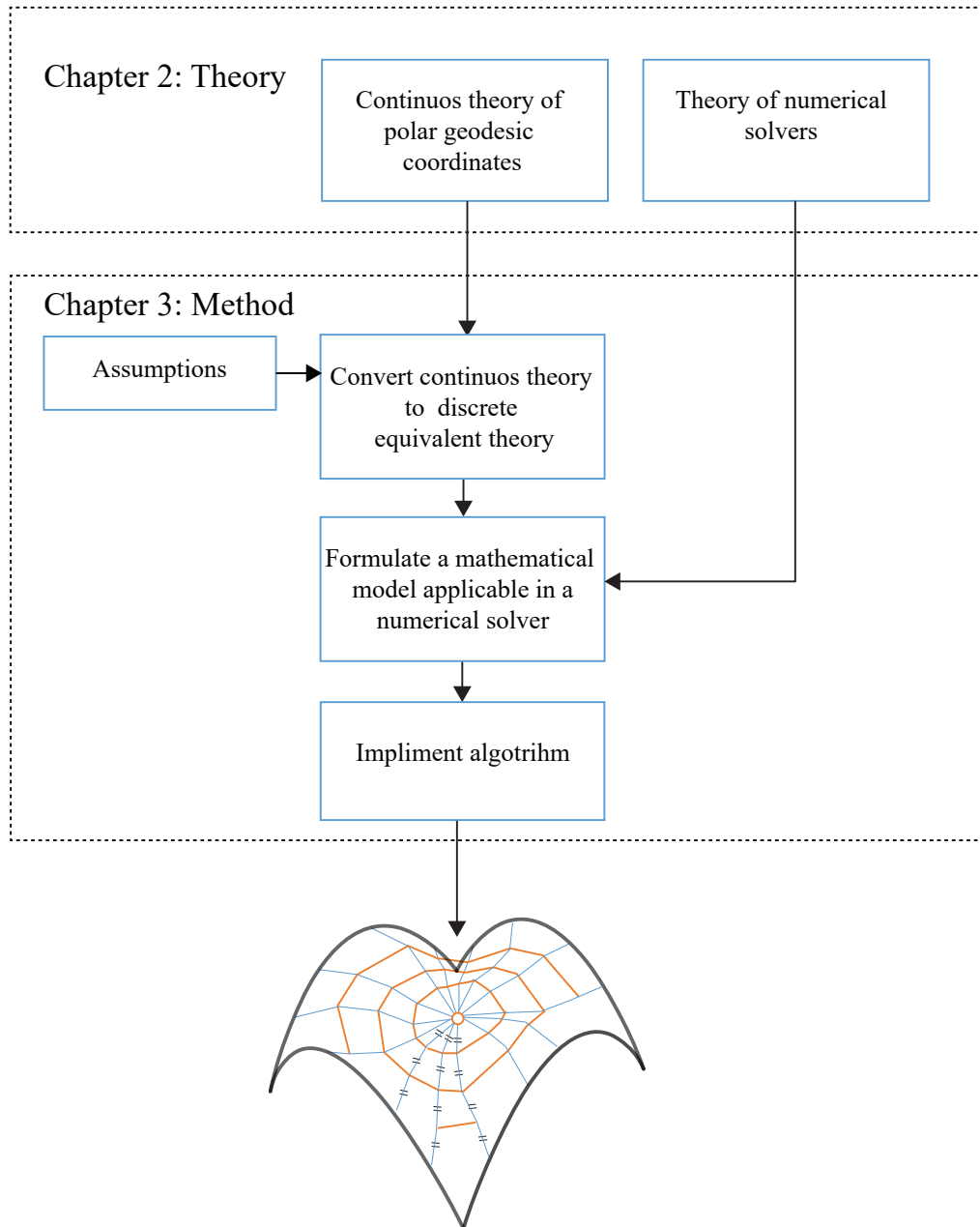


Figure 3.2: The theoretical framework of the generation of polar geodesic coordinates. From theory to formulating a mathematical model that is implemented in a numerical solver.

Both parts of the method will be implemented in a parametric framework in Grasshopper3d. To enhance the user interaction in the design process a user interface will connect Grasshopper3d with *Rhinoceros3d*, which is a 3d modelling software, see figure 3.3. Grasshopper3d and Rhinoceros3d have already in-built connection and compatibility so the purpose of the user interface is to expose specific functionality

from Grasshopper3d. The user interface will be created using *Human UI* which is an open source library for Grasshopper3d.

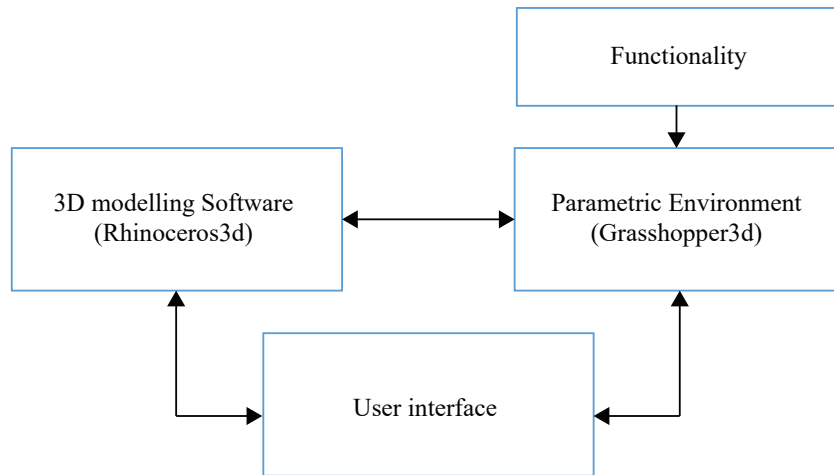


Figure 3.3: To enhance the user interaction in the design process a user interface will extend the connection between the parametric development environment and the 3d modelling software.

The user interaction and experience is chosen and illustrated in figure 3.4. It is divided into two parts referring to the different parts of this method. The intention is to ease the intractability and possibility to make many different options, in line with design scheme in figure 1.7, and the aim to place the research question in a design context.

3.1 Part 1: form-finding

As mentioned the form generation will be based on an implemented routine FDM based on routine in section 2.4.1. This will be implemented in Grasshopper3d component written in C#. The implementation will take the user intractability account, illustrated in figure 3.4, part 1. This is formalized into a flow diagram for the user implemented routine and interface illustrated in figure 3.5. This leads to the following inputs and adjustable parameters for the FDM software:

- The surface external and internal edge boundaries
- Fixed or free edge boundaries
- Loading amplitude in gravitational direction
- Force densities at different parts of domain and boundary:
 - Along external edges
 - Along internal edges
 - Internal domain

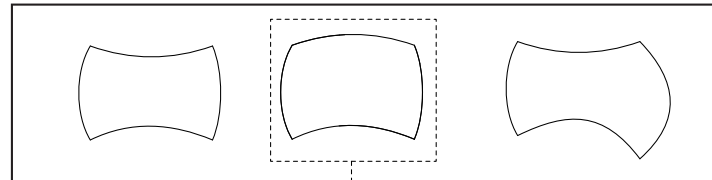
The FDM routine will output a discrete surface. This means that this surface needs to be converted to a NURBS surface for further implementation in part two of the method. This is done using a built in functionality in Grasshopper3d.

3.2 Part 2: Polar geodesic coordinates

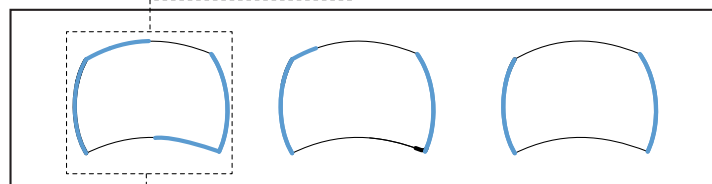
This section will describe the theoretical framework and the procedure of generation the polar geodesic coordinates. It is based on the figure 3.2.

Part 1: Form Generation

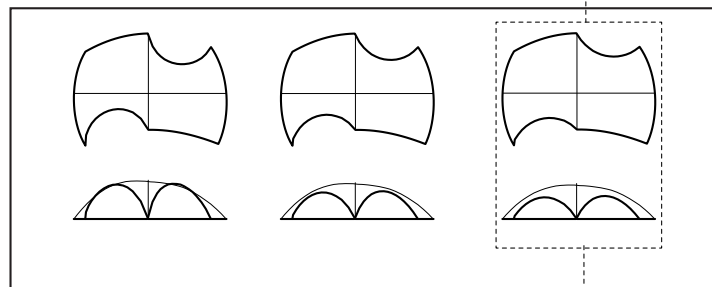
Elaborate surface border - 2d in plan



Choose free and constrained edges - 2d in plan

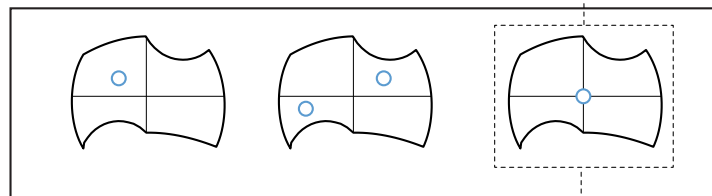


Perform form finding elaborating with different parameters - 2d in plan and section

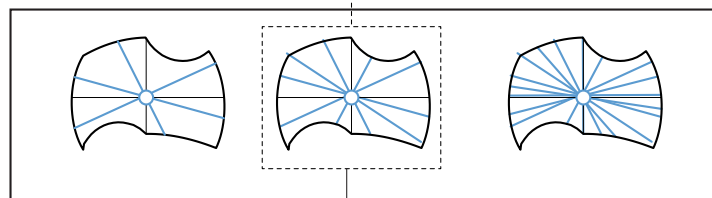


Part 2: Generation Geodesic Coordinates

Choose position and number of poles



Choose position and number the resolution of geodesics and orthogonal trajectories



Generate the polar geodesic coordinate by running the simulation

Run simulation

Figure 3.4: The method should be integrated in a easily navigated design scheme where the designer can change the design thorough different parameters.

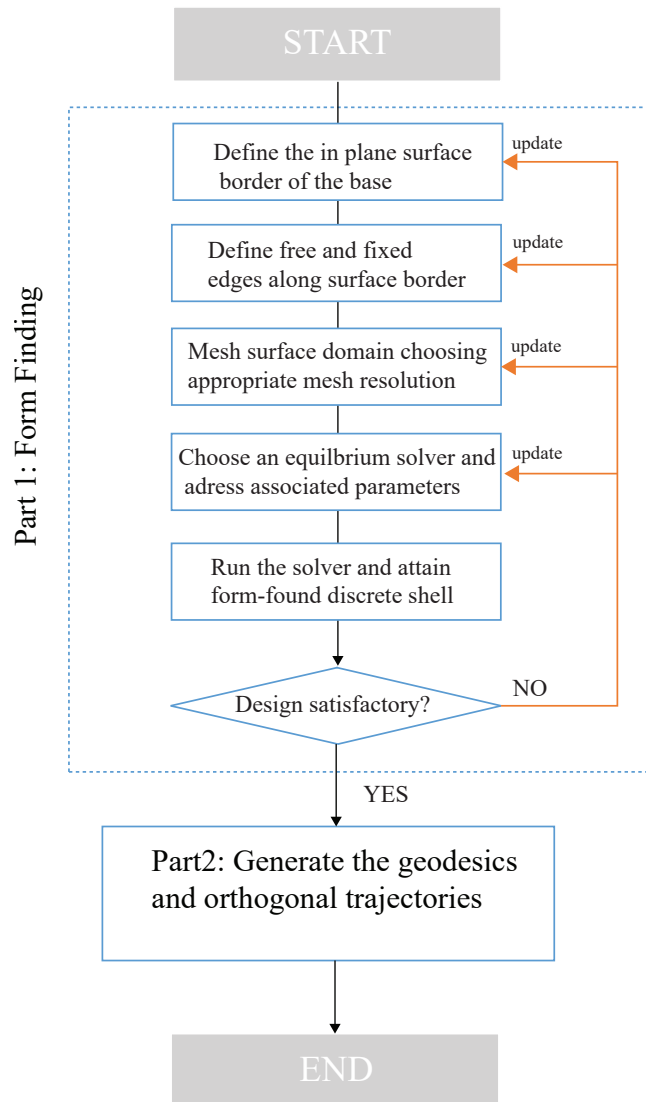


Figure 3.5: The flow diagram for the FDM routine is formalised based on the user interaction diagram of figure 3.4.

3.2.1 From continuous to discrete mathematics

This section will describe how the continuous theory have been interpreted into discrete mathematics for this thesis work. These interpretations will be qualified assumptions that through the results should be evaluated.

3.2.1.1 Discrete polar geodesic coordinates

Recall from section 2.2.2.4 that the orthogonal trajectories intersects the geodesics at a right angle, in which an equal length segment can be measured between to orthogonal trajectories along the geodesics. This means that by finding one orthogonal trajectory to a set of geodesics, you should easily the next orthogonal trajectory by measuring an equal length along the geodesics. The problem will be to find the

3. Method

first orthogonal trajectory. Therefore this method will impose using polar geodesic coordinates based on this assumption:

If generating geodesics radially from an origin point the intersection points of the first orthogonal trajectory will be found an equal length along the geodesics from the origin point.

Suppose this is true and that we have the intersection points. Connecting these points generates discrete curves in both directions. For a small enough distance this will resemble the continuous origin of the geodesic coordinates, see figure 3.6.

This method will invert this procedure. This means that it will strive to generate discrete geodesic curves with equal length segments starting from the pole. Since the segments are equal length segments their end points serve as the intersection points to the orthogonal trajectories. Connecting these points in the transverse direction creates the discrete interpretation of the orthogonal trajectories.

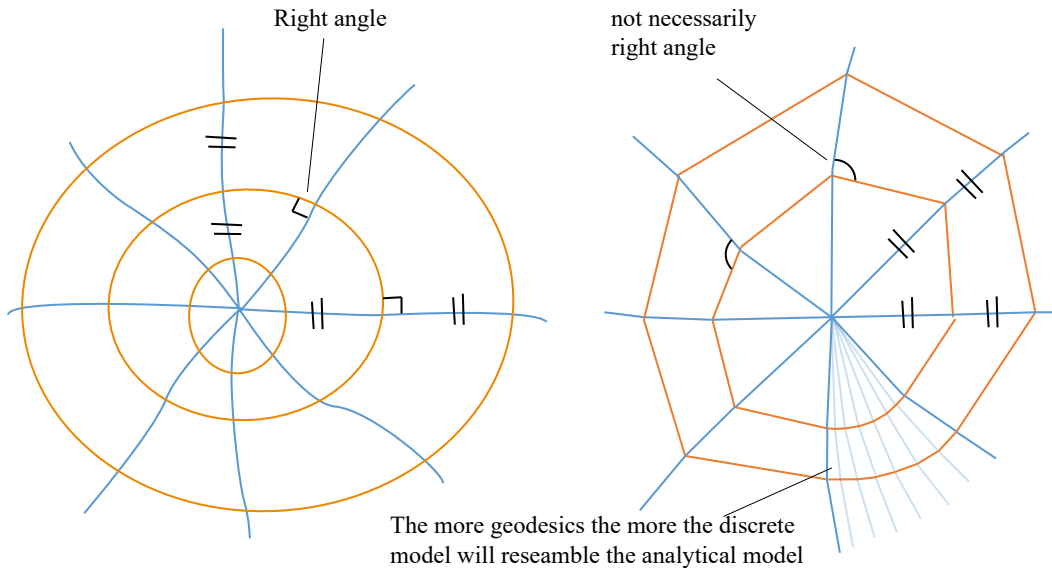


Figure 3.6: To the left the continuous definition of polar geodesic coordinates and to the right a discrete interpretation. For the discrete polar geodesic coordinate the angles are not necessarily orthogonal.

To simulate this procedure one need two things:

1. A discrete definition of geodesic curves, described in section 3.2.1.2
2. A numerical method to generate the discrete geodesics with equal segments, described in section 3.2.1.3

3.2.1.2 Discrete geodesics

The continuous definition of a geodesic curve is that in each point along the curve the geodesic curvature is zero, i.e. curve can only be curved in the normal direction. This could be interpreted as the tangent of the curve and the normal forming a

plane. For a discrete definition one can imagine three points on a surface where the points are connected through two vectors, \mathbf{A} and \mathbf{B} , starting in the middle point, see figure below. If the normal of the middle point and the two vectors lies in the same plane the geodesic curvature in the middle point can be considered zero. This means that the cross product of \mathbf{A} and \mathbf{B} is orthogonal to the normal and the projection onto the normal would be zero, i.e. the geodesic component is zero.

Based on the figure 3.7 the following condition should hold for all points of the geodesic curve.

$$\mathbf{A} \times \mathbf{B} \cdot \mathbf{N} = 0 \quad (3.1)$$

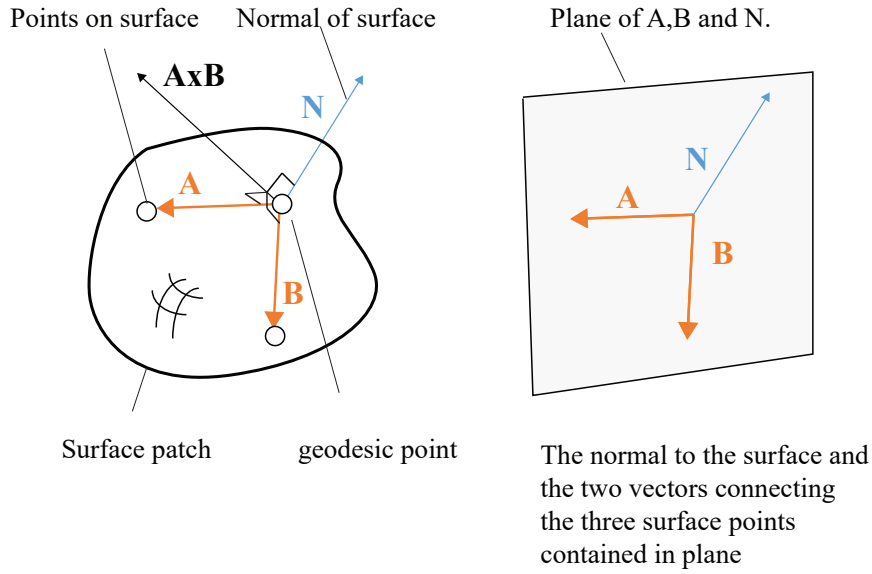


Figure 3.7: Definition of a point on a discrete geodesic curve on a continuous surface. A point, that is part of set of points forming a discrete curve, is connected by vectors \mathbf{A} and \mathbf{B} to its adjacent neighbouring points. The vectors \mathbf{A} and \mathbf{B} should be contained within a plane together with the normal vector of the surface.

For a small enough distance on the surface a collection of points with zero geodesic curvature will form a continuous geodesic curve.

3.2.1.3 Simulate geodesics using dynamic relaxation

To simulate and generate the discrete geodesics using DR a physical model will be needed to achieve the state described in equation 3.1. The model will consist of a system of springs connected, according to the left figure 3.8, spanning between two fixed points on the surface. Each node connecting these springs will have the following force relationship, also illustrated in figure 3.8:

$$\mathbf{s}_i + \mathbf{s}_{i+1} = m\mathbf{a} = \mathbf{r} \quad (3.2)$$

In equation 3.2 the sum of the spring forces, \mathbf{s}_i results in a residual force \mathbf{r} . The aim of this model is to minimize the geodesic component of the residual force in each node. The spring force for this simulation will be based on a pretension force \mathbf{s} :

$$\mathbf{s} = k(l_{t=i} - l_{t=0} * \alpha) \quad (3.3)$$

In equation 3.3 the spring, at each time step i , will strive for its initial length at $t=0$. The initial length is multiplied by a factor α , where $1 < \alpha < 0$, resulting in a contracting spring force, \mathbf{s} , when multiplied with stiffness, k . Fixing the end points and letting the nodes slide on a surface the DR simulation should converge towards the state where the residual force in each node is parallel with the normal of the surface, see bottom of figure 3.9. The sliding on the surface can be simulated by pulling the node back onto the surface in each iteration. The DR procedure can be illustrated in top of figure 3.9, where $t=0$ is the initial state and convergence is reached at $t=3$.

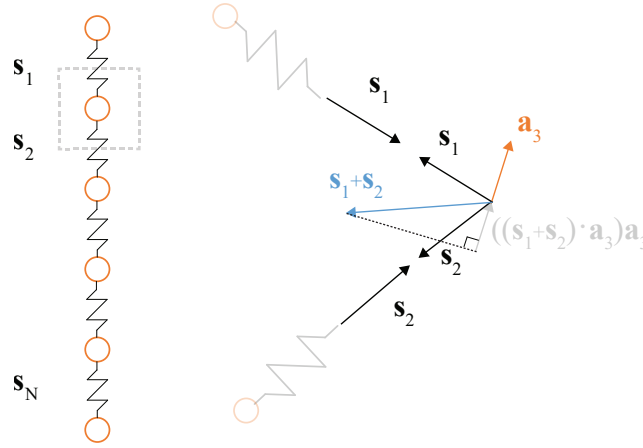


Figure 3.8: The mechanical equivalent of zero geodesic curvature is that there is no difference between the force $\mathbf{s}_1 + \mathbf{s}_2$ and its projection onto the normal, \mathbf{a}_3 , in that point.

3.2.2 Procedure

The procedure will be based on theoretical framework derived in sections 3.2.1.1, 3.2.1.2 and 3.2.1.3. From section 3.2.1.1 a possible strategy was made that stated if finding the point of the geodesics an equal distance from the pole one can generate the orthogonal trajectories, see figure 3.6. In section 3.2.1.3 a possible way to generate a geodesic fixed between two points on a surface using DR was shown. To connect these, it is needed to be assured that the points of the discrete geodesic are equally spaced. This implies that the following conditions are required for all geodesics:

1. The spring stiffness, k , is the same for all springs.
2. The initial spring length and the factor α is the same for all springs.
3. The initial lengths should be based on a reasonable guess

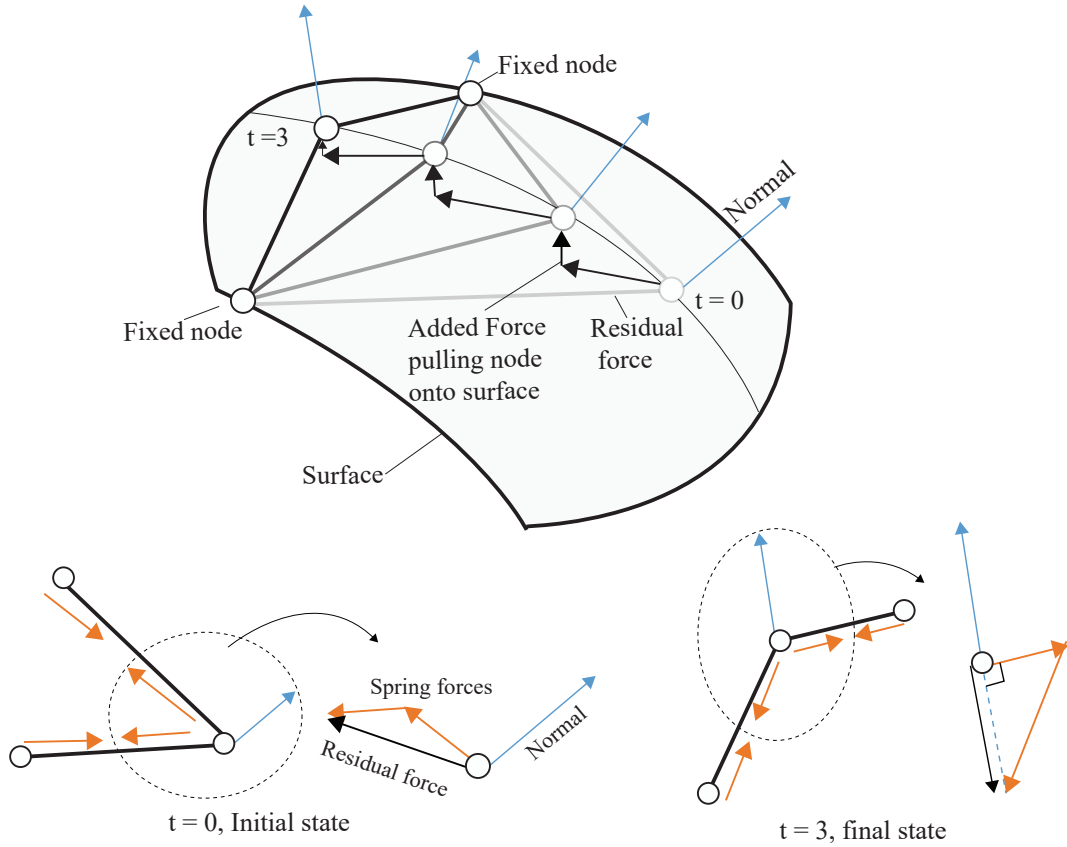


Figure 3.9: The DR procedure in which the points are connected with pretensioned springs. In the final state the residual force is parallel with the normal vector in that point.

The first two conditions will assure that the nodes between the springs will be spaced at an equal distance. The last condition indicates that it is necessary to have a small change in distance between the nodes before and after the simulation. This is achieved in this method by projecting the line between the end points of each geodesic.

Making these assumptions the procedure can now be described as follows and presented graphically in figure 3.10:

1. Decide the start and end points of the geodesics on the surface.
2. Generate an initial curve that lies on the surface based on the start and end points. Discretize the curve into segments, small enough to resemble the curve properties, of the same length. These segments will be modelled as springs in a physical model where the springs have the same stiffness.
3. Apply the same pretension in all elements and ensure that the nodes move along the surface, this can be done by either a force or just moving the point to the surface in each iteration. Start the solver, and for each iteration check

3. Method

the geodesic requirement for each point, or node.

4. When all nodes have zero geodesic curvature the solution has converged and the iterations end. The points should, due to the equal initial length and tension, still have equal distance.
5. Connect the points in the transverse direction to construct the discrete orthogonal trajectories.

This procedure will be implemented in Grasshopper3d in which the DR will be performed using the built in physics engine Kangaroo3d.

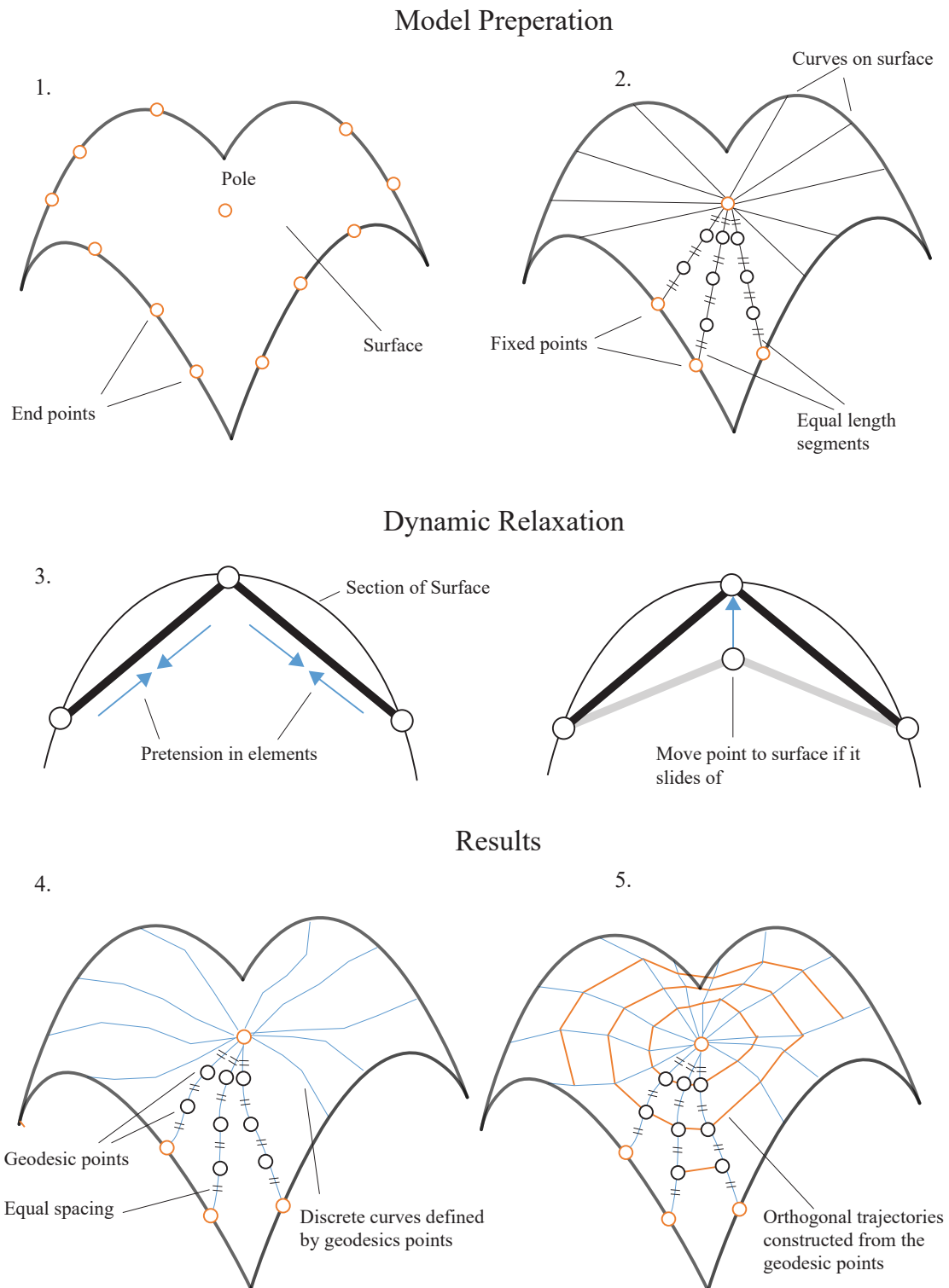


Figure 3.10: The procedure of generating the polar geodesic coordinates on a surface.

4

Results

The results of the thesis work include the idea and theory of using geodesic coordinates as a strategy for making brick patterns on complex shells and how to transform it into a computational method. The method was implemented and made into a design tool that can be used for architectural exploration in a parametric design scheme to find brick patterns on free form compression shells.

This section consists of two parts. The first presents how the model preparation in the parametric design scheme was implemented. The second part is a detailed study using the procedure of generating polar geodesics on a surface described in section 3.2.2 on a specific test case. This test case will be evaluated based on four different aspects that are relevant to ensure conformity between the application and the underlying theory, those aspects are as follows:

1. *The definition of the points of the geodesic curve.* Will the algorithm fulfill the angular requirements of the points on the geodesic, referring to definition in section 3.2.1.2
2. *The length between the geodesic points.* The basis of the idea is that the brick patterns coincide with the orthogonal trajectories which cuts the geodesics at equal length.
3. *The assumption that the discrete polar geodesic coordinate will converge towards the continuous,* referring to definition in section 3.2.1.1.
4. *Deviance going from the discrete, form founded surface, to the continuous surface.*

4.1 Model preparation and generation

This section will present how the research work is implemented as a parametric design scheme and how the geodesic coordinates generation procedure is structured. Figure 4.1 shows how the connection between Rhinoceros3d and Grasshopper3d is extended via a designed user interface, referring to figure 3.3. This connection allows for easy set up and modifications of generating a form and setting up the necessary steps for the pattern generation. The full procedure and its stages is presented in the appendix A.7.1. Since the parametric framework is open the code is exposed and one can easily modify or control the generation process. Figure 4.2 shows how the coding has been structured in Grasshopper3d. A larger picture can be found in appendix A.30.

4. Results

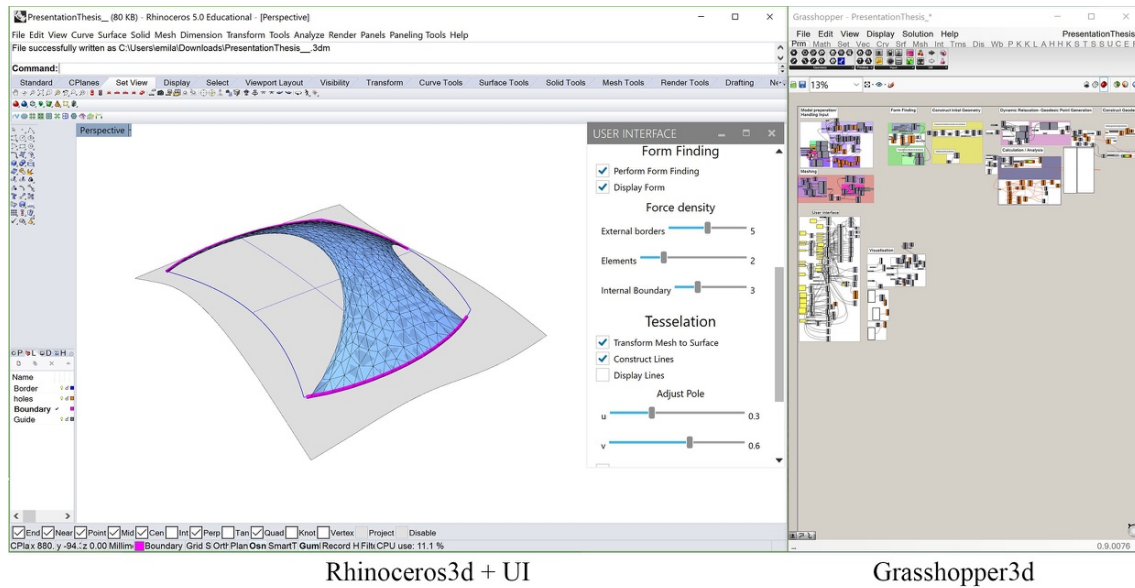


Figure 4.1: The connection between the 3dmodelling software Rhino and the parametric design plug-in is enhanced by a user interface.

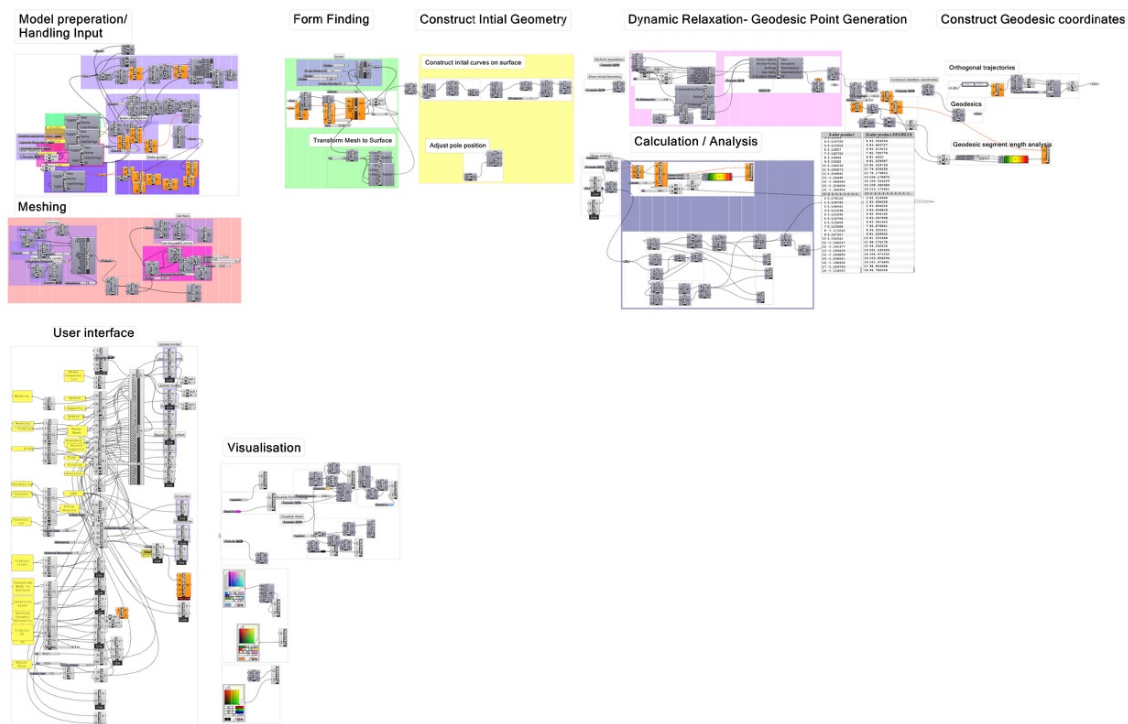


Figure 4.2: The code in grasshopper structured in different units. Starting from the input of geometry one can follow the procedure to the generation of polar geodesics on the surface.

4.2 Test case: polar geodesic coordinates on shell

This second part will show the results of a test-case where the procedure of generating polar geodesic coordinates was applied on a shell. It will challenge the assumptions and the procedure constructed in section 3.2 to model the polar geodesic coordinates based on the aspects described in section 4.

4.2.1 Visual output

This is the visual output of the polar geodesic coordinates on the shell. Blue lines are the discrete geodesics and the orange discrete curves relate to the orthogonal trajectories.

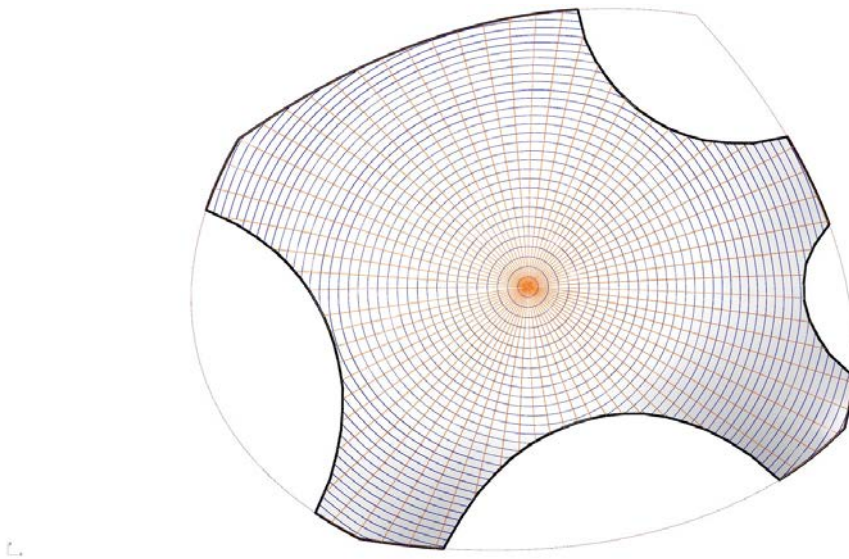


Figure 4.3: Output of discrete geodesic coordinates in top view

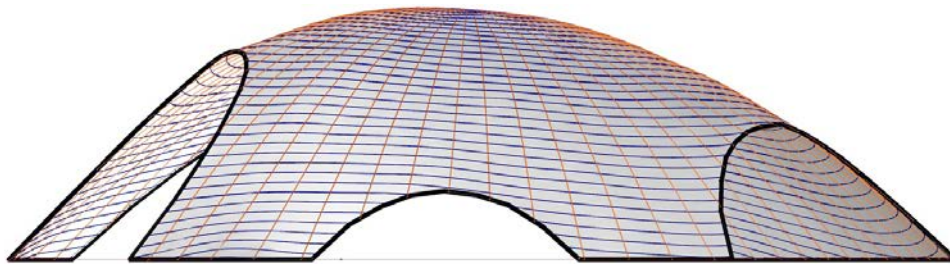


Figure 4.4: Output of discrete geodesic coordinates in right view

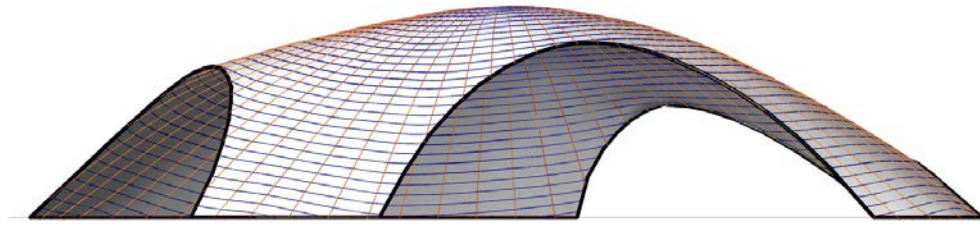


Figure 4.5: Output of discrete geodesic coordinates in front view

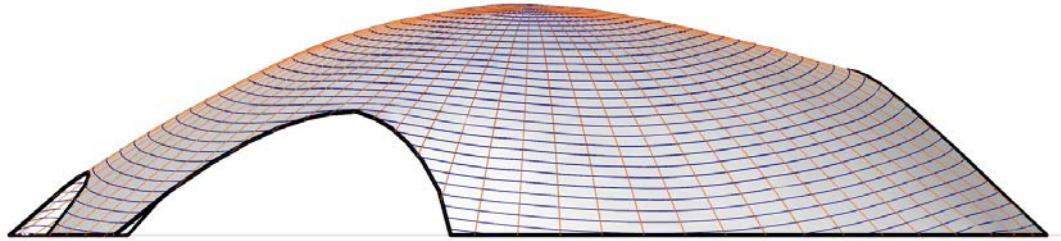


Figure 4.6: Output of discrete geodesic coordinates in back view

4.2.2 Discrete geodesics

This section analyses angle based on equation 3.1 in section 3.2.1.2 and refers to aspect 1 in section 4. The analysis is presented and described graphically in figure 4.7.

- **Maximal angle deviance from 90 °of all geodesic points: 0.97 °**
This is the highest value of all geodesics points, meaning that the deviance cannot be higher than this.
- **Average angle deviance from 90 °of the worst nodes in each geodesic curve: 0.034 °**
For each geodesic curve the nodes with highest deviance from 90 degrees was put together in a list. This measure only includes the results of those nodes.
- **Average Angle of all geodesic points: 90.000 °**
This is an average for all geodesic points in all geodesic curves.

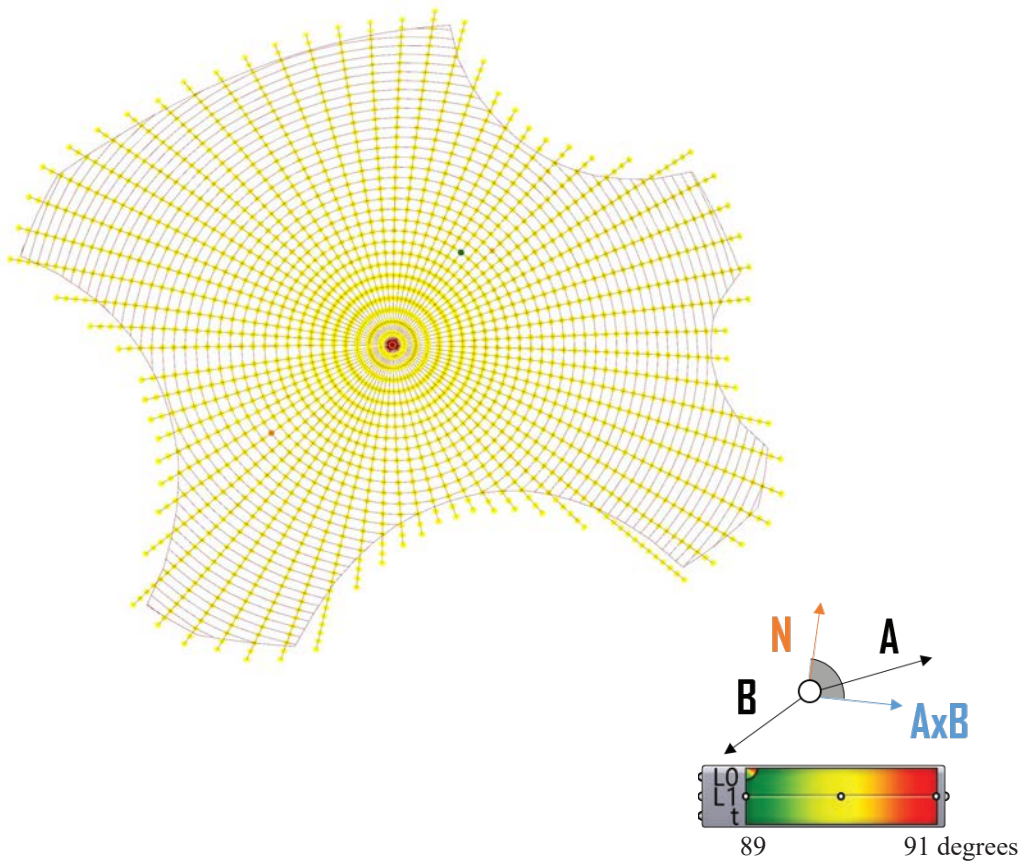


Figure 4.7: Graphical output of the angle between the normal and the cross product of the two connecting vectors to each point. The angle is evaluated in the range 89 and 91 degrees.

4.2.3 Geodesic segment length

This section analyses the length of the segments of the discrete geodesics, and refers to aspect 2 in section 4. The results are presented in figure 4.8.

- **Average geodesic segments: 1.499 length units**
This is an average for the distance between all geodesic points in all geodesic curves.
- **maximal deviation from average segment segments: 0.0005 length units**
This is the maximal length deviation compared to the average segment length.

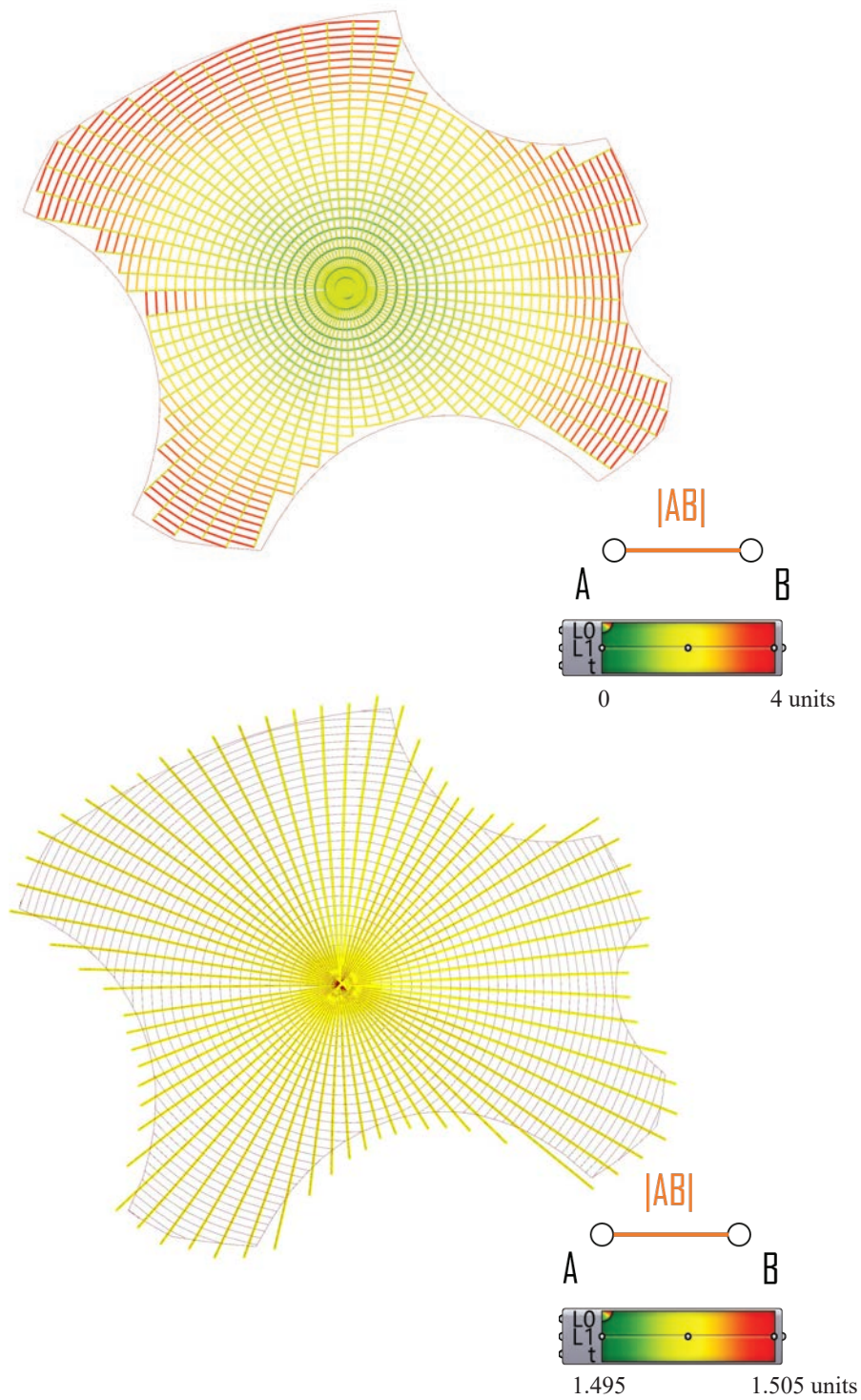


Figure 4.8: Analysis of the length of the discrete lines between the geodesic points. The figure above consists of all segments, both geodesics and orthogonal trajectories. Below the analysis is done with only the geodesic segments. The analysis shows great length consistency of the geodesic elements with small deviations.

4.2.4 Maximum angle difference of mesh face

These results refers to the analysis of the differences between the maximum and minimum angle of the mesh faces in the geodesic coordinate mesh, see figure and definition in 4.9, and refers to aspect 3 in section 4. This analysis will also investigate what happens to the results going from coarse to finer mesh resolution. Due to the computational time the fine resolution mesh is only part of a patch of the entire shell. The results are presented in figures 4.10 and 4.11.

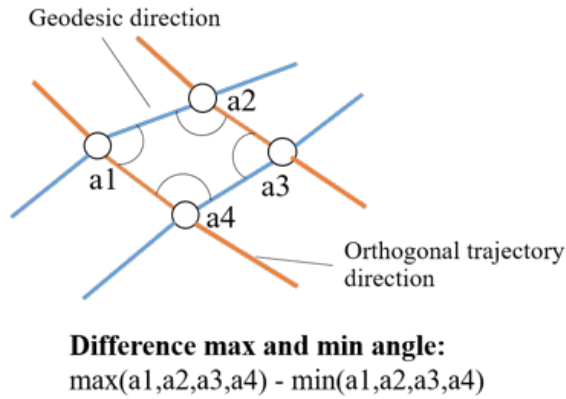
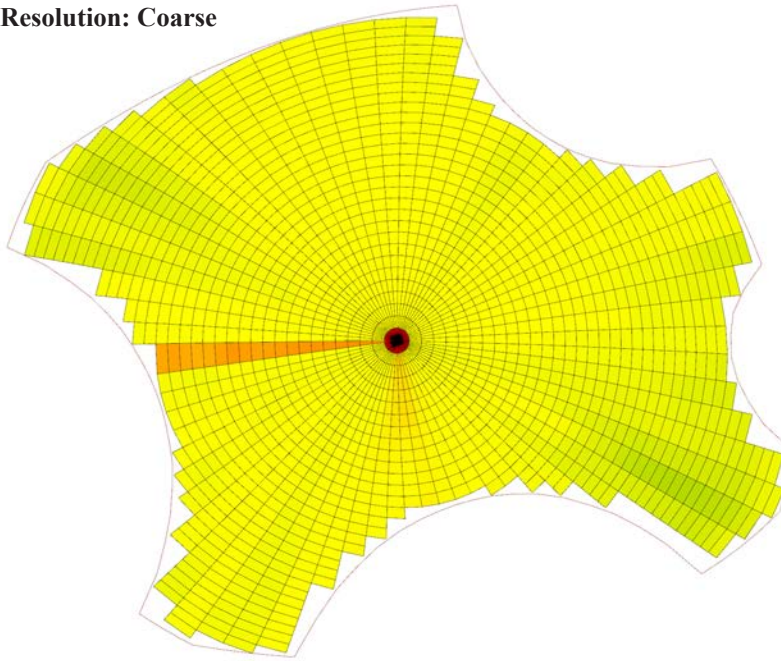


Figure 4.9: The analysis criteria where the result is the subtraction of the maximum and the minimum angle of each face.

- **Coarse resolution mesh:**
 - Average angle deviance: 7.1 °
 - Average size of mesh panel: 2.57 area units
- **Fine resolution mesh:**
 - Average angle deviance: 0.9 °
 - Average size of mesh panel: 0.13 area units

Mesh Resolution: Coarse



Mesh Resolution: Fine

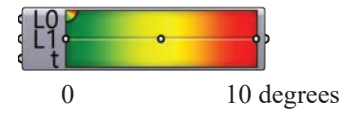
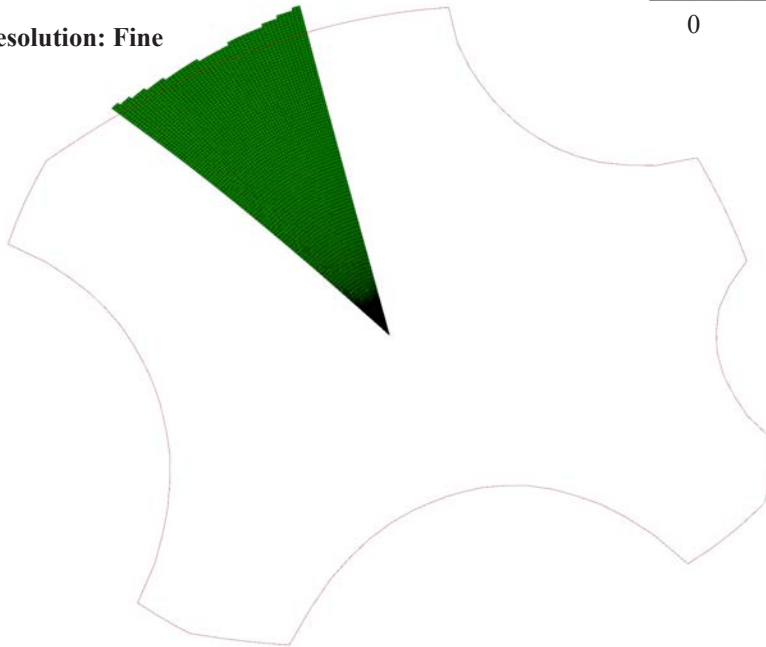


Figure 4.10: Analysis with two types of mesh resolution, the top is coarser and below is a small patch that is of very fine resolution. They are evaluated between 0 and 10 degrees.

Mesh Resolution: Fine

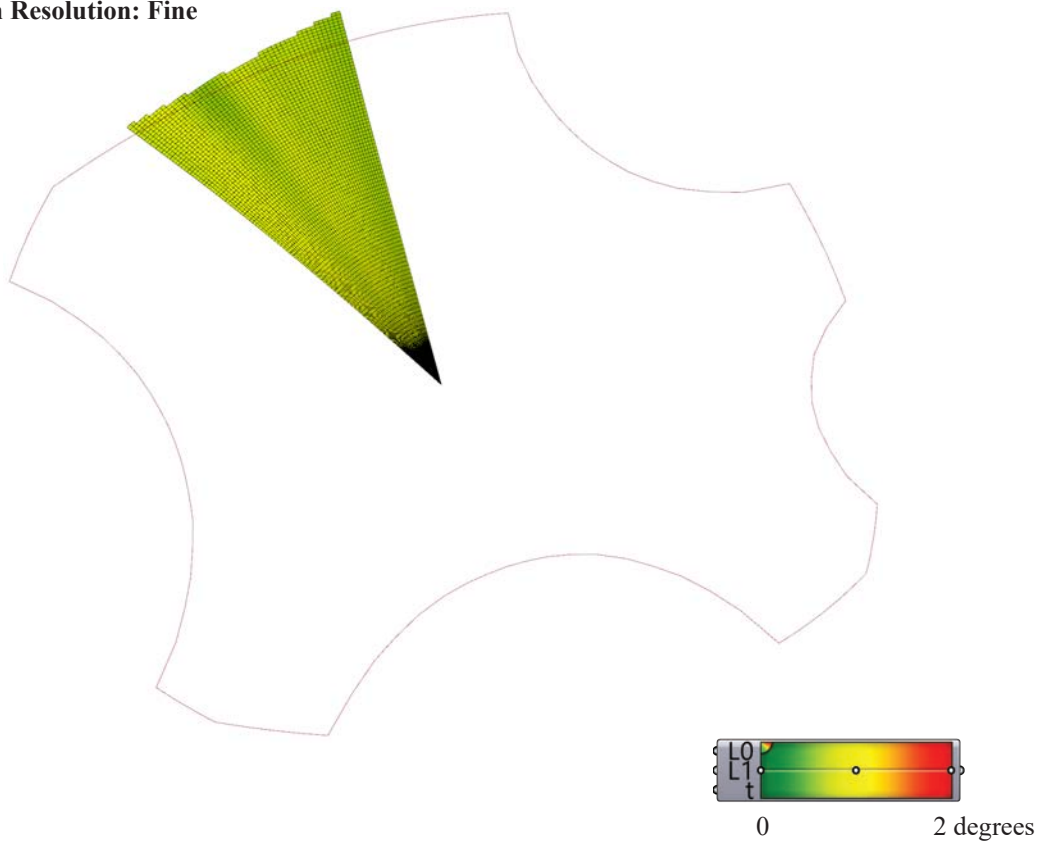


Figure 4.11: Analysis of the fine resolution mesh, same model as in figure 4.10 but with the evaluation ranging between 0 and 2 degrees to give a more detailed analysis.

4.2.5 Transformation of discrete to continuous surface

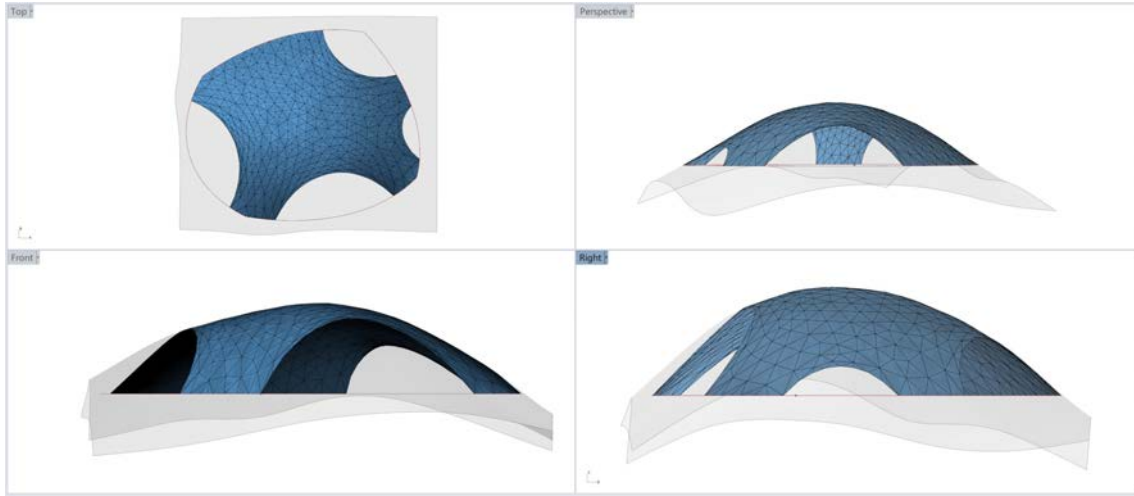


Figure 4.12: Comparison between the form-found mesh, in blue, and the surface generated from that mesh in grey which is used for the generation of geodesic coordinates.

Transforming the form found the mesh to a surface is not uncomplicated, and the NURBS surface did have small deviations from the form found mesh. To give a measure of how much the following metric was used. The average length of the mesh edges gets to resemble average panel, in this case, 4,16 *units*. The average distance to the surface was 0.025 *units*. One corner that has deviated 0.025 *units* results in an angle of 0.34 degrees.

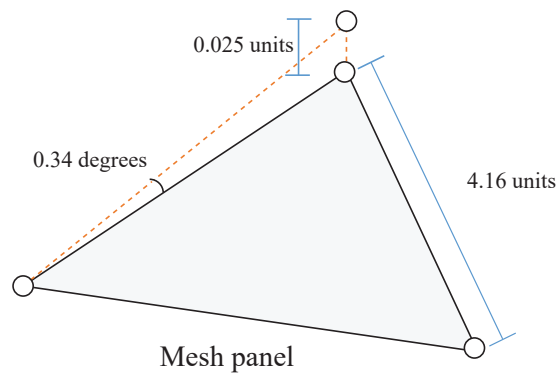


Figure 4.13: The average deviation going from the discrete surface, the form-found mesh, to the continuous surface that is used during the dynamic relaxation is relatively small compared to the size of the mesh face.

5

Discussion

In the following chapter a discussion concerning the results and methods presented in the thesis is held. Finally some recommendations for further work is presented.

5.1 Reflections

There are some areas concerning the method and results worth reflecting upon:

- Organisation of the method
- Credibility of the method - how are the results connected to the theory and hypothesis applied in the method.
- Implementation
- Design Aspects

5.1.1 Organisation of the method

The organisation of the method is based on that the form-finding and the tessellation is separated. By separating the process one gives the architect or engineer the opportunity to let the form be governed by for instance room configurations and volume or structural properties. Usually this is a luxury that can lead to a lot of problems when merging form and tessellation strategies. For steel structure and facade systems this can become quite tricky to post-process since efficient mathematical mappings is quite complicated on free-form structures. For brick structures this might not be a problem since the technique and craft implies that one allows for a certain tolerances, either through the joint or through modification of the brick itself.

5.1.2 Credibility of the method

The results and analysis of the chosen example were chosen to challenge the definitions and hypothesis made in the method. Three types of analysis were made, the first concerns the discrete geodesic definition, the second the line segment of the discrete geodesic curves and the third examines the convergence from discrete towards continuous.

The first analysis shows that there was very little deviance from the geodesic condition. The maximum deviance was less then one degree and the average deviance

was less than 0.001 degrees. This proves that the implementation can achieve the desired state made in the definition.

The second analysis is very important due to two reasons. Firstly, it is a vital part in the definition of geodesic coordinates. According to the definition two orthogonal trajectories should encapsulate equal length geodesic curves between themselves. Secondly, this is the vital and necessary part for the bricklaying. It was on this basis that the geodesic coordinates were chosen in the first place. If one could not ensure this part the method or the implementation would fall. Luckily the results show very little deviance between the segments. The maximum deviance from the average length was less than 0.04 percent.

The third analysis, was made to test the assumption that the discrete geodesic coordinates will converge towards the continuous geodesic coordinates. There were two cases, one with a coarse mesh covering the entire surface, and one with finer mesh that covers a patch of the surface. The measurement was based on measuring the difference of the internal angles of a mesh face. It is not fair to say that the difference should be zero since in the continuous theory there is not existing meshes, since they are based on line elements. What you can say is that for a very fine mesh resolution the difference should be close to zero. The result shows that it clearly converges towards smaller difference and that the fine mesh results in an average difference of 0.9 degrees for each mesh face.

5.1.3 Implementation

This section will discuss questions and aspects that are related to implementation of the method.

5.1.3.1 Computational efficiency

The method of generating the geodesics, even though giving good results, needed much computer power and therefore took long time to produce. This limited the mesh resolution of the geodesic coordinates and how fast new designs could be generated. This area can be greatly improved since the work did not intend to find the most optimal way, but rather find a way to produce geodesics and a geodesic coordinates mesh. In Rhinoceros3d there is for instance a command for creating a shortest path between two points on a surface. This is done relatively fast so there is a great potential in improving the computational power and speed required.

5.1.3.2 Form generation

The generation was done using force density method (FDM), which is a suitable method to derive efficient shapes. For brick shells it would be more beneficial to implement, or use, thrust network analysis (TNA) developed by Block and Ochsendorf [16] which ensures a compression solution. For unreinforced brick shells one must check manually if the solution only consists of compression members using FDM.

There is a TNA software implemented for Rhinoceros3d which could well have been used. The FDM was chosen based on its simplicity. This meaning quick results during form generation and simpler implementation in the parametric framework.

One down-side with the form-generation is that the form-finding algorithms produce discrete surfaces while the method of generating the geodesics are based on a continuous surface. This is not ideal since it is not without complications and the continuous surface will deviate from the discrete. Either the method needs to be modified or the form-finding needs to produce a surface. This might not be a big problem as long as the line of thrust can be kept within the thickness of the shell.

5.1.4 Design

This section will discuss aspects of designing brick patterns with geodesic coordinates.

5.1.4.1 General and polar geodesic coordinates

For some shapes and designs it seems natural to use polar geodesic coordinates for brick tessellation. Looking at domes in history they have in many cases been designed based on a center pole strategy. This can be seen in for instance Pantheon but also less flamboyant structures such as igloos. Even though it might seem natural there is a problem having this center pole. This is due to that all geometry is meeting in a small point causing detailing problems needed to be taken care of. One possibility is to leave a hole in the pole as can be seen in Pantheon. In Bath abbey they have chosen multiple poles, one for each fan vault, that meets in the aisle roof. Their approach has been to highlight rather than hide. The space created is used as extra decoration, see figure 5.1.

For some shapes the designer might like to have more control of how the geodesics should be drawn, which is not possible in a polar geodesic coordinate system. In a catenary vault it would be more natural to have bricks laid either along or orthogonal to the catenary. This would be similar to using general geodesic coordinates rather than polar geodesic coordinates. Using this approach one can design the brick patterns to follow the edge conditions for instance, as will be discussed in section 5.1.4.2. It also enables decorative and creative ways to tessellate the shell in line with the design intention.

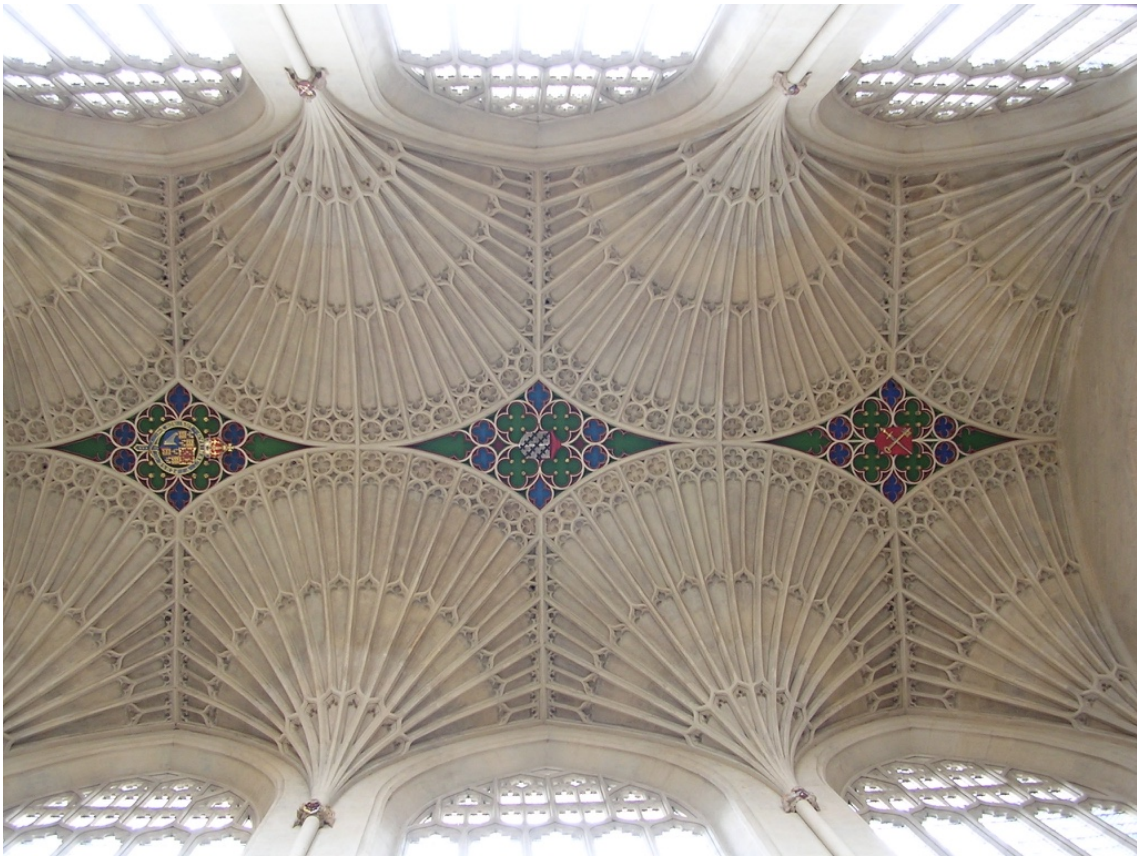


Figure 5.1: In Bath abbey each fan vault has its geometry based on a pole. The geometry then meets in the aisle roof. [47]

5.1.4.2 Edge-conditions

Considering build-ability one should think of how the edges are related to the bed joints of the bricks. Choosing arbitrary edge boundaries can make it necessary to perform modifications on the bricks or design necessary supports, like a concrete foundation. This might not be an optimal solution for a real project. Best thing would be to edge boundaries to follow the orthogonal trajectories so that they are leveled with the bed joints.

There are two ways to construct a geodesic, as described, either through a starting and an end point or by a starting point and a direction. One approach would be to design the edge-curves and let the geodesics be based on a starting point on the edge and a direction that is orthogonal. This would imply that the edge curve would become an orthogonal trajectory due to the approach of the geodesic generation. One problem might be that there is no control of how the geodesics will propagate on the surface and that they might intersect each-other at some point.

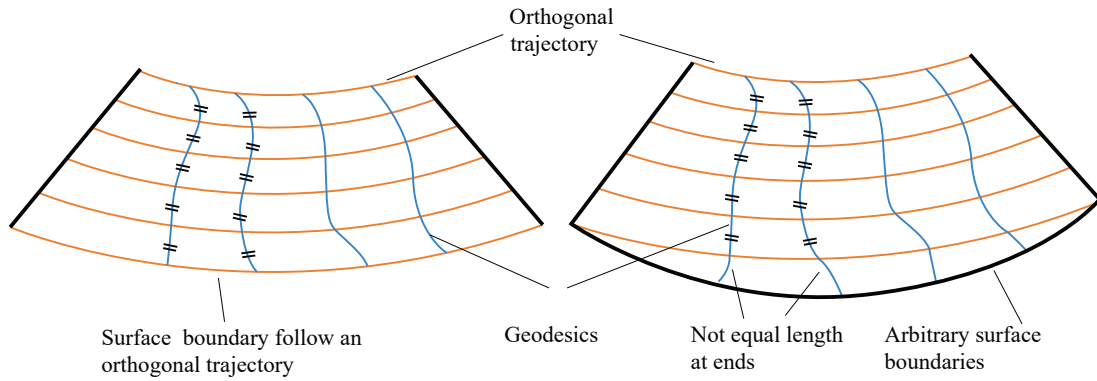


Figure 5.2: Problems that can occur along the edges if the edges and the orthogonal trajectories differ. A good design approach would be to design the edges are described by an orthogonal trajectory.

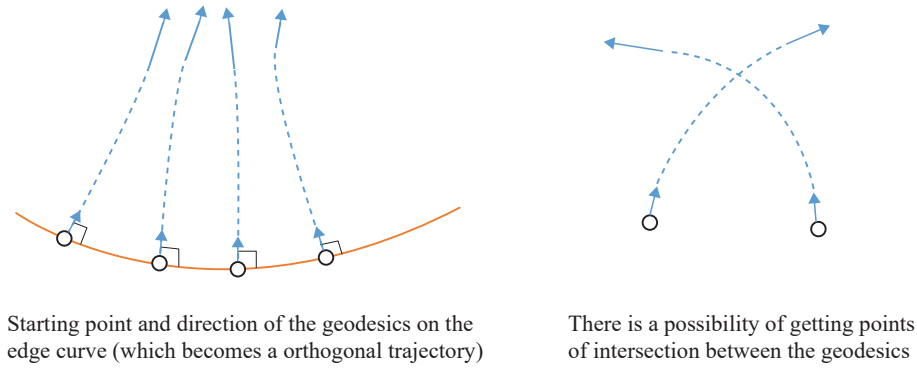


Figure 5.3: It is possible to construct the geodesic coordinates by generating geodesics orthogonal to a curve, using for instance the edge curve. There is a possibility though that the geodesics will propagate on the surface in such a way that they intersect each other.

5.2 Future work and improvements

- **Further Validation** - To prove the method and the theory of this thesis further testing and validation is needed. This means doing the same procedure on new shells or choosing different pole positions on a shell. Even though the results look very promising further evaluation is needed.
- **Geodesic generation** - The speed of generating the geodesics using dynamic relaxation was successful but the method was computationally heavy. To solve this one could either find a more efficient method or solver for this matter. Since there already existed a dynamic solver this was not of priority to implement a new dynamic relaxation solver. Implementing a specialized solver can give many advantages. One could for instance set limits for which the geodesic set is considered to be geodesic points, and focus its power on the sets that have harder time finding its position.

- **Implement general geodesic coordinates** - Within the time-frame of the thesis there was only time to present a reliable method for polar geodesic coordinates. General geodesic coordinates though could be useful where the polar geodesic polar coordinates have disadvantages, as described in the reflections. This could well be a future research task.
- **Prototyping** - Another way to validate the results would be to physically build models based on the guide lines generated with this method. Unfortunately, there was not time to make a real physical object challenging or proving the results for this thesis. It could be a good follow up in this subject to make both small models and a full scale mock-up that test this research question fully. Before a full scale model can be built a more rigorous structural design and assessment must be made.

6

Conclusion

The objective of this thesis was to investigate a new strategy for generation of brick patterns based on geodesic coordinates. This was done by combining mathematical theory of differential geometry with manufacturing processes of brick structures. The theory became the basis of a computational method constructed and implemented to generate polar geodesic coordinates on shells. The assumptions and theory of the method was evaluated on a test case where the form was derived using form-finding algorithms. The evaluation was based on the necessity to convert continuous theory of geodesic coordinates into discrete equivalent mathematics implemented in the computational method.

The output from the method applied on the test-case suggest a correlation between initial continuous theory and discrete mathematics generated by the numerical procedure. This means that the necessary conditions of the fabrication process of brick structures was met, that is that the pattern ensured consistent brick courses on the shell. Further testing will be needed to draw a general conclusion of the method. The strategy was also possible to implement in a parametric design process, proving that this can be a possible tool assisting projects in early design stages.

As concluding remark, the work in this thesis is a first step towards a general strategy of generating brick patterns on free form shells. The knowledge gained can not only apply to modern production but also be used to understand tiling patterns of historical vaults.

Bibliography

- [1] Struik, D.J. (1964) *Lectures on classical differential geometry*. 2nd edn. United States: Dover Publications.
- [2] Bär, C. 2010, *Elementary differential geometry*, Cambridge university press, Cambridge.
- [3] Adriaenssens, S., Block, P. and Veenendaal, D. (eds.) (2014) *Shell structures for architecture: Form finding and optimization*. United Kingdom: Routledge.
- [4] Pottmann, H., Asperl, A., Hofer, M. and Kilian, A. (2007) *Architectural geometry*. 1 st edn. Bentley Institute Press.
- [5] Pressley, A. (2012) *Elementary differential geometry*. 2nd edn. United States: Springer-Verlag London Limited.
- [6] Gron, O. and Naess, A. (2014) *Einstein's theory: A rigorous introduction for the mathematically untrained*. New York, NY, United States: Springer-Verlag New York
- [7] Ochsendorf, J. (2011) *Guastavino vaulting: The art of structural tile*. United States: Princeton Architectural Press.
- [8] Heyman, J. (1997) *The stone skeleton: Structural engineering of masonry architecture*. Cambridge: Cambridge University Press.
- [9] Allen, E., Zalewski, W. and Foxe, D.M. (2009) *Form and forces: Designing efficient, expressive structures [With access Code]*. United Kingdom: Wiley, John & Sons.
- [10] Domone, J. and Ilston, J. (2010) *Construction materials.; their nature and behaviour*. 4th edn. New York: Taylor and Francis Group.
- [11] Pfeifer, G. 2001, *Masonry construction manual*, Birkhäuser, Boston;Berlin;Basel;.
- [12] Mitchell, C.F. and Chapman, J. (2009) *Brickwork and masonry - A practical text book for students, and those engaged in the design and execution of structures in brick and stone*. United Kingdom: Read Books.
- [13] Mortar 2016. Britannica Academic. Retrieved 11 August 2016, from
- [14] Heyman, J. (1966) 'The stone skeleton', International Journal of Solids and Structures, 2(2), pp. 249–279. doi: 10.1016/0020-7683(66)90018-7.
- [15] Isler H., 1961. *New Shapes for Shells*. Bulletin of the International Association for Shell Structures, 8, c-3.
- [16] Block,P. (2009) *Thrust Network Analysis: Exploring Three-dimensional Equilibrium* PhD thesis. Boston: Massachusetts Institute of Technology
- [17] Williams C.J.K (1980) *Form-finding and cutting patterns for air- supported structures. Symposium on Air-supported structures: The state of art:* 1 Institution of Structural Engineers. London,99-120

- [18] Rippmann, M. and Block, P. (2011) *New Design and Fabrication Methods for Freeform Stone Vaults Based on Ruled Surfaces*, Springer Berlin Heidelberg. .
- [19] Rippmann, M., Curry, J., Escobedo, D. and Block, P. (2013) *Optimising Stone-Cutting Strategies for Freeform Masonry Vaults*, Proceedings of the International Association for Shell and Spatial Structures (IASS) Symposium 2013.
- [20] Williams, C.J.K. (1987) *Use of structural analogy in generation of smooth surfaces for engineering purposes*, Computer-Aided Design, 19(6), pp. 310–322. doi: 10.1016/0010-4485(87)90285-5.
- [21] Jabi, W. (2013) *Parametric design for architecture*. London: Laurence King Publishing.
- [22] Craig, R.R. and Kurdila, A.J. (2006) *Fundamentals of structural dynamics*. 2nd edn. United States: Wiley, John And Sons.
- [23] Anderson, S. (2003) *Eladio Dieste: Innovation in structural art*. United States: Princeton Architectural Press.
- [24] Stoker, J.J. 1969, *Differential Geometry*, Wiley-Interscience, New York.
- [25] Burström, P.G. 2007, *Byggnadsmaterial: uppbyggnad, tillverkning och egenskaper*, 2. uppl. edn, Studentlitteratur, Lund.
- [26] Green, A.E. and Zerna, W. (1992) *Theoretical elasticity*. 2nd edn. United States: Dover Publications.
- [27] Domokos, G. 1990, *THE EQUILIBRIUM EQUATIONS OF MEMBRANE SHELLS EXPRESSED IN GENERAL SURFACE COORDINATES*, Periodica Polytechnica. Architecture, vol. 34, no. 1-2, pp. 85.
- [28] Porter, D. (1895). *Notes on stereotomy*. Boston.
- [29] Ahlstrand, J.T., Eriksson, T. And Walldhör, I. 1976, *Arkitekturtermer: lexikon över svenska, engelska, tyska och franska arkitektur- och stadsplanetermer : med engelskt, tyskt och franskt register*, 2., [revid.] uppl. edn, Studentlitteratur, Lund.
- [30] Lindgren, J. And Moeschlin, J. 1985, *Tegel: tillverkning, konstruktion, gestaltning*, Svensk byggtjänst, Stockholm.
- [31] Paulsson, G. 1936, *Hantverkets bok: 4, Mureri*, Lindfors, Stockholm.
- [32] Map types (2016) Available at: <https://developers.google.com/maps/documentation/javascript/maptypes> (Accessed: 4 August 2016).
- [33] Otto, Frei, Schleyer, Friedrich-Karl, Ben-Yaakov, D. & Pelz, T. red. 1969, *Tensile structures: design, structure and calculation of buildings of cables, nets and membranes, Vol.2*, Berlin
- [34] Frei Otto Film (2015) *FREI OTTO - MODELING WITH SOAP FILMS*. Available at: <https://youtu.be/-IW7o25NmeA> (Accessed: 5 August 2016).
- [35] *Masonry 2016*. Britannica Academic. Retrieved 5 August 2016, from <http://academic.eb.com.proxy.lib.chalmers.se/levels/collegiate/article/51279>
- [36] *Building construction 2016*. Britannica Academic. Retrieved 5 August 2016, from <http://academic.eb.com.proxy.lib.chalmers.se/levels/collegiate/article/106103>
- [37] *Mercator projection 2016*. Britannica Academic. Retrieved 5 August 2016, from <http://academic.eb.com.proxy.lib.chalmers.se/levels/collegiate/article/52078>
- [38] Pottmann, H. 2013, *Architectural Geometry and Fabrication-Aware Design*, Nexus Network Journal, vol. 15, no. 2, pp. 195-208.

-
- [39] Bobenko, A.I., Suris, Y.B. and Bobenko, I. (2009) *Discrete differential geometry: Integrable structure*. Washington, DC, United States: American Mathematical Society.
 - [40] Varela and Sousa (2016) *Revising Stereotomy through Digital Technology*, Faculty of Architecture, University of Porto. .
 - [41] Poulsen, E. (2015) *Structural design and analysis of elastically bent gridshells - The development of a numerical simulation tool*. Göteborg : Chalmers University of Technology (Diploma work - Department of Applied Mechanics, Chalmers University of Technology, Göteborg, Sweden, nr: 2015:95).
 - [42] Topping, B.H.V. & Khan, A.I. 1994, *Parallel computation schemes for dynamic relaxation*, Engineering Computations, vol. 11, no. 6, pp. 513-548.
 - [43] Davis, L., Rippmann, M., Pawlofsky, T. and Block, P. (2012) *Innovative funicular tile vaulting: A prototype vault in Switzerland*, The Structural Engineer, 90(11), pp. 46–56.
 - [44] Chilton, J. (2012) ‘Form-finding and fabric forming in the work of Heinz Isler’, .
 - [45] Ekh, M., Toll, S. (2014) Lecture notes from the course Mechanics of Solids at Chalmers, Chalmers.
 - [46] Differential geometry 2016. Britannica Academic. , from <http://academic.eb.com.proxy.lib.chalmers.se/levels/collegiate/article/111075> (Accessed: 2 September 2016)
 - [47] Marshall, B.R. (2008) Geograph: Bath abbey, ceiling (C) Brian Robert Marshall. Available at: <http://www.geograph.org.uk/photo/717407> (Accessed: 23 December 2016).
 - [48] Material tour de force: The work of Eladio Dieste (no date) Available at: <http://archleague.org/2014/06/material-tour-de-force-the-work-of-eladio-dieste/> (Accessed: 19 July 2016).
 - [49] The architectural league of new york. 2017. Archleagueorg. [Online]. Available from: <http://archleague.org> (Accessed: 6 June 2016)
 - [50] Tensor analysis 2016. Britannica Academic. Retrieved 3 October 2016, from <http://academic.eb.com.proxy.lib.chalmers.se/levels/collegiate/article/71717> Interview
 - [51] Harvard GSD (2011) ‘Form and forces’ - John Ochsendorf. Available at: <https://www.youtube.com/watch?v=r-tG68WvNDM> (Accessed: 10 August 2016).
 - [52] Williams, C.J.K. Interviewed by: Adiels, E.

A

Appendix 1

The following content is in many ways relevant for the thesis but did not fit in the structure of the thesis. It is a good place for more information regarding the subjects and sections covered in the thesis.

A.1 Bricks

A.1.1 The brick

What is the essence of a brick? What one might say is the format and the materiality. A good definition is made by Mitchell [12], *Bricks are an artificial kind of stone, made of burnt or baked argillaceous or clayey earth, and the quality depends upon (a) the chemical properties of the earth, (b) the preparation of the earth, and (c) the different degrees of burning and baking*. There are many different types of clays, or silicate of alumina, with different chemical compositions. Mitchell gives a thumb-rule for a good clay, or brick earth, "*Silica, three-fifths; alumina, one fifth; iron, lime, magnesia, manganese, soda and potash forming the remaining fifth*"[12]. To get a more detailed view of chemical composition for different clays, see table A.1.

		1 Fire-Clays.		2	3	4	5 Ordinary Clays.			7	8
		Dinas.		Stourbridge.	Loam.	Blue Clay.	Burham Clay.	Terra-Cotta Clay.	London Brick Clay.	Marl.	
SiO ₂	86.2	63.4	66.7	46.5	42.92	75.2	49.5	} 43.0	
Al ₂ O ₃	2.3	23.2	27.0	38.0	20.42	10.0	34.3		
Fe ₂ O ₃3	1.9	1.3	1.0	5.0	3.4	7.7		3.0
CaO	1.0	—	.5	1.2	10.79	1.2	1.4		26.04
MgO	—	.9	—	—	.07	trace	5.1		3.5
Alkalies or Alkaline											
Chlorides	...	—	—	—	—	—	.33	.5	—		—
CO ₂	—	—	—	—	8.12	—	—		20.46
H ₂ O	—	—	—	—	6.68	5.9	—		4.0
Organic Matter	10.0	10.0	5.0	13.6	5.01	3.7	1.9		—
			99.8	99.4	100.5	100.3	99.34	99.9	99.9		100.0

Table A.1: The chemical composition of different types of brick clay. The proportions are described in percentage. [12]

A.1.2 Brick Making

The fabrication of the brick is crucial for the performance of the brick structure. Many of the properties are closely related to composition of the brick earth [12] and the kiln temperature, see figure A.17. The brick fabrication can be divided into the following steps.[25]

1. Preparation of the raw material
2. Forming of the bricks
3. Drying
4. Burning and cooling
5. Sorting

The forming of the bricks is a quite an important step for the format of the brick. There are two main principles.

1. the machine made, wire-cut, figure A.2
2. The machine-made pressed, or hand moulded, figure A.1

Wire-cut bricks usually gets very precise with a smooth surface. The pressed or molded bricks can get quite rough and the shape is usually a little bowed, curved or twisted. The deformations are in general not a problem due to the adaptability for tolerances of the mortar joints. The deformations should though not be greater than the joints allow.



Figure A.1: A traditional method of brick making is by putting it into wooden forms. Today this is not very common and the bricks are usually pressed by a machine. This method gives the brick marks of the form and also results in some deformation and transformations from the cuboid. The deformations is in general not a problem due to the adaptability for tolerances of the mortar joints. This method is more in line with traditional brick making then the wire-cutting method. [30]

There are different kinds of kilns. The principles are though the same even though they can be constructed differently. Figure A.3 describes a tunnel kiln and its different stages of the process.

A.1.3 Craftsmanship

The art of bricklaying is to combine bricks with mortar, which is a workable paste in its initial state that binds the bricks together, to form a composition of structural elements. This composition must meet the requirements of the engineer or architect

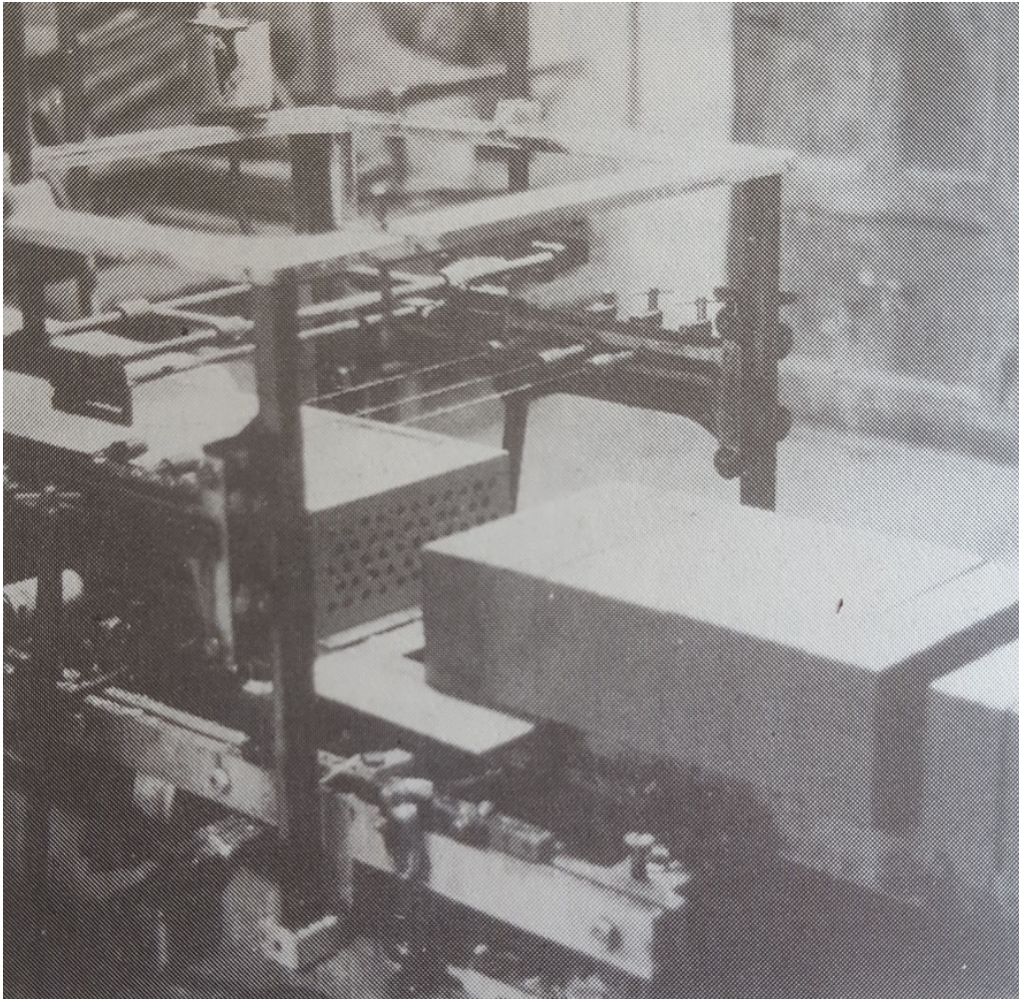


Figure A.2: An industrialised way of making bricks using a wire-cutter. This results in concise and precise forms of the brick with less deformations. The feeling of these bricks are usually more industrial.[30]

in terms of geometrical, aesthetic, structural and thermal requirements (it should be dense so that water and air cannot directly pass through). It is a very unforgiving craft since you have no margins for error due to the quick setting of the mortar. If the craftsmanship has been lacking it is very time consuming and requires much effort to correct or repair afterwards.

What differs the brick layer from other crafts is the pure simplicity, not much has changed with time and the execution is still very traditional. A description from a Swedish text book for bricklayers states *For brick laying only a few tools are required: spatula, hammer(specialized for cutting bricks), plump, spirit-level, cord and corner sticks*[31]., see figure A.4.

With the spatula the brick layer applies just enough mortar to make the brick attach to the underlying brick and assures the bed joint height is level. It is also important to apply enough mortar and pressure in the placement of the vertical joint, figure A.6 The hammer is used to cut the stones for situations where the normal format does not fit, it can be at corners or vaults. A brick layer always works within in line

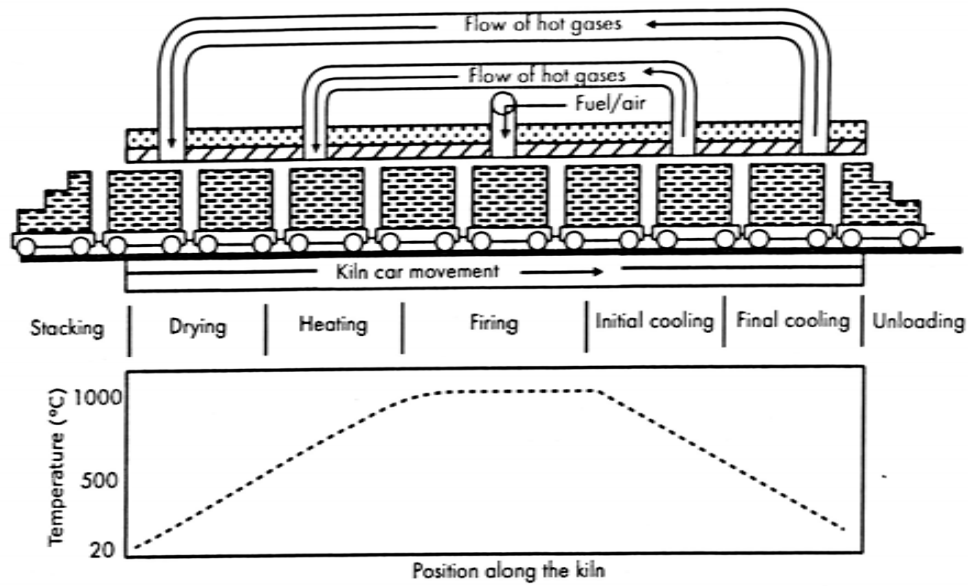


Figure A.3: Principles of a tunnel kiln. Above is the different stages and below one can follow the difference in temperature during these stages [10]

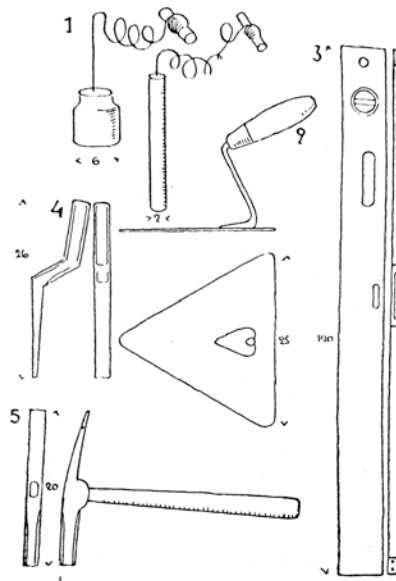


Figure A.4: Typical tools for a brick layer from a Swedish brick layer handbook from 1938. 1)Plumb 2)spatula 3)spirit level 4)Wooden jointer 5)Hammer for brick cutting [31]

with the bedding layer so the brick is always cut in the vertical direction.

The most common technique of keeping the brick level is to work with a cord attached between two corners sticks, figure A.5. When not possible a brick layer must be able to work with only a spirit level and plumb to keep ensure the geometrical entities level,figure A.6. The working stages is illustrated in the illustrations below.



Figure A.5: The bricks should all be level in the horizontal direction. The most common way to achieve this is to use string that is attached between to rods.[31]

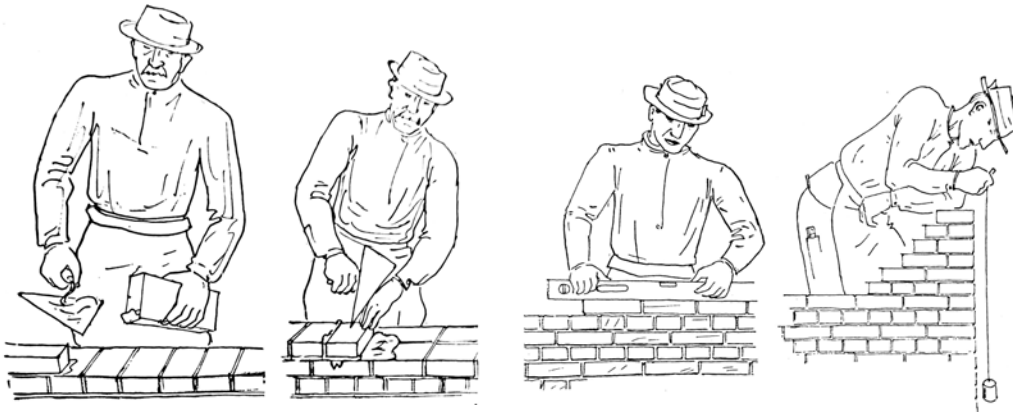


Figure A.6: To the left one can see how the bricklayer uses a spatula to apply mortar to both the brick and the place of the brick. To the right one can see how the brick layer can use both the spirit level and a plumb to ensure geometrical correctness[31]

A.1.4 Brick formats and terminology

A fundamental property of the brick wall is the unity of the single format of the bricks. There are though many different types of formats and it is usually a historical or cultural tradition that defines the dimensions in each country, see figure A.7. The most common Swedish brick format is for instance a bit larger than the Danish brick dimension. Usually the bed joint height is set depending on the brick to give an even number at say the 5th and 10th layer. Figure A.7 shows some different brick sizes and the associated height of the bed joint.

The brick composition has common terminology and the name of the brick sides are determined by which edge is facing the bed joint, see figure 1.1. The most common placement is the stretcher and header, see figure 1.1. The bed joint is the the mortar joint between the courses, one layer of bricks is called a course, and the vertical joint is called perpend. Bats are a piece of a brick, $1/2$ or $3/4$. The bats can be fabricated

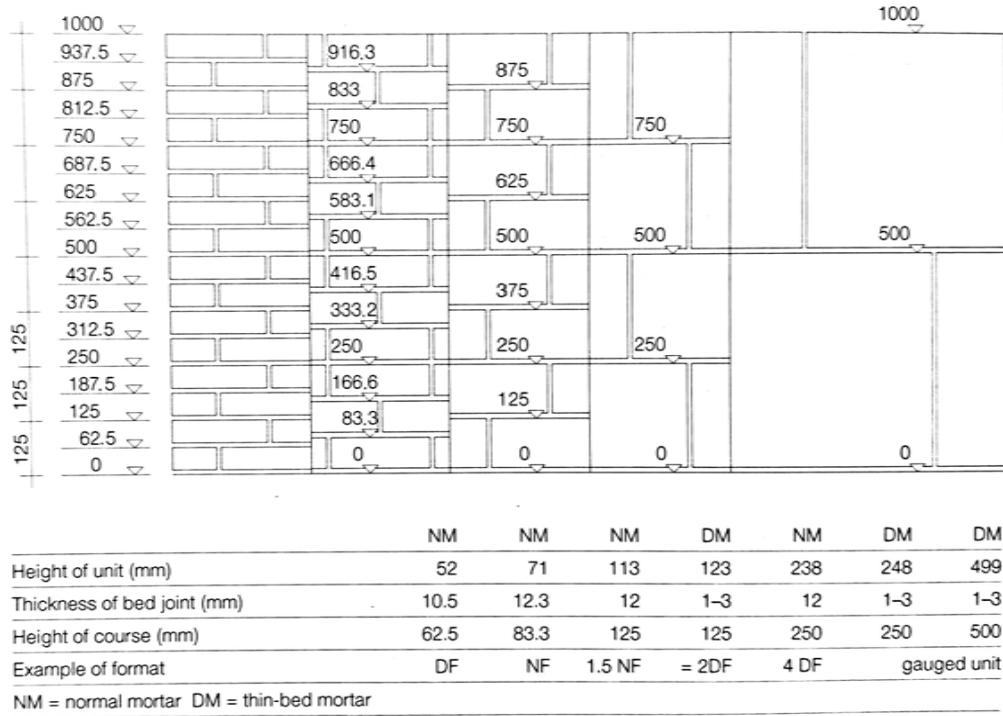


Figure A.7: Different sizes formats of typical brick constellations. [11]

but the brick layer must also be able make them himself, or herself, by splitting the brick the right size with his hammer.[12]

A.2 Differential geometry

A.2.1 First fundamental Form

The First Fundamental (FF) is the measure of the length of a surface. This is an intrinsic property since the length always is the same for real surfaces. It can tell us how its measures will behave on the surface. For example, a plane and a cylinder has the same first fundamental form which means that a line drawn on a paper has the same length as the curve on the folded cylinder by the same paper, see figure A.8.

The plane and the sphere for example does not have the same first fundamental form which is why we cannot form a paper directly to a sphere without modifications, see figure A.9. Therefore, a curve drawn on the sphere would not have a true relation to the plane as the cylinder and the plane has.

If we were to measure the line length from P and Q which is say δs . Then

$$\delta s^2 = \delta \mathbf{r} \cdot \delta \mathbf{r} = \mathbf{a}_\alpha \cdot \mathbf{a}_\beta \delta \theta^\alpha \delta \theta^\beta = a_{\alpha\beta} \delta \theta^\alpha \delta \theta^\beta \quad (\text{A.1})$$

The components of the covariant metric tensor $a_{\alpha\beta}$ described in 2.25 are also what is called the coefficients of the *first fundamental form*. It is common that these are described differently in math literature such as Struik which uses the following

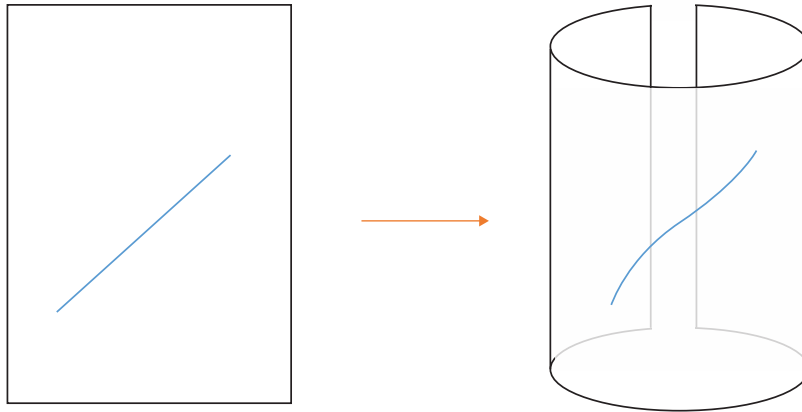


Figure A.8: The first fundamental form is way of describing how the measure of lengths on the surface will behave and propagate. If two surfaces has the same first fundamental form means that the length of a mapped curve will have the same length as before mapping. Since the plane and the cylinder has the same first fundamental form the curve will have the same length if mapping between these surfaces.

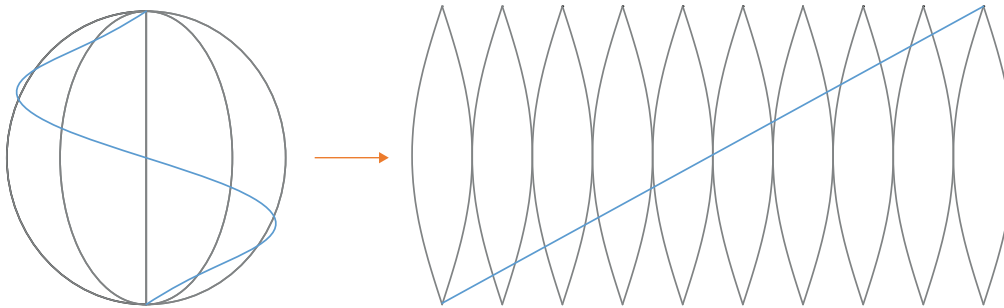


Figure A.9: The sphere and the plane does not have the same FF and therefore it is not possible to mapp these curves between the two without constraints. If flattening out a sphere on the plane, to the right, one might understand the geometrical issue graphically.

notation:

$$E = a_{11}, \quad F = a_{12}, \quad G = a_{22}$$

The curve distance P and Q can be described as following for a curve $C(t) = \mathbf{r}(\theta^1(t), \theta^2(t))$:

$$s = \int \sqrt{a_{11} \left(\frac{d\theta^1}{dt} \right)^2 + 2a_{12} \left(\frac{d\theta^1}{dt} \right) \left(\frac{d\theta^2}{dt} \right) + a_{22} \left(\frac{d\theta^2}{dt} \right)^2} dt$$

A.2.2 Second fundamental Form

The second fundamental form is the measure of how much the surface deviates from a tangent plane.[24] It is useful property in describing the curvature of the surface.

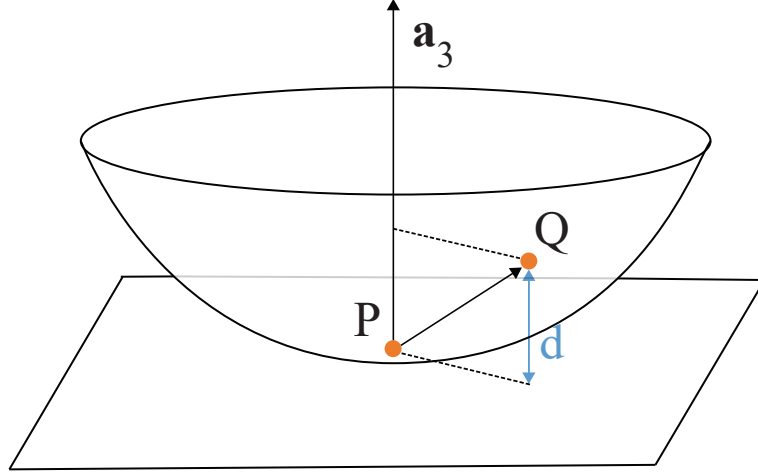


Figure A.10: A surface with a tangent plane in the point $P = \mathbf{r}(\theta^1, \theta^2)$. The point Q is described as increment from P , $Q = \mathbf{r}(\theta^1 + d\theta^1, \theta^2 + d\theta^2)$. The second fundamental form is the measure of how much the surface deviates from a tangent plane, in this figure the measure d . Redrawn from [24]

Suppose we have points P and Q on the surface that are described as $\mathbf{r}(\theta^1, \theta^2)$ and $\mathbf{r}(\theta^1 + d\theta^1, \theta^2 + d\theta^2)$.

A taylor expansion of $\mathbf{r}(\theta^1 + d\theta^1, \theta^2 + d\theta^2)$.

$$\mathbf{r}(\theta^1 + d\theta^1, \theta^2 + d\theta^2) = \mathbf{r}(\theta^1, \theta^2) + \mathbf{r}_{,1}d\theta^1 + \mathbf{r}_{,2}d\theta^2 + \frac{1}{2}(\mathbf{r}_{,11}(d\theta^1)^2 + 2\mathbf{r}_{,12}d\theta^1d\theta^2 + \mathbf{r}_{,22}(d\theta^2)^2) + \text{remainder}$$

Therefore the vector connecting P and Q , \mathbf{PQ} , can be described as

$$\mathbf{PQ} = \mathbf{r}(\theta^1 + d\theta^1, \theta^2 + d\theta^2) - \mathbf{r}(\theta^1, \theta^2) = \mathbf{r}_{,1}d\theta^1 + \mathbf{r}_{,2}d\theta^2 + \frac{1}{2}(\mathbf{r}_{,11}(d\theta^1)^2 + 2\mathbf{r}_{,12}d\theta^1d\theta^2 + \mathbf{r}_{,22}(d\theta^2)^2)$$

Projecting \mathbf{PQ} onto \mathbf{a}^3 and using the fact that $\mathbf{r}_{,\alpha} \cdot \mathbf{a}^3 = 0$.

$$d = \mathbf{PQ} \cdot \mathbf{a}^3 = \frac{1}{2}(\mathbf{r}_{,11}(d\theta^1)^2 + 2\mathbf{r}_{,12}d\theta^1d\theta^2 + \mathbf{r}_{,22}(d\theta^2)^2) \cdot \mathbf{a}^3$$

Recall from equation 2.18 that $\mathbf{r}_{,\alpha} = \mathbf{a}_\alpha$ And that $a_{\alpha\beta}$ are the coefficients of the first fundamental form. In similar fashion we define the coefficients of the Second fundamental form $b_{\alpha\beta}$

$$b_{\alpha\beta} = \mathbf{a}_3 \cdot \mathbf{a}_{\alpha,\beta} \quad (\text{A.2})$$

Applying this the second fundamental form can be written as:

$$II = b_{11}(d\theta^1)^2 + 2b_{12}d\theta^1d\theta^2 + b_{22}(d\theta^2)^2 = -d\mathbf{r} \cdot d\mathbf{a}_3$$

Reading literature by Presley, Stoker and Struik they have other conventions of describing the components of the second fundamental form, but it can be related like this.

$$e = L = b_{11}, \quad f = M = b_{12}, \quad g = N = b_{22}$$

It is appropriate to distinguish four different cases depending on the determinant of the tensor of the second fundamental form [24]. Please see illustration of these cases in figure A.11.

1. *Elliptic Case*, $b_{11}b_{22} - b_{12}^2 > 0$
2. *Hyperbolic Case*, $b_{11}b_{22} - b_{12}^2 < 0$
3. *Parabolic Case*, $b_{11}b_{22} - b_{12}^2 = 0, b_{11}^2 + b_{12}^2 + b_{22}^2 \neq 0$
4. *Planar Case*, $b_{12} = b_{11} = b_{22} = 0$

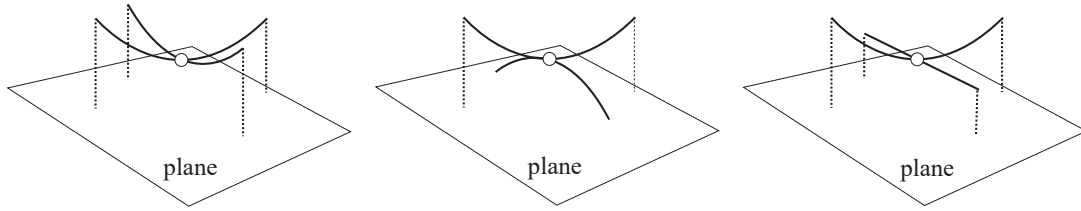


Figure A.11: On the left is the elliptic case, In the middle the hyperbolic case and to the right the parabolic case.

A.2.3 Christoffel Symbols

Applying a curve linear coordinate system on a surface means that the coordinate base vectors are dependent on the curvilinear coordinate curves, and importantly the curves do change with the surface. This means that the coordinate base vectors do change, which is a big difference to a Cartesian coordinate system where the base vectors are the same. Therefore, Christoffel Symbols are defined and used to measure the rate of change from a point P to a point Q in the base vectors of P. In the book *Einstein's Theory: A Rigorous Introduction for the Mathematically Untrained*, you can read this description "The Christoffel symbol $\Gamma_{\alpha\beta}^\gamma$, is the γ component of the change of the coordinate basis vector \mathbf{a}_β by an infinitesimal coordinate displacement $d\theta^\alpha$, per unit coordinate distance." [6]

This definition can be written in a formula as:

$$\Gamma_{\alpha\beta}^\gamma = \frac{\partial \mathbf{a}_\beta}{\partial \theta^\alpha} \cdot \mathbf{a}^\gamma \quad (\text{A.3})$$

This is what is called the *Christoffel of the Second Kind*. This leads on defining the *Christoffel of the Second Kind*.

$$\Gamma_{\alpha\beta\gamma} = \frac{\partial \mathbf{a}_\beta}{\partial \theta^\alpha} \cdot \mathbf{a}_\gamma \quad (\text{A.4})$$

According to the definition one is moving along one of the coordinate curves β with respect to parameter α , and projects the change onto coordinate vectors γ . And depending if first or second kind it is the covariant or the contravariant base vectors that the projection applies to. Since it is a scalar product the result must be a scalar. Below is a graphical interpretation of the Christoffel symbol, for both kinds.

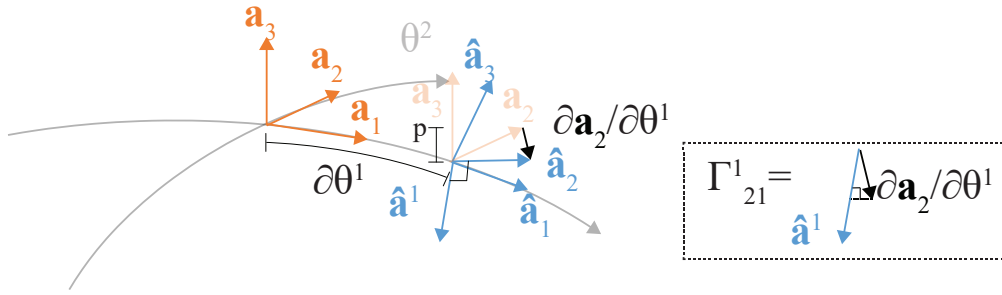


Figure A.12: Geometric representation of Christoffel Symbol of Second kind

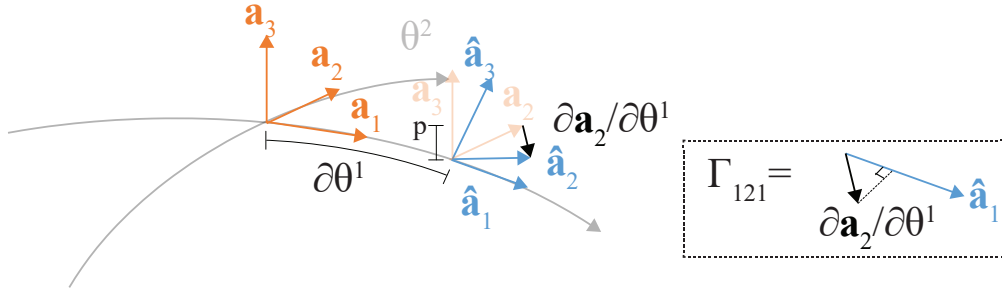


Figure A.13: Geometric representation of Christoffel Symbol of First kind

The Christoffel symbols are necessary to describe the differentiation of the covariant and contravariant basis vectors. The covariant differentiation on a surface can be defined as:

$$\frac{\partial \mathbf{a}_\beta}{\partial \theta^\alpha} = \Gamma_{\alpha\beta}^\lambda \mathbf{a}_\lambda + b_{\alpha\beta} \mathbf{a}_3 \quad (\text{A.5})$$

Notice that one needs to apply a normal component since the coordinate base vectors lie in the tangent-plane of the surface and cannot describe the changes in the normal direction. For general 3d cases it is much simpler since one can describe it much simpler:

$$\frac{\partial \mathbf{g}_i}{\partial \theta^j} = \Gamma_{ij}^k \mathbf{g}_k \quad (\text{A.6})$$

A.2.4 Gauss-Codazzi Equations

The Gauss-Codazzi Equations means the equations of Codazzi and the Gauss equation of the surface. They are important in the sense that it tells us that the first and second fundamental forms are related. Williams states [20], *"The Gauss-Codazzi equations (Gauss' theorem and the Codazzi equations) are compatibility equations, which ensure that the coefficients of the first and second fundamental forms are related in such a way that the surface 'fits together'."*

Green and Zerna[26] gives the following definition of the Codazzi equations:

$$b_{\alpha 1}|_2 = b_{\alpha 2}|_1 \quad (\text{A.7})$$

Struik writes them out as in the following [1]:

$$b_{11,2} - b_{12,1} = b_{11}\Gamma_{12}^1 + b_{12}(\Gamma_{12}^2 - \Gamma_{11}^1) - b_{22}\Gamma_{11}^2 \quad (\text{A.8})$$

$$b_{12,2} - b_{22,1} = b_{11}\Gamma_{22}^1 + b_{12}(\Gamma_{22}^2 - \Gamma_{12}^1) - b_{22}\Gamma_{12}^2 \quad (\text{A.9})$$

The Gauss equation of the surface can be written as[26]:

$$K = \frac{b_{11}b_{22} - b_{12}^2}{a} \quad (\text{A.10})$$

Equation A.10 can also be written as:

$$K = \frac{1}{4}\epsilon^{\lambda\alpha}\epsilon^{\beta\gamma}\bar{R}_{\lambda\alpha\beta\gamma} \quad (\text{A.11})$$

Where Green and Zerna calls $\bar{R}_{\lambda\alpha\beta\gamma}$ the *associated Riemann-Christoffel tensor* which is defined as.

$$\bar{R}_{\lambda\alpha\beta\gamma} = a_{\lambda\mu}\bar{R}^{\mu}_{\alpha\beta\gamma} \quad (\text{A.12})$$

Where $\bar{R}^{\mu}_{\alpha\beta\gamma}$ which is called the *Riemann-Christoffel tensor* can be written in Christoffel Symbols.

$$\bar{R}^{\lambda}_{\alpha\beta\gamma} = \Gamma_{\alpha\beta}^3\Gamma_{3\gamma}^{\lambda} - \Gamma_{\alpha\gamma}^3\Gamma_{3\beta}^{\lambda} \quad (\text{A.13})$$

Equation A.13 shows what A.10 can be written in terms of the first fundamental form, since Christoffel symbols can be written in the first fundamental form components.

A.2.5 Gaussian and Mean Curvature

Two measures to describe the curvature of a surface are what is called *Gaussian Curvature* and *Mean Curvature*. Both can be described through the principal curvatures or in terms of first and second fundamental form.

The mean curvature, H , is the mean value of the principal curvatures.

$$H = \frac{\kappa_1 + \kappa_2}{2} = \frac{b_{11}b_{22} - 2b_{12}a_{12} + b_{22}a_{11}}{2(a_{11}a_{22} - (a_{12})^2)} \quad (\text{A.14})$$

The Gaussian curvature, K , is the product of the two principal curvatures.

$$K = \kappa_1 \kappa_2 = \frac{b_{11}b_{22} - (b_{12})^2}{a_{11}a_{22} - (a_{12})^2} \quad (\text{A.15})$$

The geometrical meaning of the Gaussian curvature can be seen in figure A.14. A point of positive Gaussian curvature is a point where you have positive principal curvature in both directions as in a sphere. This is a point where you have two parabolas whose openings are directed the same way. A negative Gaussian curvature means that you have two parabolas but where they are directed in opposite directions. Zero Gaussian curvature is a result of one or both Principal curvatures are zero as in a cylinder.

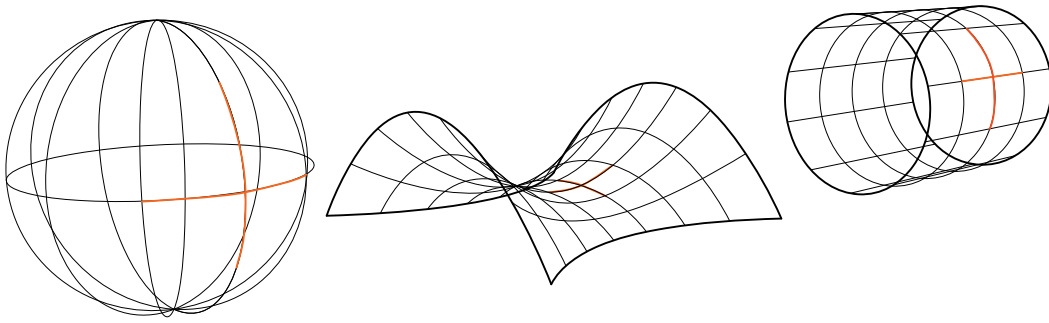


Figure A.14: To the left is a sphere which has positive curvature in two directions. In the middle is a hyperparaboloid which has both positive and negative curvature in its saddle point, which results in negative Gaussian curvature. To the right is the cylinder which has positive in one and zero curvature in the second direction which results in zero Gaussian curvature.

Surfaces of no *mean curvature* is what we are calling minimal surfaces. Usually we define that as a surface of the smallest area spanned by a given closed space curve, even though this is not always true according to Struik [1].

A.2.5.1 Principal Curvature

The directions in the tangent plane for which κ_n , normal curvature, takes maximum and minimum values are called principal directions. There are always two principal curvatures κ_1 and κ_2 corresponding to the principal directions and the directions are always orthogonal to each other. [1]

The principal curvatures are the roots of the determinant of the combined matrix of the two tensors $b_{\alpha,\beta}$ and $a_{\alpha,\beta}$, see below. [5]

$$\begin{vmatrix} b_{11} - \kappa a_{11} & b_{12} - \kappa a_{12} \\ b_{12} - \kappa a_{12} & b_{22} - \kappa a_{22} \end{vmatrix} = 0 \quad (\text{A.16})$$

and the principal vectors corresponding to the principal curvature κ are the tangent vectors $\mathbf{t} = \xi \mathbf{a}_1 + \eta \mathbf{a}_2$. [5]

$$\begin{pmatrix} b_{11} - \kappa a_{11} & b_{12} - \kappa a_{12} \\ b_{12} - \kappa a_{12} & b_{22} - \kappa a_{22} \end{pmatrix} \begin{pmatrix} \xi \\ \eta \end{pmatrix} = \begin{pmatrix} 0 \\ 0 \end{pmatrix} \quad (\text{A.17})$$

A.3 Tensor Analysis

This thesis uses a fare amount of tensor analysis. Tensor can be described as following [50] *"Tensor analysis, branch of mathematics concerned with relations or laws that remain valid regardless of the system of coordinates used to specify the quantities. Such relations are called covariant. Tensors were invented as an extension of vectors to formalize the manipulation of geometric entities arising in the study of mathematical manifolds."*

A.3.1 Index notation

The index notation simplifies writing quantities as well as equations. In the index notation there are two types of indices, *free indices* and *summation indices*.

Free indices are those who are used only once per quantity. If you have a Cartesian coordinate system the integer will take values 1,2 and 3. It is possible to use several free indices.[45]

$$a_\alpha \Leftrightarrow a_1, a_2, a_3$$

$$a_{\alpha\beta} \Leftrightarrow a_{11}, a_{12}, a_{13}, a_{21}, a_{22}, a_{23}, a_{31}, a_{32}, a_{33}$$

Summation indices are used twice per quantity and indicates a summation of that index. Using Cartesian coordinates it will range from 1 to 3.

$$a_{\alpha\alpha} \Leftrightarrow \sum_{\alpha=1}^3 a_{\alpha\alpha}$$

$$a_\alpha b_\alpha \Leftrightarrow \sum_{\alpha=1}^3 a_\alpha b_\alpha$$

A.3.2 2nd order Tensors

2nd order tensors are physical quantities that describe how vectors change with e.g direction and position in space. A 2nd order tensor \mathbf{T} is represented in a orthonormal coordinate system $\{\hat{\mathbf{e}}_1, \hat{\mathbf{e}}_2, \hat{\mathbf{e}}_3\}$ as [45]

$$\mathbf{T} = T_{\alpha\beta} \hat{\mathbf{e}}_\alpha, \hat{\mathbf{e}}_\beta \quad (\text{A.18})$$

A.4 Material

A.4.1 Material Properties

Bricks belongs to the group of materials called ceramics. There are some general properties that applies to clay based ceramic materials.[25]

- Hard and brittle

- They have little or no creep and plastic deformation
- Heat resistant
- Resistant against acid and biological attacks
- Have small volumetric deformations, i.e. no deformations related to heat and moisture.

The mechanical of physical properties of bricks are that they are very favourable under pure compression and unfavourable. The very high compressive strength is in contradiction to it tensile and flexural capacity. In figure A.15 to the left one sees how the compressive strength relates the flexural strength and the modulus of elasticity.

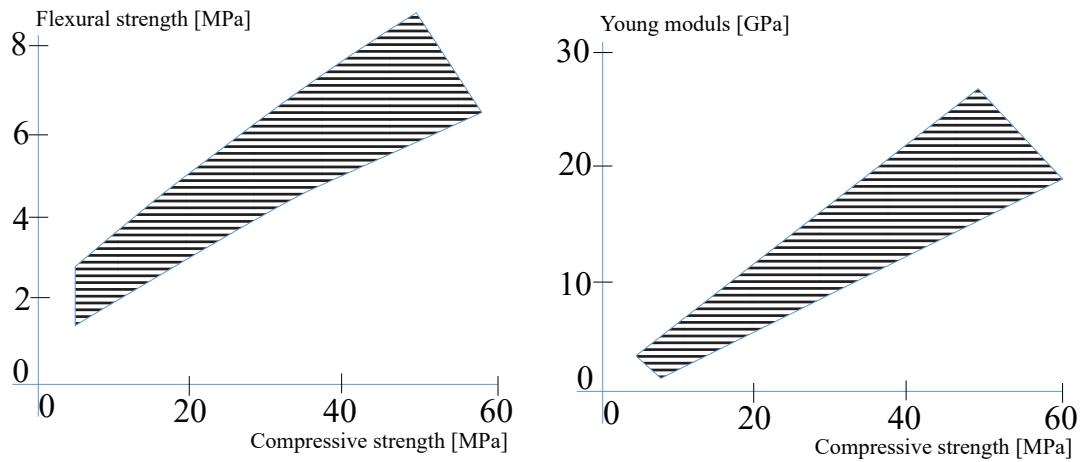


Figure A.15: The flexural strength and Young modulus compared to the compressive strength of bricks. These pictures are remakes from[25]

Figure A.16 shows the elasticity modulus of brick compares to other materials. Notice the very low Elasticity modulus compared to for instance steel which could go well over 200 GPa.

The properties of bricks are very much controlled and related to the composition of the raw material and the kiln temperature. This give the possibility to design the brick for the right circumstances and demands during the fabrication process, which can result and in a wide range of different bricks. The figure A.17 shows how for instance the density and the pore properties change with the temperature.[25]

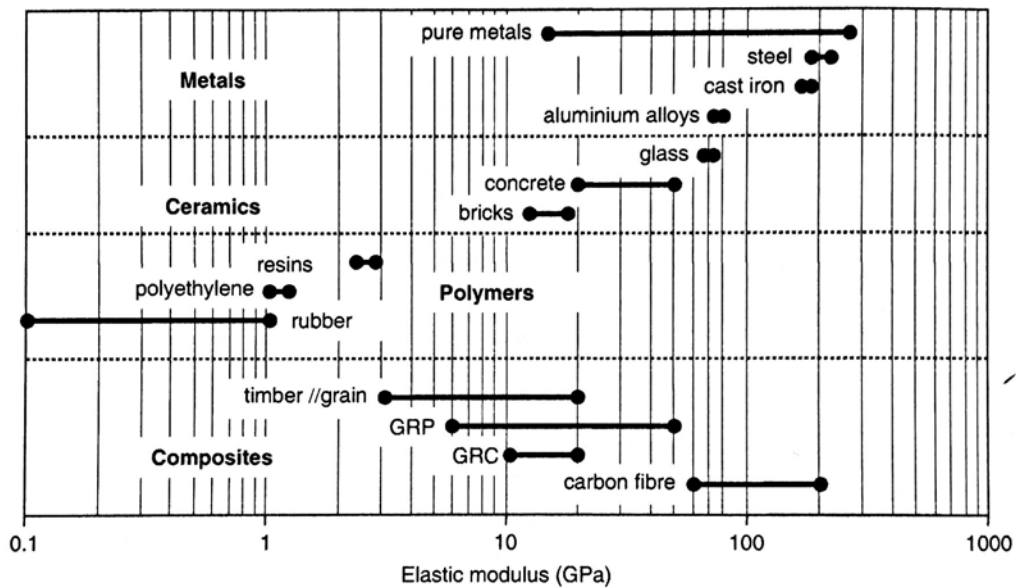


Figure A.16: Brick are part of category called ceramics which has relatively low elastic modulus compared to most metals. [25]

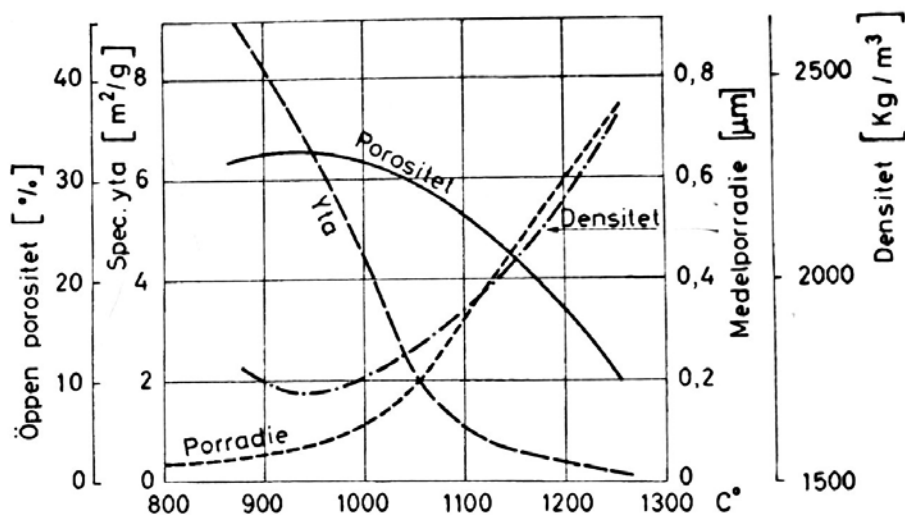


Figure A.17: The properties of bricks are very much controlled and related to the composition of the raw material and the kiln temperature. [10]

A.4.2 Mortar

Mortar is material used in building construction to bond brick, stone, tile, or concrete blocks into a structure. Mortar consists of inert siliceous (sandy) material mixed with cement and water in such proportions that the resulting substance will be sufficiently plastic to enable ready application with the mason's trowel and to flow slightly but not collapse under the weight of the masonry units.[13]

Main ingredients of mortar are:

- *Water*
- *Aggregates* - The aggregates in mortar is mostly *sand*. Sand is a rock mixture

- of rock particles of different sizes from 10 mm in diameter down to $75\mu\text{m}$.
- *Binder* - Widely used binders are based on one of these categories
 - *Hydraulic cements*, which react chemically with water at normal site temperatures.
 - *lime-silica mixtures*, which react only in the presence of high-pressure steam.
 - *lime-pozzolan mixtures*, which set slowly at ambient temperatures, or pure lime which sets slowly in air by carbonation.
- *Admixtures*, examples are: plasticisers, super plasticisers, accelerators, retarders.
- *Pigments*

A.5 Geometry

A.5.1 Stereotomy

Long before computers practitioners of stereotomy managed to create structures and patterns of very complex surfaces. The book *"Le premier tome de l'Architecture"* was released in 1567 by *Philibert de l'Orme* and is considered to contain the first description and definition of stereotomy[40]. Stereotomy is defined as "the science or art of cutting solids into certain figures or sections". It includes, and the term is sometimes used as a synonymous with, the art of cutting stones for masonry shells. [28]. Even though miss-used sterotomy is not the science of cutting stone but more the theoretical and mathematical construction of these shapes and solids. *"This is a practice not so much concerned with the actual physical means to cut through stone, but with the intellectual means to find the correct shapes to be produced."*[40]. in figure A.18 one can see an example of sketches and drawings of shapes that are constructed by different kinds of solid elements. One of the most famous examples in architecture is Hotel de Ville by *Jules Hardouin Mansart*, see figure A.19.

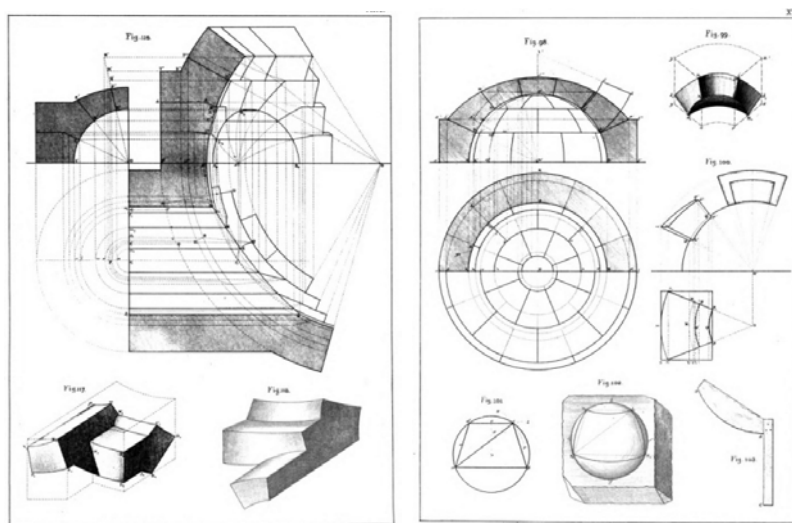


Figure A.18: Sketches and drawings from a notebook of Stereotomy from 1896 showing how structures are discretized and how those elements are constructed.[28]



Figure A.19: The stone vault at Hotel de Ville by *Jules Hardouin Mansart* is a famous example of stereotomy in architecture [49]

These methods are not very common today since it involves quite complex building elements that need to be manufactured. Though it is possible to read the research of the Block Research Group where they have investigated in how to use computational methods and digital fabrication to generate these kind of geometries. Figure A.20 and A.21 show how geometry and solids are generated digitally[18] and finished stone blocks that are digitally fabricated[19].

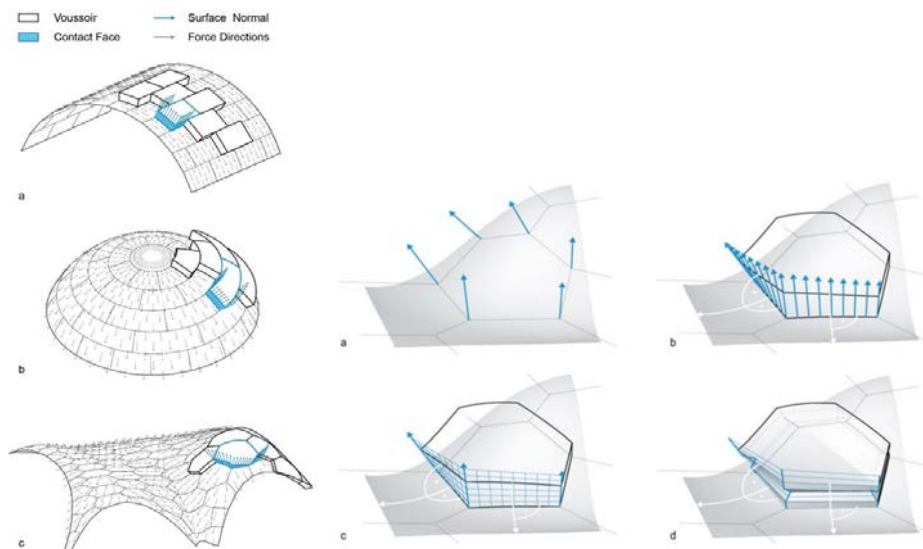


Figure A.20: Blocks can be generated from a discrete surface representation with computational methods [18]



Figure A.21: Stone blocks that have been fabricated using digital fabrication methods [19]

A.6 Form Finding

A.6.1 Graphical Methods

Graphical methods are one of the basic categories of form finding, but not less powerful. An example of these is called *graphic static* or *force polygon method*. This method can be used to seek a form of equilibrium such as arches or analysing already designed structural members such as trusses. The method originates from the work of *Karl Culmann* published in *Die graphische statik* in 1866. Graphic Statics has had much influence for modern structural design in the late 19th century and early 20th century and was used by modern structural pioneers such as *Rafael Guastavino*, *Antoni Gaudí*, *Felix Candela* and *Robert Maillart* [9]. Figure A.22 shows the method applied on a vault consisting of different shaped blocks.

The main idea of the force polygons, which are represented in what is called a reciprocal force diagram, is that the polygons should always be closed to ensure that the forces are in equilibrium. In figure A.23 a hanging cable is illustrated where the internal forces and global forces are constructed as triangles, and since they are closed polygons the structure is in equilibrium. The powerful aspect of graphic statics is the illustrative way of expressing the force connections and how the design relates the force patterns.

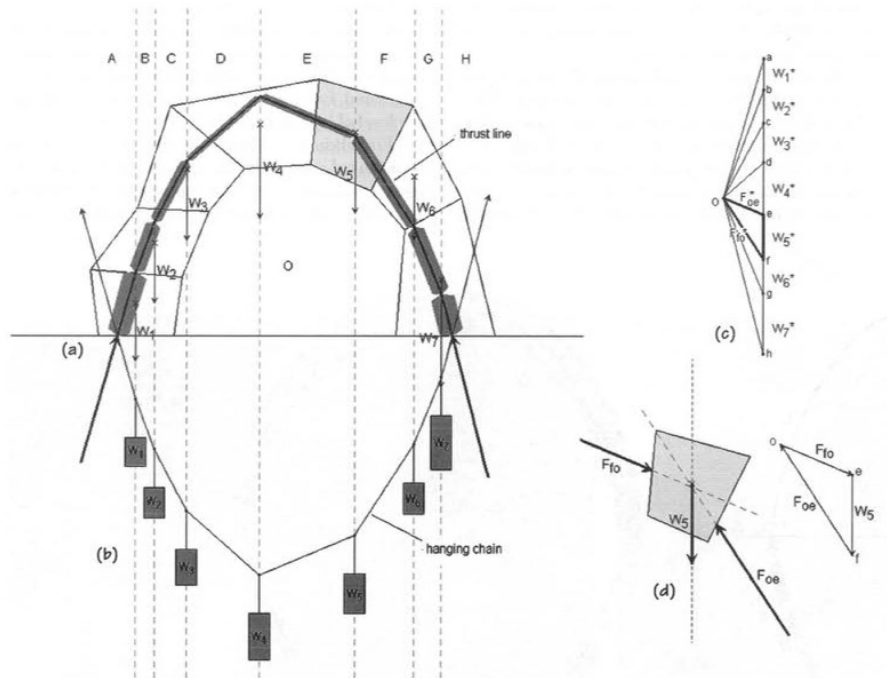


Figure A.22: Graphic statics applied to vault with differently shaped elements. To the right on can see triangles forming of the internal and external forces which illustrates equilibrium.[9]

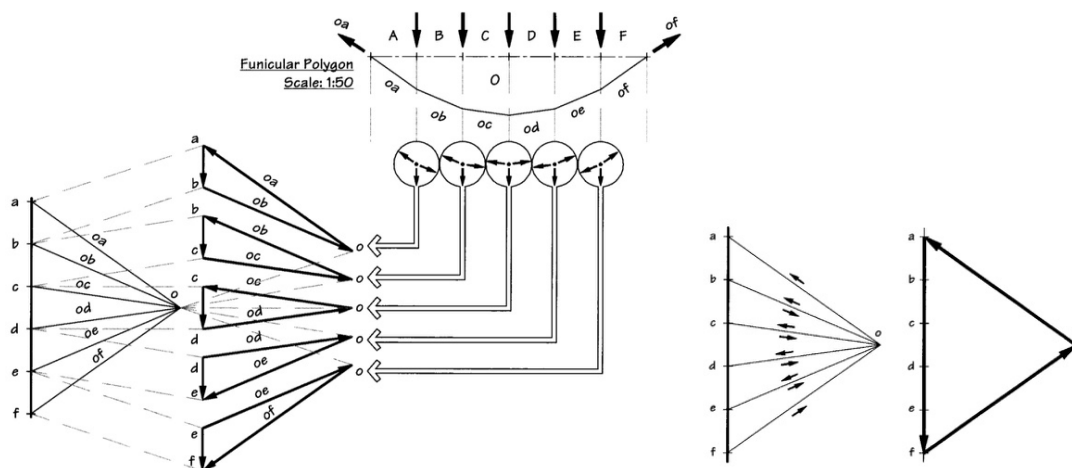


Figure A.23: Example of graphic statics applied to a hanging cable. Figure to the left shows the collected force polygons and how they relate to the internal forces of the hanging cable. To the right one can see the global equilibrium illustrated. [9]

A.6.2 Analytical Methods

It is possible to analytically derive shapes of pure tension or compression, most common example might be the catenary but it is also possible to derive various shell forms. This method allows the engineer to decide a certain stress distribution

that governs the shape. It is not very common since it easily gets very complicated applying it to complex demands, both architectural and structural. Williams [3] describes in the book *Shell Structures for Architecture* how to attain the mathematical expressions for both arches and shells, with varying constraints. You might also read *Tensile Structures Volume 2, Cable nets*[33] by Frei Otto for a descriptive way to analytically describe single cables and cable nets.

A.6.3 Physical methods

Using physical models to understand and communicate design has been a vital part in proceeding in the field of structural engineering. Many have seen the hanging cable models of *Gaudi* but the modern pioneers in this field was structural engineers and architects such as *Frei Otto* and *Heinz Isler*. During the 20th century both of them elaborated with physical models to understand the shapes and design of light weight structures. Otto is most known for his works with membrane structures and soap film models, while Isler worked much with compression shells.[44]

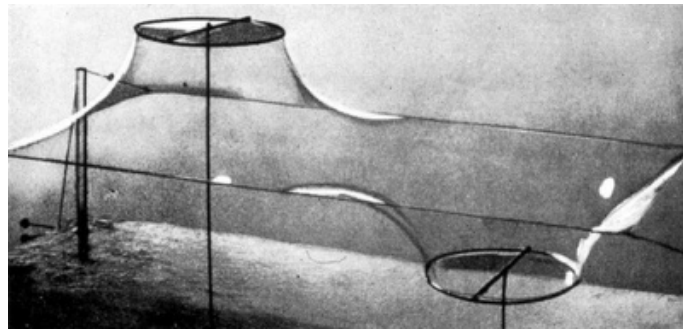


Figure A.24: Soap-film experiment to achieve minimal surfaces from the research of Frei Otto [34]

The need for physical models can be for various reasons. *"Designers of structures have used small-scale models when it is beneficial to do so, especially in order to raise the engineers confidence in the design being proposed. This may have been for many reasons. For example:"* [3]

- The available calculation methods were too complex or time-consuming
- It would be too costly to build a full-size prototype
- It was believed that normal structural analysis methods would not adequately model the structure.
- The geometry of the structure could not be defined using a mathematical equation
- There were no other means available

A.7 Results

This section will complement the and show results that did not fit inside the results section.

A.7.1 Model preparation

This section shows the different stages of model preparation in the design framework, described in 4.1.

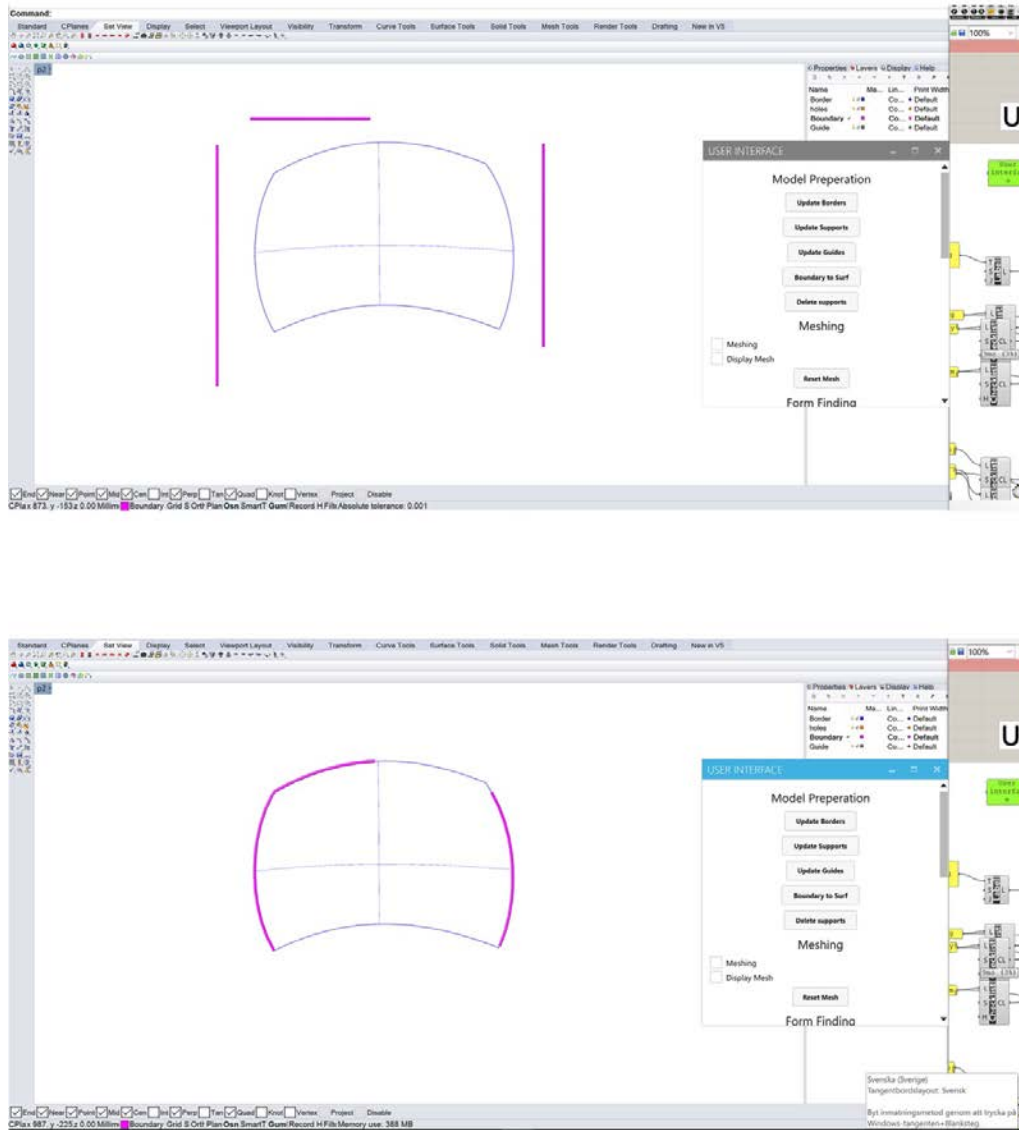


Figure A.25: It is easy to apply and change the boundary conditions. One can draw initial lines that are then projected onto the edge of the bottom form.

A. Appendix 1

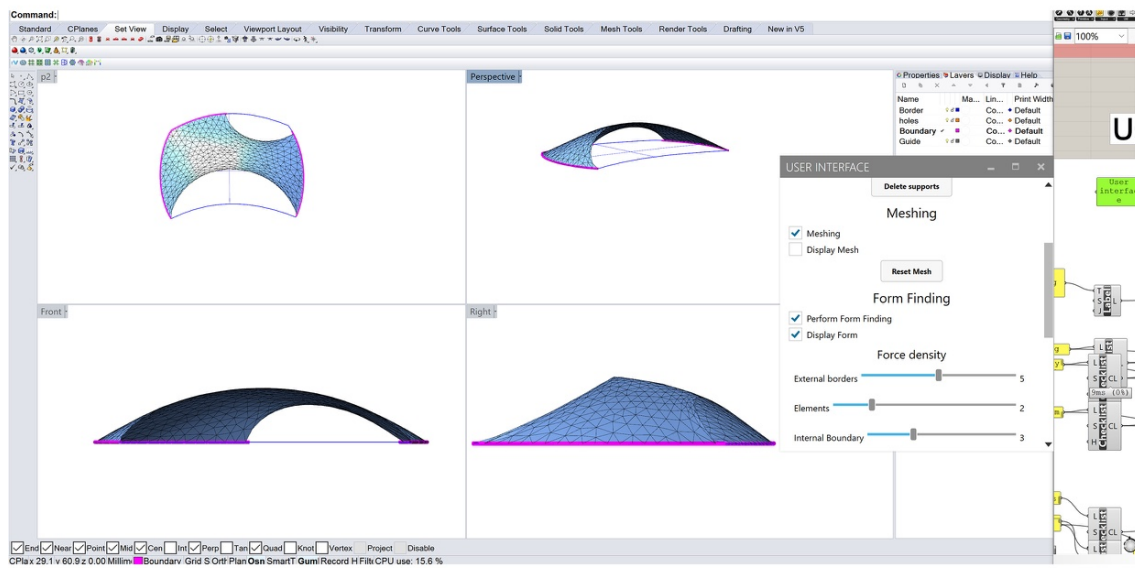
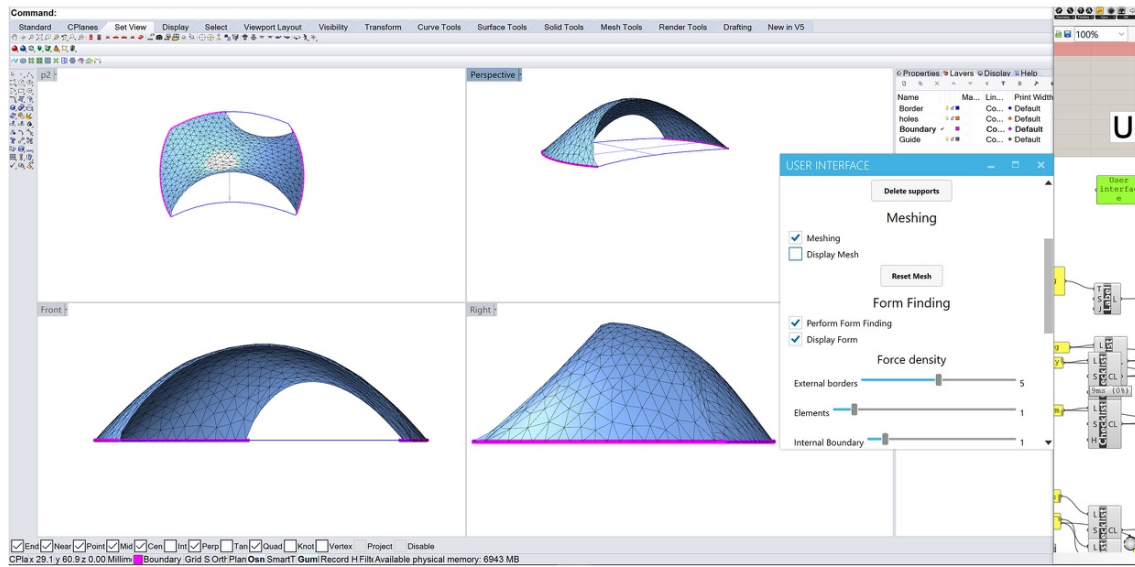


Figure A.26: It is possible to change the force densities to get different properties and attributes to the form.

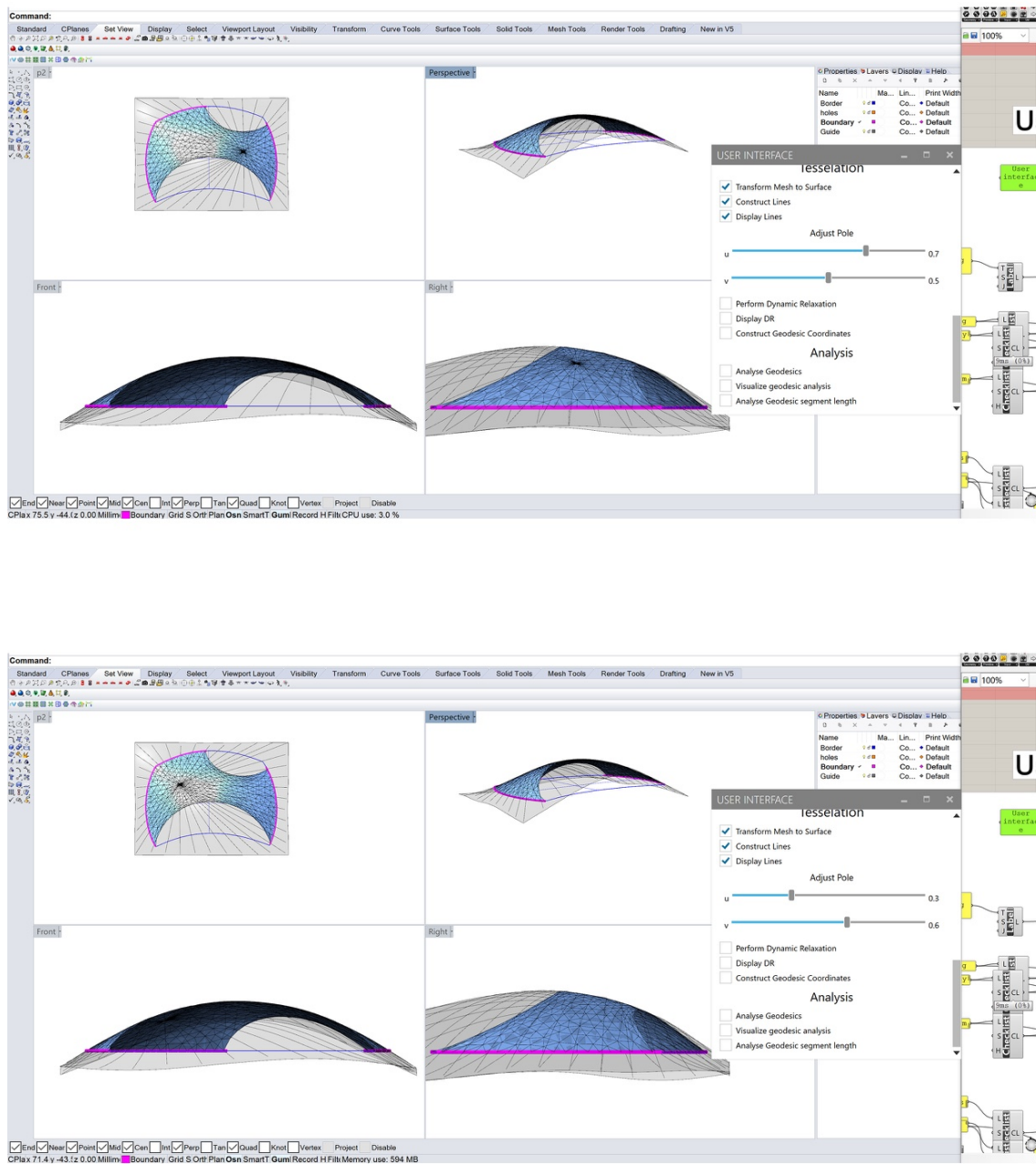


Figure A.27: It is possible to adjust the position of the pole depending on the aesthetics or the properties of the form itself.

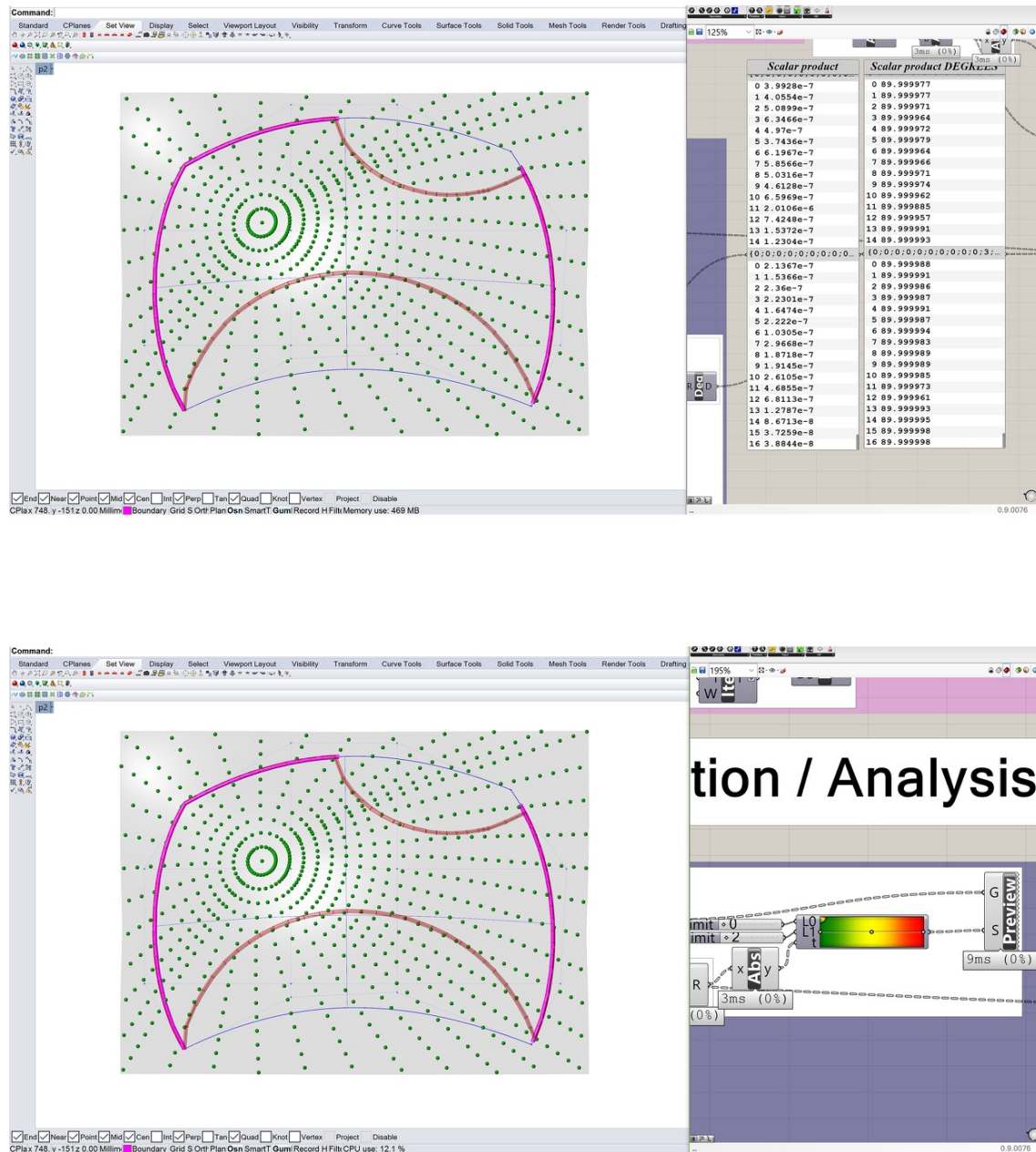


Figure A.28: Dynamic relaxation is applied to generate the geodesics. it is possible to analyse during the process by either looking at the values for each point, top picture, or look graphically, bottom picture.

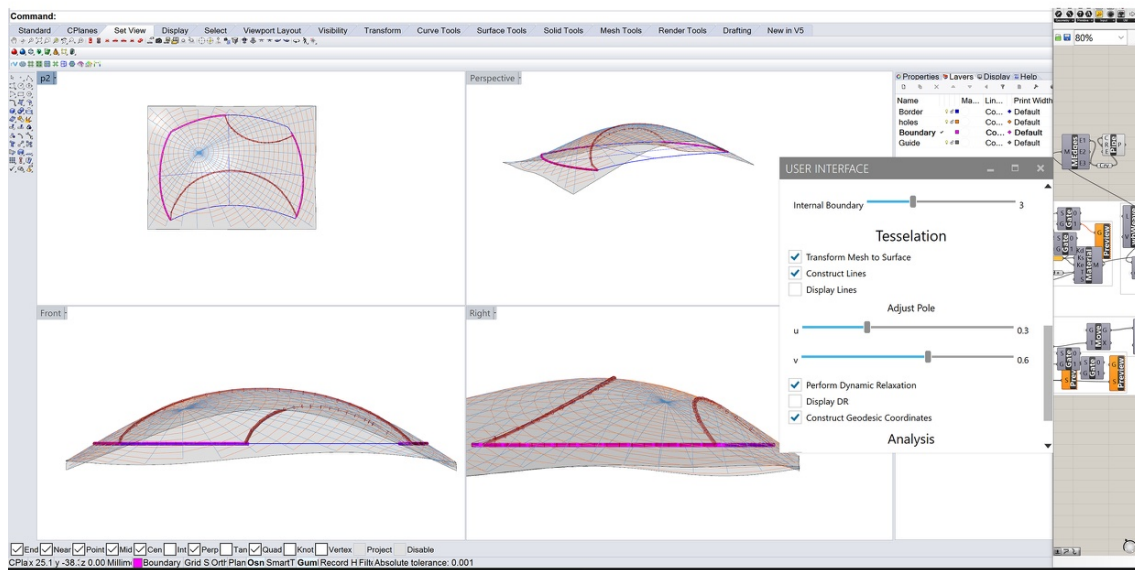
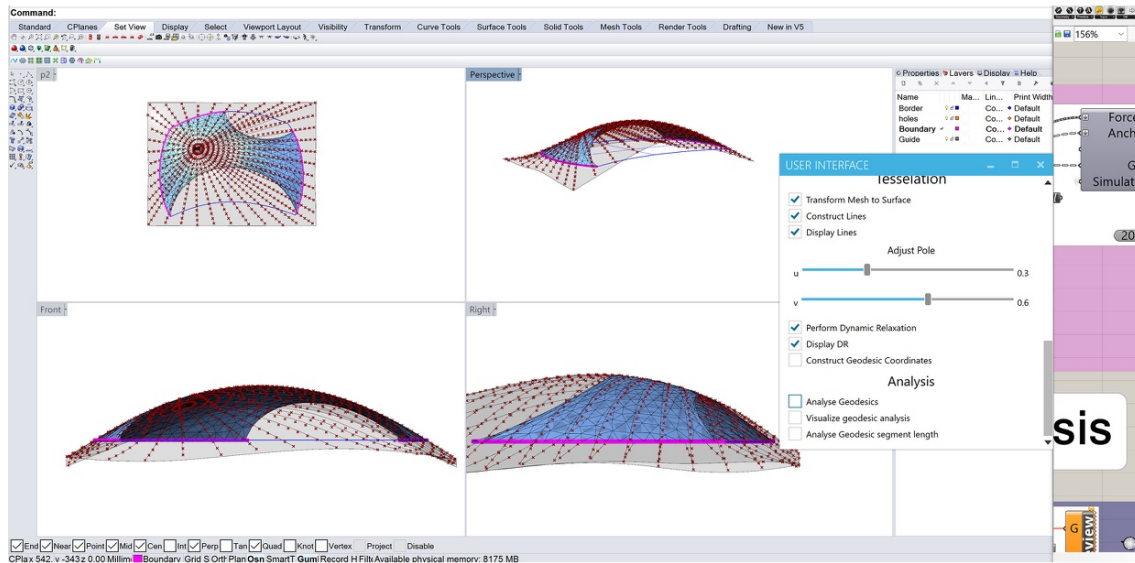


Figure A.29: The generation of the geodesics are done at this stage. And it is now possible to generate the polar geodesic coordinate based on the points from the previous stage.

A.7.2 Parametric Framework

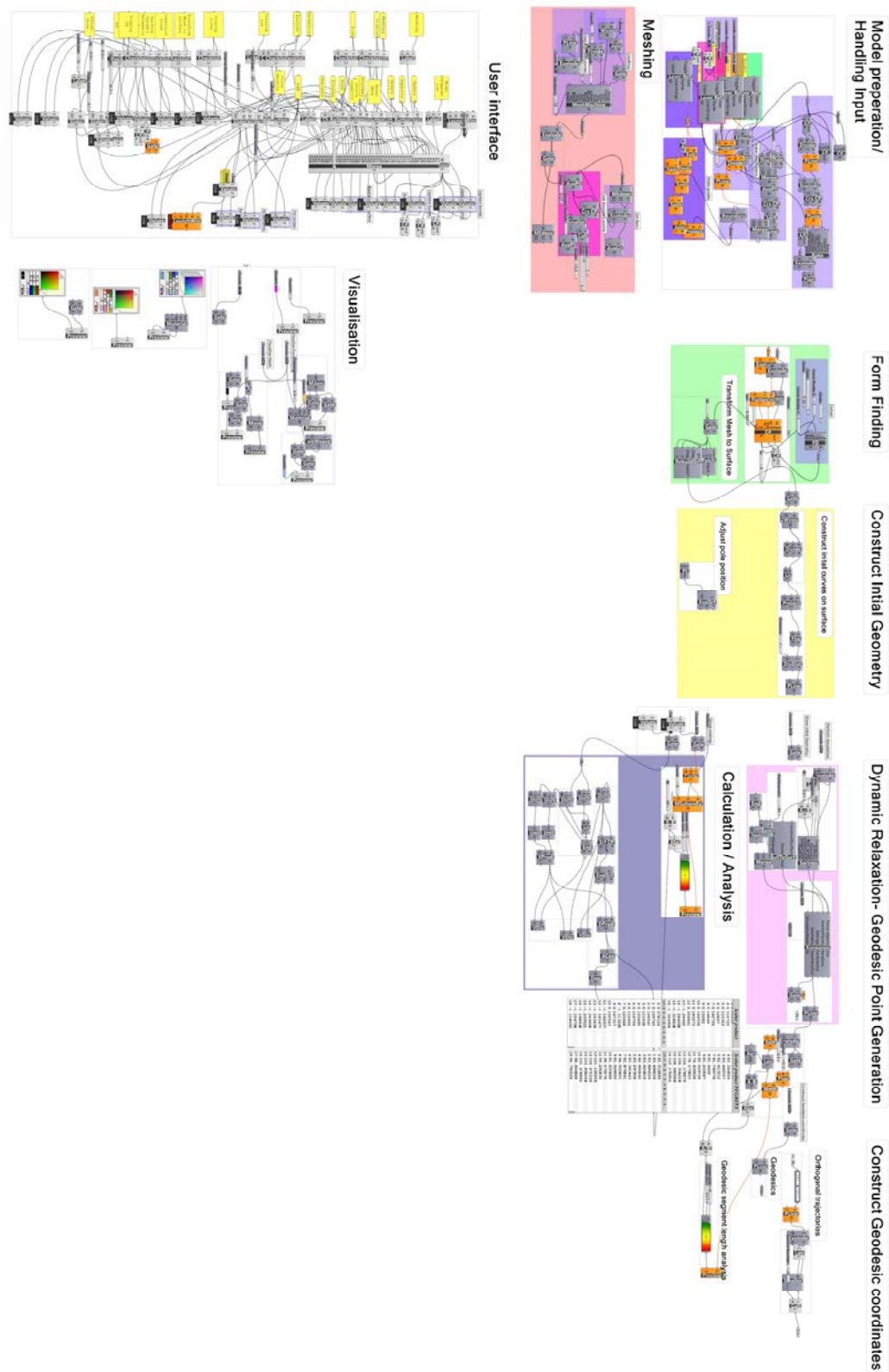


Figure A.30: The grasshopper definition made for this thesis.